UNIVERSIDAD COMPLUTENSE DE MADRID
FACULTAD DE FARMACIA

TESIS DOCTORAL

Transmission of Antimicrobial Resistance in the Intensive Care Unit Environment

Transmisión de Resistencia a Antimicrobianos en el ambiente de la Unidad de Cuidados Intensivos

MEMORIA PARA OPTAR AL GRADO DE DOCTOR

PRESENTADA POR

Sonia Aracil Gisbert

DIRIGIDA POR

María Teresa Coque González
Fernando Baquero Mochales

Madrid

UNIVERSIDAD COMPLUTENSE DE MADRID
FACULTAD DE FARMACIA

TESIS DOCTORAL

Transmission of Antimicrobial Resistance in the Intensive Care Unit Environment
Transmisión de Resistencia a Antimicrobianos en el ambiente de
la Unidad de Cuidados Intensivos

MEMORIA PARA OPTAR AL GRADO DE DOCTORA

PRESENTADA POR

Sonia Aracil Gisbert

DIRECTORES

Dra. María Teresa Coque González
Dr. Fernando Baquero Mochales

UNIVERSIDAD COMPLUTENSE DE MADRID

FACULTAD DE FARMACIA

TESIS DOCTORAL

Transmission of Antimicrobial Resistance in the Intensive Care Unit Environment
Transmisión de Resistencia a Antimicrobianos en el ambiente de la Unidad de Cuidados Intensivos

MEMORIA PARA OPTAR AL GRADO DE DOCTORA

PRESENTADA POR

Sonia Aracil Gisbert

BAJO LA DIRECCIÓN DE LOS DOCTORES

María Teresa Coque González

Fernando Baquero Mochales

PROGRAMA DE DOCTORADO EN

MICROBIOLOGÍA Y PARASITOLOGÍA

“Science is like art, it is creative.

We are not creative if you are only talking to some people.

We need to talk to everybody.”

MAY-BRITT MOSER

Nobel Prize in Physiology or Medicine 2014

AGRADECIMIENTOS

A TERESA COQUE, gracias por darme la oportunidad de aprender y crecer a tu lado. En estos años, no sólo has sido una gran mentora y un ejemplo de dedicación y perseverancia, sino que también te has convertido en una de esas amigas que sabes que nunca perderás en la vida. Tu inteligencia, tu pasión por la investigación y por la vida, tu paciencia y tu apoyo incondicional han sido una fuente de inspiración, no solo para pensar con rigor científico, sino también para creer en una misma. Gracias por cada consejo, cada empujón y cada momento de alegría en esta etapa de crecimiento no solo académico, sino también personal. Contigo he aprendido que todo esfuerzo vale la pena siempre que saques fuerzas y empeño, a no rendirme ante las dificultades y a confiar en mí misma.

A FERNANDO BAQUERO, gracias por valorar este trabajo desde el principio, por haberte implicado sobremanera, por compartir tu infinito conocimiento, y por esas bromas que, a veces, no terminaba de entender. No hay mejor manera de hacer ciencia que añadiendo un toque de humor. Siempre recordaré las conversaciones tan interesantes que hemos tenido tanto científicas como de la vida y la cultura.

A ANA ELENA PÉREZ COBAS, gracias por haberme dado luz en la oscuridad y por ser un apoyo fundamental durante esta etapa. Aunque siempre seremos un poco oscuras las dos, estos años los has iluminado estos años con tu pasión, dedicación a la investigación e inteligencia, y estoy orgullosa de poder llamarte amiga.

A mis compañeros del EcoEvoBiome Lab, sobretodo a NATALIA GUERRA-PINTO y MIGUEL D. FERNÁNDEZ-DE-BOBADILLA, gracias por haber empezado esta aventura conmigo y haber llenado estos años de alegría. A SILVIA SERRANO, persona incondicional en mi vida, y CAROLINA LÓPEZ, a veces confundidas como hermanas.

Al Evodynamics Lab, sobretodo a JERÓNIMO RODRÍGUEZ-BELTRÁN, que también ha compartido conmigo toda esta etapa. Hemos podido crecer juntos y espero que siga siendo así. A CRISTINA HERENCIAS, LAURA ÁLVARO, PAULA RAMIRO y LAURA JARABA grandes compañeras y amigas.

A CRUZ SORIANO y RAÚL DE PABLO, por su dedicación a la investigación y por haber hecho posible este proyecto.

A mis compañeras de piso ANDREA y PAULA, y ANITA e IRENE, por haber llenado de alegría estos años y por ser tan irremplazables en mi vida. No sé que haría sin vosotras, gracias por tanto.

A mis hermanas de otra sangre ISA, PATRI, IRENE y AINHOA, gracias por todos estos años y por seguir estando ahí. Sois unos pilares fundamentales en mi vida.

A mis amigxs de Madrid, por ser un grupo tan guay e incondicional, vuestros regalos siempre quedarán en mi corazón.

Y, por último, a mi familia, a mis PADRES, mi HERMANO y mis ABUELOS. No ha sido fácil este camino, sobretodo los últimos años, y sé que siempre estaréis incondicionalmente de mi lado. Va para vosotros. Y para ti, VICENTE.

INDEX OF CONTENTS

ABBREVIATIONS

16S RNA	16 Svedberg (unit of measure) RNA
2GC	Second-Generation cephalosporins (antibiotic, β-lactam)
3GC	Third-Generation cephalosporins (antibiotic, β-lactam)
4GC	Fourth-Generation cephalosporins (antibiotic, β-lactam)
ABC	ATP-binding cassette (transporter, protein)
ABR	Antibiotic-resistance (resistome)
AMC	Amoxicillin-Clavulanate (antibiotic, penicillin, β-lactam)
AMP	Ampicillin (antibiotic, penicillin, β-lactam)
AmpC	Ampicillin-resistance cephalosporinase (enzyme, class C β-lactamase)
AMR	Antimicrobial Resistance (antibiotics, heavy metals, biocides)
ANI	Average Nucleotide Identity
ARB	Antibiotic-Resistant Bacteria
ARG	Antibiotic Resistance Gene
AST	Antibiotic Susceptibility testing
ATM	Aztreonam (antibiotic, monobactam, β-lactam)
BLAST	Basic Local Alignment Search Tool
BRC	Central Venous Catheter-related Bloodstream Infections
BSI	Bloodstream infection
CDC	Centers for Disease Control and Prevention
CDS	Coding sequence
CFU	Colony Forming Unit
CHL	Chloramphenicol (antibiotic)
CIP	Ciprofloxacin (antibiotic, fluoroquinolone)
CLSI	Clinical and Laboratory Standard Institute
CTX	Cefotaxime (antibiotic, 3GC, β-lactam)
CTX-M	Cefotaximase (Type M, class A β-lactamase)
CZD	Ceftazidime (antibiotic, 3GC, β-lactam)
DDST	Double Disk Synergy Test
DIN	DNA integrity number
DNA	Deoxyribonucleic Acid
ESBL	Extended-Spectrum Beta-Lactamase
EUCAST	European Committee on Antimicrobial Susceptibility Testing
FEP	Cefepime (antibiotic, 4GC, β-lactam)
FOX	Cefoxitin (antibiotic, second-generation cephalosporin, β-lactam)
GC	Guanine-Cytosine
GMN	Gentamicin (antibiotic, aminoglycoside)
GTDB	Genome Taxonomy Database
HAI	Hospital-acquired infection
HCCA	α-Cyano-4-hydroxycinnamic acid (matrix used in MALDI-TOF MS)
HURyC	Hospital Universitario Ramón y Cajal
ICU	Intensive Care Unit
IMI	Imipenem
Inc	Incompatibility (referred to plasmid families)
K-NN	K-nearest neighbors' algorithm
KPC	*Klebsiella pneumoniae* carbapenemase
LB	Lysogenic Broth
LDA	Linear discriminant analysis
LEFSe	LDA effect size
MALDI-TOF-MS	Matrix-Assisted Laser Desorption/Ionization-Time of Flight-Mass Spectrometry
MDR	Multi-drug Resistant
MDRO	Multi-drug Resistant organism
MEM	Meropenem (antibiotic, carbapenem, β-lactam)

MGE	Mobile genetic element
MH	Mueller-Hinton (culture media)
MIC	Minimal Inhibitory Concentration
MLST	Multi-Locus Sequence Typing
MOB	Mobilization gene (plasmid)
MRSA	Methicillin-resistant *Staphylococcus aureus*
NAV	Ventilator-associated pneumonia
NCBI	National Center for Biotechnology Information
NDM	New Delhi MBL (class B β-lactamases)
NICU	Neonatal Intensive Care Unit
NMDS	Non-metric multidimensional scaling
OXA-48	Oxacillinase-48 (class D β-lactamase)
p-value	Probability-value
p0	Pooling of DNA from fecal samples from patients at admission (0)
p1	Pooling of DNA from fecal samples from patients after 5d admitted (1)
PATO	Pangenome Analysis Toolkit
PCA	Principal component analyses
PCR	Polymerase Chain Reaction
PD	Phylogenetic diversity
PG	Plasmid Group
PT	Pulsotype or PFGE-type
PFGE	Pulsed-Field Gel Electrophoresis
PubMLST	Public Databases for molecular typing and microbial genome diversity
QIIME	Quantitative Insights Into Microbial Ecology
R	Resistant to the antibiotic
REDCap	Research Electronic Data Capture
RESCap	Resistome Capture
rMLST	Ribosomal Multi-Locus Sequence Typing
RNA	Ribonucleic acid
rRNA	Ribosomal Ribonucleic acid
S	Susceptible to the antibiotic
SARS-CoV	Severe Acute Respiratory Syndrome-Coronavirus
SNP	Single Nucleotide Polymorphism
ST	Sequence Type
SXT	Trimetoprim-sulfametoxazol (antibiotic, sulfonamide)
TE	Tris-EDTA
TEM	Temocillin (antibiotic)
TEM	Class A β-lactamase, first detected in a patient called Temoniera
TET	Tetracycline (antibiotic)
TOB	Tobramycin (antibiotic, aminoglycoside)
UTI	Urinary tract infection
VIM	Verona-Integron Metallo- β-lactamase (class B β-lactamase)
VRE	Vancomycin-Resistant Enterococci
WHO	World Health Organization
WGS	Whole Genome Sequencing

FIGURES

TABLES

ANNEXES

RESUMEN

La resistencia antimicrobiana (RAM) es uno de los principales problemas de salud pública y global debido a su impacto en la salud, humana, animal y medioambiental. En los últimos años, las dimensiones ambientales de la RAM han adquirido una relevancia notable, ya que el uso de antibióticos en humanos, animales y plantas contribuye al vertido de microorganismos resistentes y antimicrobianos al medio ambiente, aumentando la polución microbiana, creando nuevos reservorios y disminuyendo la biodiversidad microbiana en distintos hábitats. Un tema de interés creciente en el estudio de la RAM es el ambiente hospitalario, especialmente en áreas de alto riesgo como las Unidades de Cuidados Intensivos (UCIs), que favorecen la amplificación, transmisión y evolución de microorganismos multirresistentes. La concentración e interacción de individuos (pacientes y personal médico), la abundancia de reservorios microbianos (agua, superficies, dispositivos médicos), las presiones de selección, y las intervenciones terapéuticas facilitan la transmisión y persistencia de estos microorganismos.

La hipótesis de esta tesis plantea que la adquisición y transmisión de bacterias resistentes a antibióticos (BRAs) y genes de resistencia a antibióticos (GRAs) en UCIs están influenciadas tanto a nivel individual (microbioma del paciente) como colectivo (ambiente hospitalario). Los objetivos de la tesis son: i) evaluar el papel del microbioma intestinal de los pacientes en la transmisión de GRAs dentro de la UCI y ii) analizar la contribución del ambiente hospitalario en la persistencia y diseminación de BRAs y plásmidos RAM, tomando como modelo el patógeno oportunista *Serratia marcescens*. Para ello, planteamos un estudio longitudinal prospectivo llevado a cabo en la UCI del Hospital Universitario Ramón y Cajal entre marzo de 2019 y diciembre de 2021, donde se recogieron muestras clínicas (heces) y ambientales (lavabos, superficies) y se aplicaron técnicas de microbiología clínica convencional, -ómicas (genómica y metagenómica) y análisis bioinformáticos. La tesis se estructura en cuatro capítulos que exploran una *unidad de análisis* (subdividida en pacientes y medioambiente) con diferentes *indicadores* (microbioma/resistoma, especies, clones, plásmidos), aspectos complementarios para la comprensión de la transmisión de la RAM.

El **capítulo 1** analiza la contribución de los pacientes en la aparición y transmisión de RAM en una UCI. El análisis del microbioma de los pacientes, utilizando una estrategia de "muestras agrupadas" de heces ("pooling samples"), reveló que las estancias prolongadas en la UCI alteran significativamente el microbioma gastrointestinal. Los

pacientes recién admitidos (p0) presentaron mayor diversidad alfa y riqueza microbiana que los pacientes de larga estancia (p1), cuya composición microbiana era más heterogénea (diversidad beta). Esto sugiere un efecto notable de las intervenciones y el uso de antimicrobianos, especialmente en los pacientes de larga estancia. En p0 predominaban taxones asociados con una microbiota gastrointestinal sana, como *Clostridiales* y *Ruminococcaceae*, mientras que en p1 dominaban *Enterococcus* y *Staphylococcus*.

El análisis del resistoma mostró un mayor número de GRAs en p0, principalmente de resistencia a macrólidos, tetraciclinas, aminoglicósidos y β-lactámicos. Sin embargo, la presencia de GRAs clínicamente relevantes, como carbapenemasas (*bla*$_{\text{OXA-48}}$, *bla*$_{\text{KPC}}$, *bla*$_{\text{VIM-1}}$), se asoció a brotes epidémicos hospitalarios registrados entre diciembre 2019 a marzo 2020. Estos resultados subrayan el papel de la UCI en la selección y diseminación de patógenos resistentes a antibióticos, capaces de persistir en el microbioma de los pacientes y afectar a la seguridad del paciente aumentando el riesgo de infección o colonización por BRAs.

El ***capítulo 2*** analiza la aparición de BRAs y GRAs que codifican resistencia a antibióticos β-lactámicos de primera elección (cefalosporinas de tercera generación y carbapenémicos) tanto a nivel individual (colonización e infección en pacientes) como colectivo (brotes epidémicos). En las muestras fecales de los pacientes predominaban *Enterococcus*, *Staphylococcus*, *Escherichia coli* y *Klebsiella*. Los episodios de infección, eventualmente acompañados de colonización intestinal, se relacionaron principalmente con neumonías asociadas a ventilación mecánica y traqueobronquitis, siendo *Klebsiella pneumoniae* y *Pseudomonas aeruginosa* resistentes a carbapenémicos los mayores desafíos clínicos. Esto sugiere la contribución de diferentes factores y vías de transmisión cruzada (endógena y exógena) en el desarrollo de infecciones nosocomiales.

El ***capítulo 3*** explora el papel de los reservorios medioambientales en la persistencia y evolución de BRAs, tomando como modelo la bacteria *Serratia marcescens.* El "ambiente hospitalario del paciente" parece contribuir a la transmisión y endemicidad de patógenos. Se observó la coexistencia en lavabos de diversas poblaciones de *Serratia* con gran variabilidad genotípica y fenotípica que se agruparon en un único "*S. marcescens* complex" (SMC) utilizando diferentes herramientas bioinformáticas de clasificación taxonómica. Estas poblaciones, previamente consideradas como distintas especies de este género bacteriano, mostraron variabilidad en la expresión de AmpC, asociada a diferentes fenotipos de sensibilidad, lo que contrasta con la noción tradicional

de resistencia intrínseca a β-lactámicos. El fenotipo "basal-like", previamente descrito en otras especies pero no en *Serratia*, explica la eficacia de los tratamientos contra infecciones por *Serratia* y resalta la importancia de discriminar las poblaciones del SMC en el laboratorio clínico antes de iniciar el tratamiento terapéutico. Las cepas del SMC aisladas de los lavabos presentaron mayor cantidad de plásmidos que las de pacientes. Esto refuerza el papel de los lavabos como reservorios de clones y plásmidos epidémicos de alto riesgo, incluyendo aquellos que codifican carbapenemasas.

El ***capítulo 4*** explora la diversidad, evolución y contexto genético de los plásmidos de resistencia a antibióticos, tomando como modelo un plásmido IncL pOXA-like, uno de los más conservados y endémicos en nuestro hospital. La presencia de variantes similares de IncL que contienen $bla_{\text{VIM-1}}$ o $bla_{\text{OXA-48}}$ (pB77-Csm, pOXA-48) en distintas especies indica un riesgo significativo de transferencia de plásmidos en los lavabos hospitalarios, resaltando su importancia como reservorios abióticos de clones y plásmidos de relevancia clínica.

Esta tesis demuestra la dinámica de la RAM en el ambiente de las UCIs, revelando cómo el microbioma y resistoma de los pacientes evolucionan durante la estancia hospitalaria y contribuyen a modificar el microbioma hospitalario medioambiental. Estos resultados contribuyen a una mejor comprensión de la aparición y transmisión de la RAM en el ambiente hospitalario, y de las rutas de transmisión endógenas y exógenas, orientando el desarrollo de estrategias de intervención más efectivas.

ABSTRACT

Antimicrobial resistance (AMR) is a growing global threat, exacerbated by its multi-centric impact across human, animal, and environmental health systems. The environmental dimensions of AMR have become increasingly apparent as the use of antibiotics in humans, animals, and plants contributes to disseminating resistant microorganisms and antimicrobial agents into the environment, increasing microbial pollution, creating new reservoirs, and reducing microbial diversity across distinct habitats. A growing topic of interest in AMR research is the healthcare-built environment, particularly high-risk areas such as Intensive Care Units (ICUs), which favors the amplification, transmission and evolution of multidrug-resistant microorganisms. The concentration and interaction of individuals (patients and healthcare workers), the abundance of microbial reservoirs (water, surfaces, medical devices), selection pressures, and therapeutic interventions facilitate the transmission and persistence of those microorganisms.

The hypothesis of this thesis is based on the fact that the acquisition and transmission of antibiotic-resistant bacteria (ARB) and antibiotic-resistant genes (ARGs) in ICUs are influenced at both individual (patient microbiome) and collective (hospital environment) levels. The objectives of this thesis are: i) to evaluate the role of the patient gut microbiome in the transmission of ARGs within the ICU, and ii) to analyze the contribution of the hospital environment to the persistence and spread of ARBs and AMR plasmids, using the opportunistic pathogen *Serratia marcescens* as a model. To address this, we developed a prospective longitudinal study conducted between March 2019 and December 2021 in the ICU of Ramón and Cajal Hospital, recovering patient (feces) and environmental (sinks, surfaces) samples and integrating conventional clinical microbiology techniques, -omics (genomics and metagenomics) and bioinformatic analyses. The thesis is structured into four chapters that explore a *unit of analysis* (divided into patients and the environment) using different *indicators* (microbiome/resistome, species, clones, plasmids), providing complementary aspects for understanding AMR transmission.

Chapter 1 analyzes the contribution of patients to the emergence and transmission of AMR in an ICU. The patient microbiome analysis, using a pooled sampling strategy of fecal samples, revealed that extended ICU stays significantly alter the gut microbiome.

Newly admitted patients (p0) showed higher alpha diversity and richness than long-term patients (p1), whose microbial composition became more heterogeneous (beta diversity), likely influenced by medical interventions and antimicrobial use, especially for long-term patients. Taxa associated with healthy gut microbiota, such as *Clostridiales* and *Ruminococcaceae*, were more abundant in p0, while *Enterococcus* and *Staphylococcus* dominated p1.

The resistome analysis revealed higher ARGs in p0, primarily conferring resistance to macrolides, tetracyclines, aminoglycosides, and β-lactams. The presence of clinically relevant ARGs, including carbapenemases (e.g. $bla_{\text{OXA-48}}$, bla_{KPC}, $bla_{\text{VIM-1}}$), was associated with nosocomial outbreaks recorded between December 2019 and March 2020. These findings underscore the ICU's role in selecting and spreading antibiotic-resistant pathogens capable of persisting in the patient microbiome even after hospital discharge, thereby influencing the community ecology of antibiotic resistance and compromising patient safety by increasing the risk of colonization or infection by ARBs.

Chapter 2 examines the emergence of ARBs and ARGs encoding resistance to first-line β-lactams, third-generation cephalosporins, and carbapenems at both individual (colonization and infection in patients) and collective (epidemic outbreaks) levels. We found a predominance of *Enterococcus*, *Staphylococcus*, *Escherichia coli,* and *Klebsiella* in feces. Episodes of infection, often accompanied by intestinal colonization, were primarily linked with ventilator-associated pneumonia and tracheobronchitis, with carbapenemase-producing *Klebsiella pneumoniae* and *Pseudomonas aeruginosa* posing the greatest clinical challenges. This highlights the contribution of multiple factors and cross-transmission routes (endogenous and exogenous) in developing nosocomial infections.

Chapter 3 explores the role of environmental reservoirs in the persistence and evolution of ARBs, using *Serratia marcescens* as a model. The ”patient care environment” contributes to pathogen transmission and endemicity, although its influence has not been extensively studied outside epidemic outbreaks. Diverse genotypic and phenotypic *Serratia* populations coexisted in sinks and were grouped into a single “*Serratia marcescens* complex” (SMC). These populations were previously considered distinct species within this bacterial genus. Variability of AmpC expression associated with different susceptibility phenotypes contrasted with the traditional notion of intrinsic resistance to β-lactams. The “basal-like” phenotype, previously described for other species but not for *Serratia*, explains the efficacy in treating *Serratia* infections and

reinforces the need to identify SMC populations before implementing therapeutic interventions. Counterintuitively, those strains in sinks harbored more plasmids than patient strains. This underscores the role of sinks as reservoirs of high-risk epidemic clones and plasmids, including those encoding carbapenemases.

Chapter 4 investigates the diversity, evolution, and genetic context of antibiotic resistance plasmids, focusing on the highly conserved and endemic IncL pOXA-like plasmid in the hospital. The presence of similar IncL plasmid variants harboring *bla*$_{\text{VIM-1}}$ or *bla*$_{\text{OXA-48}}$ (pOXA-48, p77-Csm) across different species suggests a high level of plasmid mobility across hospital sinks, highlighting their relevance of abiotic reservoirs of clones and plasmids of clinical relevance.

This thesis demonstrates the dynamics of AMR in the ICU environment, revealing how patient microbiomes and resistomes evolve during hospitalization and contribute to modifying the environmental hospital microbiome. These findings enhance our understanding of the emergence and transmission of AMR in hospital settings, as well as endogenous and exogenous transmission routes, guiding the development of more effective intervention strategies.

INTRODUCTION.
INTRODUCCIÓN.

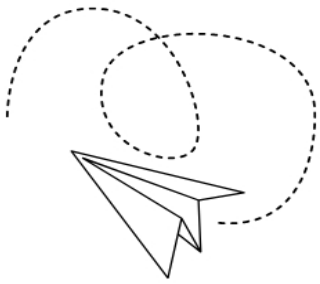

1.1 The Environmental Dimensions of Antimicrobial Resistance

The problem of AMR. Antimicrobial resistance (AMR) is recognized as one of the top ten Global Health challenges of the 21st century, requiring a multidisciplinary approach and involving major economic sectors, including pharmaceutical, agriculture, food industry, and healthcare (EClinicalMedicine, 2021). Antimicrobials are agents intended to kill or inhibit the growth of microorganisms, which include antibiotics, fungicides, antiviral agents, and parasiticides (United Nations Environment Programme, 2023). Some heavy metals, disinfectants, antiseptics, other pharmaceuticals, and some natural products may also have antimicrobial properties. Antimicrobials are widely used in healthcare for humans and animals, as well as in agriculture for crops and animal production. AMR occurs when microbes (such as bacteria, viruses, fungi, and parasites) develop the ability to adapt against the effects of an antimicrobial to which they were initially susceptible. As a result, antimicrobials become less effective, making infections more challenging to treat in patients and animals. This can lead to increased morbidity and mortality rates and a risk of spreading resistant microbes (EClinicalMedicine, 2021).

According to recent reports from 2019, 4.95 million deaths were associated with drug-resistant infections, of which 1.27 million were directly attributable to drug-resistance (Antimicrobial Resistance Collaborators, 2022). Six pathogens were responsible for more than 250,000 deaths associated with AMR (*Escherichia coli, Staphylococcus aureus, Klebsiella pneumoniae, Streptococcus pneumoniae, Acinetobacter baumannii,* and *Pseudomonas aeruginosa*) and have been identified as priority pathogens from the World Human Organization (WHO) (WHO Bacterial Priority Pathogens List, 2024). The list was intended to inform research and development priorities related to pathogens with multidrug resistance that cause severe and often deadly infections in healthcare settings. Carbapenem resistance in Gram-negative bacteria (e.g. *Enterobacteriaceae, Pseudomonas, Acinetobacter*) saw a substantial increase in attributable burden from 1990 to 2021. Under the alternative scenario in which new antimicrobials are developed for Gram-negative bacteria, a forecasted 11.1 million AMR deaths were reported to be averted by 2050, in which AMR burden is forecasted to increase to 8.22 million associated deaths and 1.91 million attributable deaths (Antimicrobial Resistance Collaborators, 2024).

Research on AMR has traditionally focused on antibiotic-resistant bacteria (ARB) isolated from healthcare facilities, where they often cause patient infections. However,

the emergence and spread of AMR also involve animals and plants and the interfaces between these organisms and their environments (United Nations Environment Programme, 2023). Thus, most ecosystems contribute to AMR's emergence, acquisition, and spread (Berendonk *et al.*, 2015), making it necessary to approach the problem under the perspective of One Heath (United Nations Environment Programme, 2023).

The Environmental Dimension of AMR. Microorganisms, especially bacteria, can acquire resistance to antibiotics in water, soil, and air by contact with resistant microbes that may have evolved naturally or have been introduced into the environment through human and/or animal waste containing antibiotic resistant genes (ARGs) (Berendonk *et al.*, 2015). When antimicrobials are released into the environment, even at sub-inhibitory concentrations, they can select resistant microorganisms and contribute to the emergence of new AMR genes. Water systems such as rivers, lakes, and oceans, which accumulate drug and microbial pollution over time, may harbor microorganisms enriched in ARGs and/or evolve towards AMR and, afterwards, become a source of AMR spread to different One Health sectors (United Nations Environment Programme, 2023). This is why AMR requires a response based on a comprehensive systems perspective, such as “One Health,” an integrated, unifying approach that aims to sustainably balance and optimize the health of people, animals, and global ecosystems (Hernando-Amado *et al.*, 2019). This shift from traditional sector-specific epidemiological surveillance based on individual cases to genomic-enhanced surveillance on a One Health perspective provides more precise risk assessments and expands the prevention and control of infection across sectors (Dalton *et al.*, 2020; Struelens and Ludden, 2024). Understanding the “hospital antibiotic-resistant environment”, which refers to the sum of conditions that surround patients at a given space and time including pathogens, is crucial to implementing integrated, efficient interventions and public health strategies to fight AMR (Coque *et al.*, 2023). All anthropogenic policies in every sector have an influence on health that should be substantiated (Health-in-all-Policies) (PAHO, 2024), and the policies influencing the microbiosphere affect antibiotic resistance that requires continuous surveillance.

1.2 Surveillance of Antimicrobial Resistance

Measuring AMR involves tracking the prevalence and spread of ARBs and ARGs across different environments, populations, and healthcare settings. However, much of the available data comes primarily from hospital records and, more recently, from data obtained in farms, which feed local and regional surveillance systems. The information on AMR is typically derived from a few sources using similar indicators, methodologies, and models for different purposes (Coque *et al.*, 2023). To assess how well a test or indicator is working (validity) and the consistency of the measurement (reliability), it is crucial to carefully choose "units of analysis" and "indicators" and understand how to measure AMR.

The ***unit of analysis*** in AMR refers to the sample of study and may correspond to disparate human groups (from single individuals to social, professional, or health-risk groups), healthcare settings (tertiary, secondary, primary, or single wards), economic (One Health, economic growth sectors) and environmental (sewage ad water treatment facilities) sectors (Coque *et al.*, 2023), and even animals and plants. Traditionally, populations are analyzed at tertiary (hospitals) and secondary healthcare centers (long-term care facilities), where the concentration of high-risk groups of people and life-sustaining equipment (e.g. ventilators), indwelling catheterization, and frequent drug use facilitate the emergence and spread of AMR. Within hospitals, some wards concentrate on groups and factors at higher risk than others, such as the Intensive Care Units (ICUs).

A wide range of ***indicators*** exist in AMR surveillance. In hospitals, they mainly refer to the percentage of pathogens resistant to a particular antibiotic (pathogen–antibiotic pairs) at particular sites, the proportion of healthcare-associated infections (HAIs) with AMR cases in population-based studies as markers for significant emergent threats, and the density of antimicrobial use and/or consumption as drivers of AMR (Coque *et al.*, 2023). Some bacterial species acquire and spread ARGs that confer resistance to first-line antibiotics and are included in the priority pathogen lists of the WHO, which includes opportunistic pathogens of the taxonomic groups of *Enterobacterales*, *P. aeruginosa,* enterococci, and staphylococci (WHO Bacterial Priority Pathogens List, 2024). However, none of these "watch lists" considers the heterogeneity within a species from which certain lineages or clones can contribute more significantly to transmitting ARGs within the bacterial community (Riley, 2014; Rodríguez *et al.*, 2021; Aracil-Gisbert *et al.*, 2024). Diversity within clonal complexes with periodic

emergences of new genotypes enables the permanence of bacterial intraspecies diversity that makes it difficult to rank and predict the risks of critical sub-populations. Genomic typing to track AMR and outbreak investigations is progressively implemented in national and international surveillance programs, demanding a high level of agreement between genotypes and phenotypes (European Centre for Disease Prevention and Control, 2021).

Recent evidence indicates that water systems (e.g. sinks and other drains) in healthcare facilities can become contaminated with multidrug-resistant organisms (MDROs), which cause up to one-third of HAIs (Perkins *et al.*, 2019; European Centre for Disease Prevention and Control, 2024a). They include non-Legionella water opportunistic pathogens such as *Enterobacterales* (*Klebsiella* spp., *Serratia marcescens*), *P. aeruginosa* or *A. baumannii* which are within the WHO list of priority pathogens (European Centre for Disease Prevention and Control, 2024a). All these species are often isolated from water systems during and beyond outbreaks, and recently *S. marcescens* has been persistently able to be maintained in hospital water reservoirs (Kizny Gordon *et al.*, 2017; Aracil-Gisbert *et al.*, 2024; Kim *et al.*, 2024). Its capacity to acquire carbapenemases and survive in water, soils, and the rhizosphere offers an excellent model to analyze the consequences of the wide range of interactions among biotic and abiotic elements (**Figure 1**) (Aracil-Gisbert, Baquero and Coque, 2024).

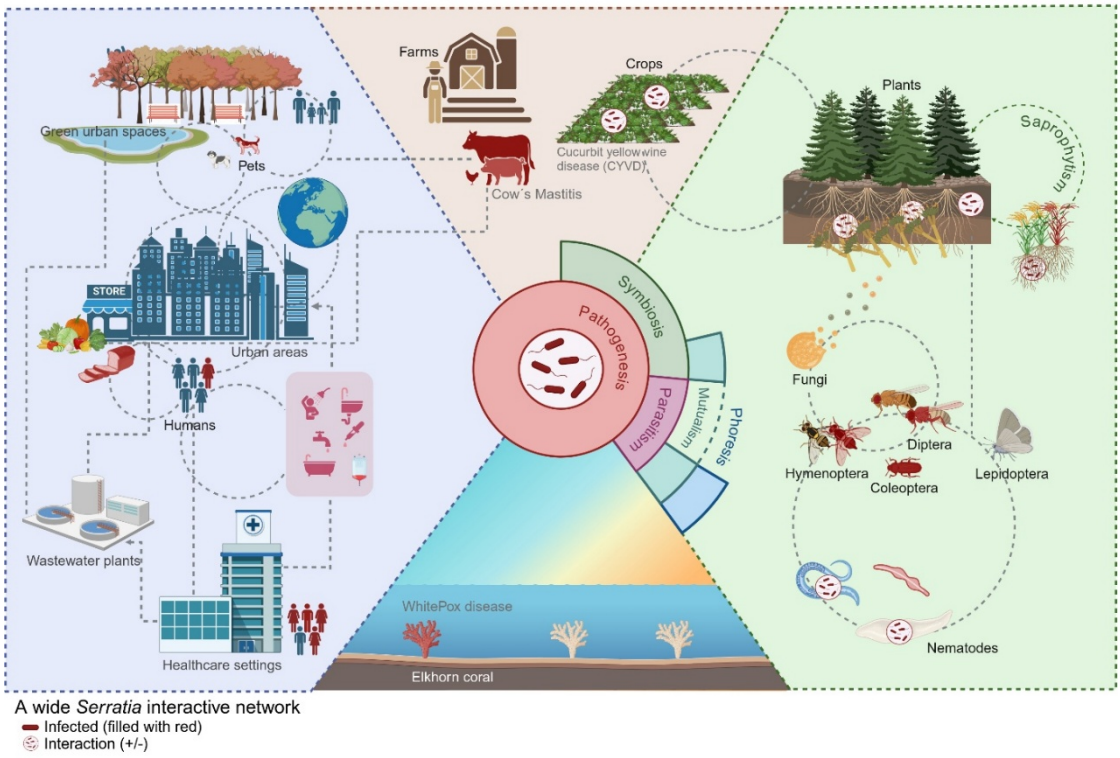

Figure 1 | The interactive network of *S. marcescens,* an environmental opportunistic pathogen able to establish different microbial interactions.

The molecular epidemiology of ARGs within human, animal, or environmental backgrounds, and the mobile genetic elements (MGEs) on they are located, such as plasmids, transposons, integrons, or insertion sequences, reveals the promiscuity of the genetic determinants encoding AMR. This exchange of genetic material often results in complex mosaic elements, which complicates the accuracy and interpretation of diagnostic and surveillance results and the identification of transmission pathways (Coque *et al.*, 2023).

Metagenomics and genomics represented novel approaches to studying the distribution of ARGs in human and environmental microbiome. These methods help to study relevant traits such as the genomic contexts and the mechanisms that drive the selection of specific ARGs (Berendonk et al., 2015). Other relevant and still unexplored microbiomes are those associated with the built environment (Gilbert and Stephens, 2018). Within this, the "hospital-built environment", is an issue of increasing interest in research agendas to understand the emergence, transmission and persistence in the healthcare network (Dalton *et al.*, 2020; Coque *et al.*, 2023).

1.3 The Hospital Built Environment

The "hospital-built environment" refers to the structure of the inpatient care environment (buildings and wards) along with fixtures, fittings, and furniture (Dalton *et al.*, 2020). It also includes surrounding areas accessible to patients (communal reception areas, gardens, and other outside spaces), patients' belongings, and items that can act as microbial reservoirs or provide anchor points for cross-transmission. A hospital ward microbiome consists of the combined microbiomes of patients, healthcare workers, and water systems, all of which coexist, interact, and evolve, affected by the building confinement (**Figure 2**). Selective pressures such as the overall use of antimicrobials and antiseptics or breaching infection control measures may contribute to the spread and/or maintenance of ARBs (Mahnert *et al.*, 2019).

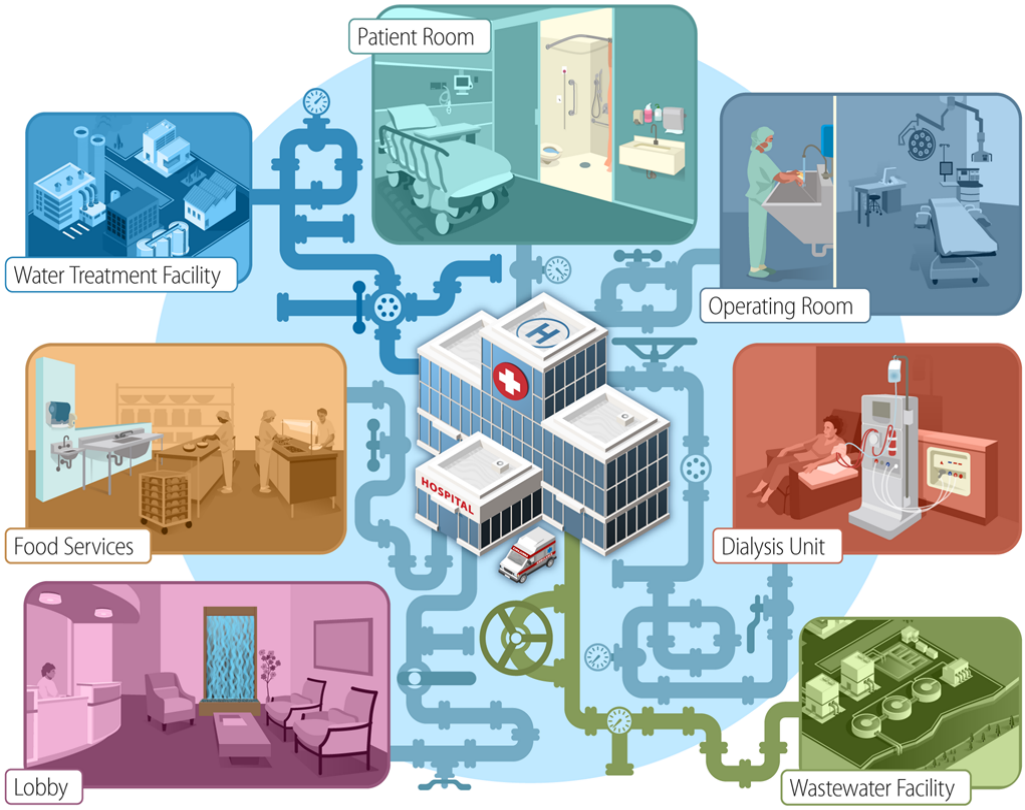

Figure 2 | The hospital built environment.
Source: Centers for Disease Control and Prevention (CDC) (European Centre for Disease Prevention and Control, 2024a).

Contamination of high-touch surfaces with MDROs such as methicillin-resistant *Staphylococcus aureus* (MRSA) or vancomycin-resistant enterococci (VRE) (Knelson *et al.*, 2014; Freedberg *et al.*, 2022), as well as contamination of water systems with Gram-negative bacteria such as *Enterobacterales* (e.g. *S. marcescens, K. pneumoniae*) or *P. aeruginosa* (Kizny Gordon *et al.*, 2017; Diorio-Toth *et al.*, 2023; Aracil-Gisbert *et al.*, 2024), is well documented during outbreak situations. Infection prevention and control measures may mitigate cross-transmission of MDROs between patients and their close environment to minimize potential outbreaks (Kizny Gordon *et al.*, 2017).

Patient occupancy influences the global environmental conditions (e.g., temperature, relative humidity, use of conditioned air systems, healthcare worker contacts, frequency of use of medical devices) as well as the abundance and composition of human-associated microbial communities in the patient rooms and nurse stations (Ramos *et al.*, 2015). Indeed, humans are the predominant source of colonizing microbes in the hospital setting, with the gut being a substantial reservoir of MDROs, particularly in patients receiving antibiotics (Wellington *et al.*, 2013). It has been suggested that the

risk of acquiring HAIs increases for patients admitted to a room previously occupied by an infected or/and colonized patient, even after disinfection (Mitchell et al., 2015). The longer a patient stays, the more closely the room's microbiota resembles that of the patient. The presence of highly diverse, stable, and beneficially designed microbiomes inside healthy buildings could result in lower exposures to resistances in the future (Mahnert *et al.*, 2019). Several interventions to mitigate the spread of AMR must be addressed in various ways to reduce the absolute number of ARB, limit transmission, and support the maintenance and restoration of susceptible populations (Baquero *et al.*, 2015).

1.4 Transmission pathways for AMR in the hospital setting

Most ARBs of clinical relevance are primarily colonizing opportunistic pathogens (COPs) that can be spread through different transmission routes, potentially leading to their uptake and subsequent carriage, colonization, or even disease in humans (Price *et al.*, 2017; Huijbers, Flach and Larsson, 2019). In hospitals, ***cross-transmission***, defined as the spread of microorganisms in the healthcare setting, occurs through direct contact (patient to patient, via healthcare workers), indirect contact (contaminated surfaces or objects, devices, reservoirs, sinks), and air (**Figure 3**). Patient-to-patient transmission is a prominent mechanism for the emergence of ARB, especially in ICUs. From a theoretical perspective, with ICU patients confined to their beds, ARB spread predominantly as a vector-borne disease, with the temporarily contaminated hands of healthcare workers acting as vectors (Bonten, 2012). Proper hand hygiene before and after patient contact and barrier precautions reduce the likelihood of hands becoming contaminated. However, the capacity and resources of the healthcare setting can influence the spread of ARB, particularly when clinical staff are managing increasing patient loads. Cleaning procedures (Verhougstraete *et al.*, 2024), hospital size, patient density, clinical staff actions, and differences in individual transmitter abilities (Del Campo *et al.*, 2019) are critical in spreading and colonizing bacteria.

The likelihood of new patients becoming colonized by an ARB due to the presence and density of already colonized patients and environment in a first contact is called ***colonization pressure*** (Bonten, 2012). Some patients may acquire MDROs that were present in the room before their admission, indicating cross-transmission through the "contaminated" environment and the patient (Dalton *et al.*, 2020). Several factors influence ARB transmission between environmental reservoirs (abiotic surfaces or water

sinks) and ICU individuals (patients and clinical staff), such as infection control policies or the type of surface material (e.g. porous or non-porous), fixtures and water infrastructures (Plipat *et al.*, 2013) or the proximity of medical devices and environmental reservoirs (Aracil-Gisbert *et al.*, 2024). The plethora of reservoirs and the continuous patient and clinical staff turnover greatly difficult identifying the source of bacterial contamination responsible for outbreaks and HAIs.

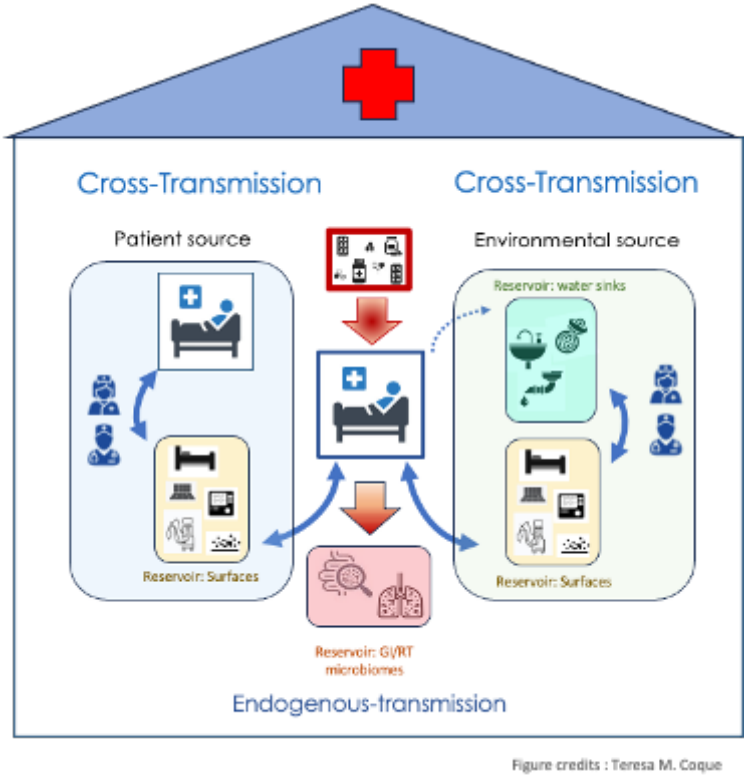

Figure 3 | Transmission pathways in a hospital ward

The overuse of antibiotics and sanitation protocols in hospitals can exert selective pressure on microorganisms, promoting the survival of those resistant to common disinfectants and antimicrobial agents (Dalton *et al.*, 2020). The more frequently these products are used, the more likely resistant organisms are to survive in colonized areas inside or outside the host, outcompeting susceptible ones (Baquero *et al.*, 2024). The *endogenous transmission* refers to the spread of ARGs within a bacterial population in a colonized patient (León-Sampedro *et al.*, 2021), facilitated by horizontal gene transfer of ARGs, which includes conjugative transfer via MGEs, transformation via uptake of naked DNA, cell-to-cell gene transfer by microvesicles, and transduction via bacteriophages (Hernando-Amado *et al.*, 2019; Liu *et al.*, 2022). Specifically, conjugative gene transfer

mainly relies on circular plasmids that act as shuttles and reservoirs of ARGs, transposons, and integrons (Li *et al.*, 2024). In fact, the proliferation and dissemination of ARB owing to selective pressures exerted by antimicrobial compounds is primarily the main causative agent of transmission of ARGs (Hernando-Amado *et al.*, 2019).

Many microorganisms producing antibiotics are found in natural environments, and ARBs can be selected at very low antibiotic concentrations (Andersson and Hughes, 2012). An increase in the proportion of ARB can be indicative of the selection pressure (Huijbers, Flach and Larsson, 2019), in which the larger the ecosystem exposed to antibiotics, such as in hospitals, the higher the possibility of colonizing and infecting human populations. Some hospital practices are intended to reduce the antimicrobial exposure experienced by ***bystander*** microorganisms, which are not the treatment targets but are selected as "collateral damage" of therapeutic interventions. Overgrowth of these ***off-target*** resistant microbes can disrupt the normal microbiota and lose the ***colonization resistance*** (van der Waaij, Berghuis-de Vries and Lekkerkerk-v, 1971), promote antimicrobial resistance within the patient's microbiome, or increase the risk of transmission of antibiotic-resistant microorganisms between individuals (Morley, Woods and Read, 2019).

HYPOTHESIS AND OBJECTIVES.
HIPÓTESIS Y OBJETIVOS.

The risk of acquiring and transmitting opportunistic bacterial pathogens in hospitals is especially high in ICUs. Such risk is associated with the patient's individual characteristics (e. g. severity, genetics, frailty associated with severe underlying diseases, natural or iatrogenic immunodeficiencies) and external local factors (e. g. antibiotic exposure, non-antibiotic therapy, supine position, parenteral nutrition, use of ventilators, local demographic factors, local interventions, ward architectural design). These factors also influence the structure and function of the intestinal microbiota at both the individual (resistance/susceptibility to antimicrobials) and the collective level (increasing colonization pressure). Key issues such as AMR selection, transmission, and persistence in hospitals remains poorly understood. This is due to the scarcity of comprehensive longitudinal studies with information before and after implementing interventions, limitations of available tools to analyze resistomes accurately, and the reductionistic nature of antimicrobial surveillance, which typically focuses on isolates from patients with severe infections and/or therapeutic failures.

The **working hypothesis** of this thesis is that the acquisition and transmission of ARBs and ARGs in ICUs are influenced by the "patient-care microbial environment", which comprises both the patient microbiome/resistome and the hospital-built microbiome.

The **main objective** of this thesis is to address some critical knowledge gaps that facilitate the transmission of AMR (ARBs and ARGs) at both the individual (patients) and collective (ICU) levels.

The **specific objectives** are:

1) To evaluate the contribution of the patient microbiome/resistome to the transmission of ARGs in the ICU environment (**Chapter 1**)
2) To establish the dynamics of ESBL and carbapenemase genes in the ICU environment (**Chapter 2**)
3) To assess the contribution of the "hospital-built environment" of the ICU to the transmission and persistence of ARBs, based on the single-model organism *S. marcescens* shared by patients and built-environment (**Chapter 3**)
4) To analyze the influence of the "hospital-built environment" on the transmission and persistence of AMR plasmids, based on the single-model plasmid IncL pOXA-like (**Chapter 4**)

MATERIAL AND METHODS.
MATERIAL Y MÉTODOS.

3.1 The Study Design

This thesis work was developed within a prospective and longitudinal study conducted in the large Intensive Medicine ICU of the Ramón and Cajal University Hospital (HURyC), a 1,200-bed tertiary hospital in the Northern area of Madrid (Spain), the top center of a public health system attending a population of 600,000 inhabitants. The ICU comprises 14 patient rooms, one nurse control, two nurse lounges, two dirty hospital rooms, two storage rooms, one pharmacy room, and one office for the clinical staff, each fully equipped with all the necessary instruments (**Figure 4**).

The study was divided into three periods based on demographics and operational changes in this ICU area: **period A**, when the ICU operated normally (March 2019 to March 2020); **period B**, after SARS-CoV-2 quarantine and thus harboring with SARS-CoV-2 patients (July 2020 to February 2021); and **period C**, in which the area was emptied of patients and remodeled for other hospital uses (March 2021 to December 2021).

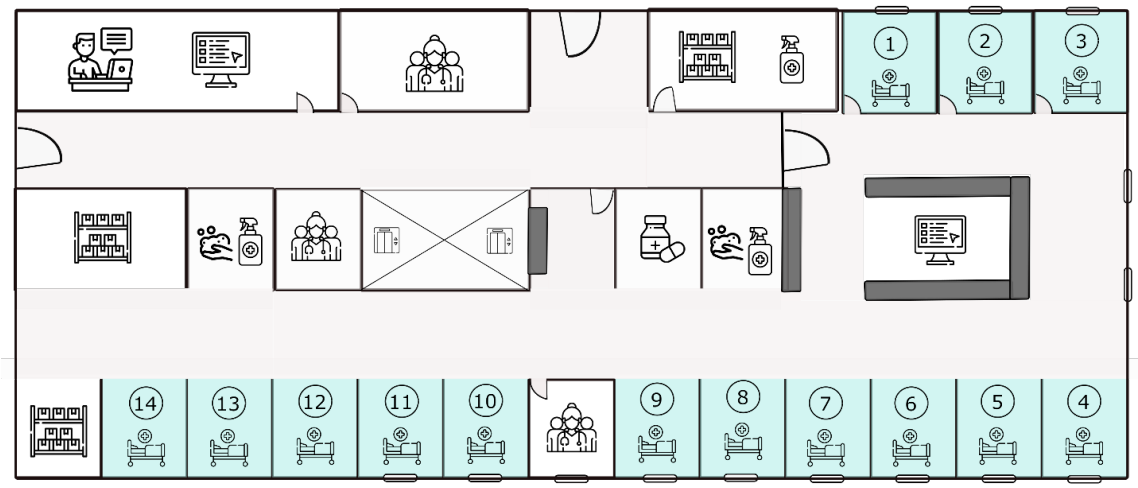

Figure 4 | ICU area during the study period (March 2019- December 2021).
The ward includes common elements found in ICUs, such as patient rooms, nursing stations, a monitoring area, and utility rooms.

3.2 Sampling and processing

This work analyzed patient and environmental samples.

Patient sampling. All patients admitted to the Intensive Medicine ICU at HURyC during period A were included in the study (n=349). However, due to the SARS-CoV-2 pandemic and the displacement of the ICU unit to another floor, the sampling was not continued for further periods. Patient's stools were collected daily during period A (>5 g of feces) from admission to discharge using disposable containers (DDBiolab, Barcelona, Spain) or Flexi-Seal™ FMS (Convatec, London, United Kingdom), and samples were stored at -20ºC until processing. Then, those patient samples were categorized per week according to the patient's stay length into two groups: i) "group 0" comprising **newly admitted patients** (samples collected at 0-5 days at admission), and ii) "group 1" comprising **long-term patients** (samples collected from 5 days at admission). One sample per patient per week was selected from those groups for DNA extraction and culturomics. Individual patient and pooled samples (see section **3.8**) were analyzed during this thesis.

Patient demographics and clinical and epidemiological metadata were collected by collaborating physicians and managed using REDCap (Research Electronic Data Capture) (https://www.project-redcap.org/), hosted at the Bioinformatics Unit of HURyC. REDCap (Research Electronic Data Capture) is a secure, web-based software platform designed to support data capture for research studies, providing 1) an intuitive interface for validated data capture; 2) audit trails for tracking data manipulation and export procedures; 3) automated export procedures for seamless data downloads to common statistical packages; and 4) procedures for data integration and interoperability with external sources (Harris *et al.*, 2009, 2019).

Environmental sampling. Environmental samples were recovered during periods A, B, and C. We sampled "wet" abiotic samples, consisting of sinks (surface, drainage, and p-trap) and "dry" abiotic samples (bed rails, ventilator's touchscreen, and pot) (**Figure 5**). Room and sink surfaces were sampled with polyurethane sponges placed in a sterile bag impregnated with 10 mL HiCap Neutralizing Broth (EZ-10HC-PUR, EZ Reach™ Sponges, World Bioproducts, Bioing sro, Czech Republic). Sink drainage and p-trap samples were collected using standard sterile swabs and aspiration probes, respectively. Samples were immediately processed by culturomics.

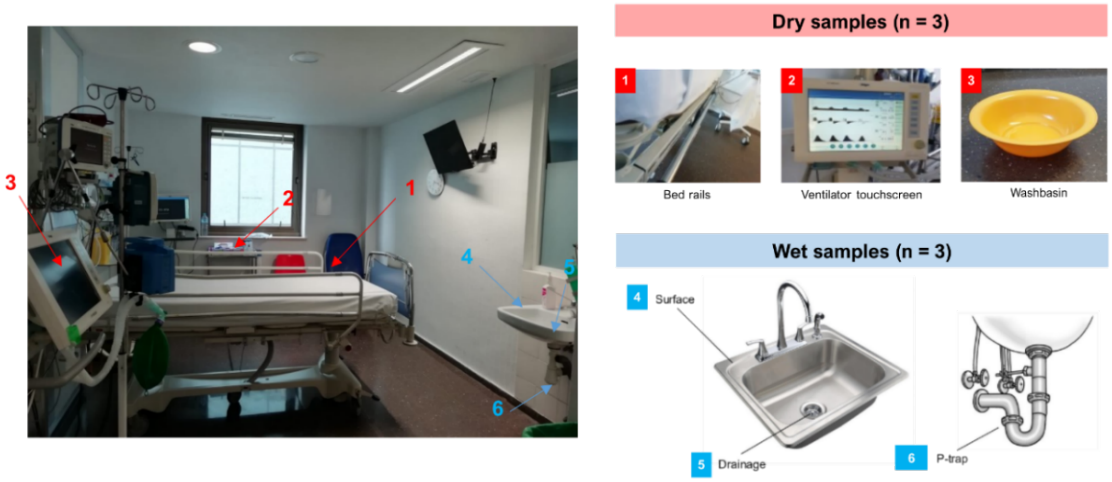

Figure 5 | ICU room with the sampling points from both dry and wet samples.

3.3 Bacterial isolates

This thesis was based on clinical and environmental bacterial isolates recovered during the prospective study described in section **3.2**, as well as clinical isolates independently collected from the Microbiology Department at HURyC as part of their routine diagnostic and surveillance activities and stored in their strain collections. They were used for comparative genomic analysis in sections **4.3** and **4.4**.

For section **4.3,** which analyzes the hospital population dynamics of *Serratia*, we included 66 environmental *Serratia* isolates (our prospective study) and 98 clinical *Serratia* isolates collected through the years in the Microbiology Department. They include 93 blood isolates causing individual episodes of BSI between 2003 and 2016 (Pérez-Viso *et al.*, 2024), and five clinical isolates (two broncho-aspirates, two wound exudates, and one bone sample) involved in hospital outbreaks of VIM-1 and OXA-48 producers between 2016 and 2018 (Pérez-Viso *et al.*, 2021).

For section **4.4**, which analyzes the diversity of plasmids carrying carbapenemase genes, we included 25 isolates of different species of *Enterobacterales* carrying IncL-*bla*$_{\text{VIM-1}}$ and IncL-*bla*$_{\text{OXA-48}}$ plasmids. They were recovered during our prospective longitudinal study, and also from polyclonal plasmid outbreaks in our institution for years (Tato *et al.*, 2010; Pérez-Viso *et al.*, 2021), coming from the strain collection of the Microbiology Department.

3.4 Culturing and Identification

Fecal samples were suspended into 0.9% NaCl at a 1:2 ratio, vortexed, and 60-120 µl was inoculated into different culture media (**Table 1**). Plates were incubated at 37ºC for at least 48-72h. Environmental sponge samples from the environmental surfaces were plated by spreading the sponge into the plates. Then, the plates were incubated for 48h at 37ºC. Colonies of different morphotypes (size, color, and shape) for both types of samples were subcultured and then incubated for 24h at 37ºC.

Bacterial identification was performed using MALDI-TOF Biotyper® (Bruker), enabling rapid and unbiased microorganism identification down to the species level within minutes. Bacterial colonies were transferred to the target titanium plate using a tip. When colony morphologies suggested the presence of a Gram-positive bacteria, 1µl of formic acid was added. Finally, a volume of 0.7µl of the α-cyano-4-hydroxycinnamic acid (HCCA) matrix substance included in the manufacturing instructions is added to each plate's colonies. The equipment employed was MALDI-Biotyper Realtime (Bruker Daltonics, Germany), and the spectrum was analyzed with the FlexControl 3.0 software, comparing the spectrum with the database. A reliability score of >2 was considered for species bacterial identification.

Bacterial isolates were stored at -80°C in 1,500 µl of LB broth + 15% glycerol until analysis.

Table 1 | Culture media

Media	Classification	Identification target	Commercial brand, City, Country	Type of sample or use	Notes
HiChrome™ UTI Agar	Differential, non-selective	Gram-negative and Gram-positive	HiMedia, Modautal, Germany	Feces	
Difco™ mEnterococcus agar	Non-differential, selective	VRE	Beckton Dickinson, New York, United States	Feces	Supplemented with 4mg/ml Vancomycin
CHROMagar™ ESBL Biplate	Differential, selective	ESBL producers, Gram-negative	Beckton Dickinson, New York, United States	Feces, Water, Environmental	
CHROMagar™ mSuperCARBA™	Differential, selective	Carbapenemase producers, Gram-negative	Beckton Dickinson, New York, United States	Feces, Water, Environmental	
CHROMagar™ Orientation	Differential, non-selective	Gram-negative and Gram-positive	Beckton Dickinson, New York, United States	Water, Environmental	
Lysogenic Broth (LB) Lennox Agar or Broth*	Non-differential, non-selective	Gram-negative	Condalab, Madrid, Spain	Bacterial isolation	
BBL™ Mueller Hinton II Agar or Broth, Cation adjusted	Non-differential, non-selective	Gram-negative	Beckton Dickinson, New York, United States	Antibiotic susceptibility	

*The difference of these culture media with the conventional Luria-Bertani medium is the sodium chloride concentration (5 g/L vs 10 g/L, respectively).

Abbreviations: UTI (Urinary tract infection), VRE (Vancomycin-resistant enterococci), ESBL (Extended-spectrum beta-lactamase).

3.5 Antibiotic susceptibility

Antibiotic susceptibility testing (AST) defines the *in vitro* activity of an antibiotic against a bacterial population. AST was applied to different antimicrobial agents in the collection of microorganisms studied using disk diffusion and minimum inhibitory concentration (MIC) methods. Other phenotypic and genotypic assays were performed to characterize β-lactam mechanisms of resistance: AmpC β-lactamase expression induction tests, and PCR to screen the presence of genes encoding ESBLs and carbapenemases.

Disk-diffusion. This technique, also known as the agar diffusion test or Kirby-Bauer test, uses paper discs impregnated with a specific concentration of antibiotics, which are placed on a Mueller Hinton (MH) plate inoculated with a bacterial suspension of 0.5 McFarland in physiological saline (equivalent to $1.5x10^8$ CFU/ml). These plates were incubated at 37ºC for 16-20 hours. Afterward, we measured the diameter of the growth inhibition zone (in mm) and compared these sizes to databases, categorizing the antibiotic susceptibility into susceptible (S), intermediate (I), or resistant (R) following CLSI (CLSI, 2023) and EUCAST (https://www.eucast.org/mic_distributions_and_ecoffs/) guidelines. The disk diffusion test cannot differentiate bacteriostatic and bactericidal activity. The antibiotics tested were amoxicillin-clavulanic acid (AMC, 20/10 µg), ampicillin (AMP, 10 µg), cefoxitin (FOX, 30 µg), ceftazidime (CZD, 10 µg), cefotaxime (CTX, 5 µg), cefepime (FEP, 30 µg), aztreonam (ATM, 30 µg), temocillin (TEM, 30 µg) and meropenem (MEM, 10 µg). Non-β-lactams were also studied as follows: ciprofloxacin (CIP, 5 µg), chloramphenicol (CHL, 30 µg), gentamicin (GMN, 10 µg), tobramycin (TOB, 10 µg), tetracycline (TET, 30 µg) and sulfamethoxazole-trimethoprim (SXT, 25 µg).

MIC methods. The most common methods for determining MIC are agar dilution, broth dilution, and the Epsilon test (E-test). We used broth microdilution using commercial MicroScan panels (Beckman Coulter, Nyon, Switzerland). The antibiotics tested were AMP, AMC, CTX, CAZ, FEP, AZT, MEM, imipenem (IMI), ertapenem (ERT), GMN, TOB and CIP. E-test serves to quantitatively determine the MIC using an impregnated plastic strip with a pre-establish gradient of antibiotic placed on an inoculated plate with a bacterial suspension of 0.5 McFarland in physiological saline and incubated at 37ºC for 16-20 hours. The antibiotics tested were AMC, FOX, MEM, and CZD.

Production of ESBLs and carbapenemases. We employed the Double Disk Synergy Test (DDST), Hodge test, and PCR confirmation for ESBL and carbapenemase production. DDST was used to detect ESBLs in which two disks of antibiotic (inhibitor of β-lactamase and cephalosporin) were placed 20-30 mm from a previously inoculated plate with a bacterial suspension. We combined AMC (20/10 µg) with CTX (5 µg), CZD (10 µg), FEP (30 µg), or ATM (30 µg) (Kaur *et al.*, 2013). Plates were incubated at 37ºC for 16-20h, and any deformation of the inhibition halos in the antibiotic interaction space of the plate was recorded. Hodge test was used to detect the presence of carbapenemases. A carbapenem-containing disk was placed in the center of an inoculated plate with a bacterial suspension of a susceptible strain (e.g., *E. coli* ATCC25922). The testing strain is streaked from the edge of the disk towards the edge of the plate, forming straight lines of bacteria. The plate is incubated at 35ºC for 16-20h. The growth of the susceptible strain in the vicinity of the tested strain was recorded. The antibiotic contained in the plates was MEM (10 µg). PCR screening confirmed the ESBL and carbapenemase genes of phenotypically suspected carbapenemase production (see section **3.9**).

Induction of AmpC β-lactamases. The induction of the AmpC β-lactamase was measured using an inoculated plate with a bacterial suspension of the tested microorganism. Two types of antibiotic disks are placed: an inducer of AmpC production (e.g., IMI or FOX, strong and medium inducers, respectively) and indicators of hydrolysis of antibiotic (e.g. aminopenicillin, 2GC or 3GC) (Dunne and Hardin, 2005; Gupta, Tak and Mathur, 2014). We employed FOX (30 µg) and IMI (10 µg) confronting AMC (20/10 µg), CZD (10 µg), and CTX (5 µg).

3.6 DNA extraction

We extracted genomic DNA from clinical stool samples and bacterial strains using different methods and commercial kits. Conventional DNA extraction protocols use lytic agents such as heat, alkaline solutions, and/or detergents. Commercial kits combine those procedures with specific beads to disrupt and homogenize samples and/or columns to purify DNA. This method allows for obtaining high-purity DNA, high yield, and stability.

For ***fecal samples***, 250 mg of stools were *in situ* extracted using the QiAmp PowerFecal Pro DNA kit (Qiagen, Venlo, The Netherlands) following manufacturer instructions. The kit uses novel bead tubes with optimized chemistry for efficient bacterial lysis and streamlined inhibitor removal technology. Cell lysis occurs by mechanical and

chemical methods using manufacturer buffers and homogenization via Vortex Adapter to Vortex-Genie 2 (Qiagen, Venlo, The Netherlands), and further inhibitor removal and DNA isolation are conducted using manufacturer MB Spin columns with buffer.

For ***bacterial monocultures,*** we used a solution-based method using Wizard® Genomic DNA Purification Kit (Promega, Fitchburg, USA) that was employed for Gram-negative bacteria following manufacturer instructions. It employs a sample-based method from one ml of an overnight bacterial culture on LB Broth that was pelleted and lysed using heat and lysis solution. For PCR screening of bacterial isolates, a boiling method was often employed by diluting one to two colonies into TE and boiling them in a thermal block for ten minutes.

Genomic DNA from pure bacterial cultures was used for PCR gene screening and genomics, and stool samples were used for metagenomics.

3.7 DNA quantification

DNA quantification was performed using fluorometry, spectrophotometry, and electrophoresis, employing the Qubit fluorometer, the NanoDrop spectrophotometer, and the TapeStation, respectively. They have distinct advantages and limitations.

Fluorometry. The **Qubit™ 3 Fluorometer** (Invitrogen, ThermoFisher, Waltham, USA) was used to measure the specific DNA concentrations using the manufacturer's Broad Range and High Sensitivity reagents. This fluorescence-based technology provides highly sensitive and specific DNA quantification by utilizing DNA-binding dyes that emit fluorescence proportional to the amount of DNA present. It is particularly useful for samples with low concentrations of DNA, offering higher sensitivity.

Spectrophotometry. The **NanoDropTM 2000/2000c Spectrophotometer** (ThemoFisher, Waltham, USA) was used to measure DNA purity. It quantifies DNA by measuring absorbance at 260 nm, providing a rapid and straightforward assessment of DNA concentration and purity by calculating 260/280 and 260/230 ratios. However, it is less sensitive than Qubit and can be affected by contaminants such as proteins and phenol.

Electrophoresis. The **TapeStation 2200** (Agilent, Waldbronn, Germany) measured the DNA quality, integrity, and fragment length of the pooled DNA samples. This method combined capillary electrophoresis with a fluorescence-based detection system, which provides a detailed DNA integrity number (DIN) that quantifies the level of DNA

degradation and ensures sample quality. Together, these techniques complement each other, providing a comprehensive understanding of DNA concentration and purity.

Together, these techniques complement each other, providing a toolbox for measuring DNA concentration and purity.

3.8 DNA pooling design

Pooled testing is a screening approach that combines DNA samples from different people into a single test, reducing labor loads and material expenditures. The pooled DNA sample is tested first for the presence of the desired genetic target, and, if the result is negative, all DNA aliquots in the pool can be considered as negative, saving the cost of testing each DNA sample separately. In this work, we used this approach not only to rapidly screen for the presence of genes of interest in clinical practice but also to analyze the entire microbiome input of patients admitted to an ICU weakly.

To do that, we classified the stool DNA samples according to the patient's stay within five days of admission (group 0) and samples from patients for more than five days (group 1) (see section **3.2**). We combined them in pools by mixing equimolar DNA concentrations by selecting one sample per patient per week from groups 0 and 1, resulting in weekly pools. These pooled samples (p) were designed as "p0" and "p1", respectively. Each DNA pooled sample contained a minimum amount of 1,000 ng, which is necessary for library preparation and sequencing.

3.9 DNA amplification

Conventional PCR amplification was employed to amplify ARGs and to identify the microbiome profile of 16S rRNA sequences. This approach uses sequence-specific primers, DNA polymerase, nucleotides, and thermal cycling to replicate target DNA regions exponentially. The application of this technique allowed the amplification of specific gene families related to ESBLs (*bla*$_{\text{TEM}}$, *bla*$_{\text{CTX-M}}$, *bla*$_{\text{SHV}}$) (Monstein *et al.*, 2007) and carbapenemases (*bla*$_{\text{VIM}}$, *bla*$_{\text{OXA-48}}$, *bla*$_{\text{KPC}}$, *bla*$_{\text{NDM}}$, *bla*$_{\text{GES}}$) (Poirel *et al.*, 2011). All PCR reactions were carried out in T100 Thermal Cycler (Biorad, California, USA) using positive, negative, and blank reaction controls. The conditions and components of each reaction varied depending on the size of the fragment to be amplified. Primers and conditions used in this study are shown in **Table 2**.

Table 2 | Primers used in this study

Primer name	Oligonucleotide sequence 5'-3'	Gene	Reaction	Polymerase	Conditions	Reference
TEM-164.SE TEM-165.AS	TCGCCGCATACACTATTCTCAGAATGA ACGCTCACCGGCTCCAGATTTAT	*bla*TEM	2 µl for each primer (10µm), 1 µl DNA template, 25 µl polymerase mix, fill to a final volume of 50µl	2X PCRBIO HS Taq Mix Red (PCRBIO Systems)	Multiplex PCR: Initial denaturation 1 cycle 15 min 95ºC; 30 cycles 30s 94ºC, 30s 60ºC, 2 min 72 ºC; Final extension 1 cycle 2 min 72ºC	(Monstein *et al.*, 2007)
SHV.SE SHV.AS	ATGCGTTATATTCGCCTGTG TGCTTTGTTATTCGGGCCAA	*bla*SHV				
CTX-M-U1 CTX-M-U2	ATGTGCAGYACCAGTAARGTKATGGC TGGGTRAARTARGTSACCAGAAYCAGC	*bla*CTX-M				
VIM-F VIM-R	GATGGTGTTTGGTCGCATA CGAATGCGCAGCACCAG	*bla*VIM	2 µl for each primer (10µm), 2 µl DNA template, 25 µl polymerase mix, fill to a final volume of 50µl	2X PCRBIO HS Taq Mix Red (PCRBIO Systems)	Multiplex PCR: Initial denaturation 1 cycle 10 min 94ºC; 36 cycles 30s 94ºC, 40s 52ºC, 50s 72 ºC; Final extension 1 cycle 5 min 72ºC	(Poirel *et al.*, 2011)
OXA-48-F OXA-48-R	GCGTGGTTAAGGATGAACAC CATCAAGTTCAACCCAACCG	*bla*OXA-48				
NDM-F NDM-R	GGTTTGGCGATCTGGTTTTC CGGAATGGCTCATCACGATC	*bla*NDM				
KPC-F KPC-R	CGTCTAGTTCTGCTGTCTTG CTTGTCATCCTTGTTAGGCG	*bla*KPC				
GES-F GES-R	CTGGCAGGGATCGCTCACTC TTCCGATCAGCCACCTCTCA	*bla*GES	2 µl for each primer (10µm), 1 µl DNA template, 25 µl polymerase mix, fill to a final volume of 50µl	2X PCRBIO HS Taq Mix Red (PCRBIO Systems)	Initial denaturation 1 cycle 15 m 95ºC; 30 cycles 30s 94ºC, 90s 57ºC, 90s 72ºC; Final extension 1 cycle 10 min 72ºC	(Bogaerts *et al.*, 2013)
Forward 16S	TCGTCGGCAGCGTCAGATGTGTATAAG AGACAG+CCTACGGGNGGCWGCAG	V3-V4 16S rRNA	5 µl for each primer (1µm), 2.5 µl DNA template, 12.5 µl polymerase mix, fill to a final volume of 25µl	KAPAHiFi HotStart ReadyMix (2X) (KAPA Biosystems)	1 cycle 95ºC 3 min; 25 cycles of 95ºC 30s, 55ºC 30s, 72ºC 30s; 72ºC 5 min	(Illumina, 2013)
Reverse 16S	GTCTCGTGGGCTCGGAGATGTGTATA AGAGACA+GGACTACHVGGGTATCTAATCC					

3.10 DNA separation

We used conventional gel electrophoresis and pulsed-field gel electrophoresis (PFGE) to separate DNA fragments of low (<30kb) and high (>30kb) molecular weight, respectively (Sambrook, Fritsch and Maniatis, 1989).

Conventional gel electrophoresis was employed to study PCR products and DNA extraction's integrity. This method employs an electric field to move negatively charged molecules through a gel matrix, typically made of agarose or polyacrylamide. A concentration of 1.5-2X agarose was used with a current of 700A and a voltage of 100-120mV for 20-40min, attending to the size of the fragment due to smaller fragments (<100bp) need a higher agarose concentration, lower voltage, and higher time than bigger fragments.

PFGE is used to separate larger DNA molecules with periodic changes in the direction of the electric field. In this case, it was used to analyze the clonal relationship between isolates. 3000 U of XbaI (Takara, Japan) were used following the PulseNet website protocols (https://pulsenetinternational.org/protocols/pfge/). Comparison of XbaI-genomic digested patterns revealed different pulsotypes (> four bands) from which we selected a set of isolates for further typing by whole genome sequencing (WGS) according to spatiotemporal distribution, pulsotype, and antibiotic susceptibility in the case of *Serratia* isolates.

3.11 Genomics

Genomics implies the study of genomes (the entire gene set), in this case, bacterial genomes, to analyze their structure, function, evolution, mapping, and even editing applications. We employed short-read and long-red sequencing to analyze bacterial genomes using Illumina and Oxford Nanopore technologies in this thesis.

Short-read sequencing. DNA was extracted automatically using the Chemagic DNA Bacterial External Lysis Kit (PerkinElmer, Waltham, USA) following manufacturer recommendations. Fragmentation of 4 µg DNA in a 46-µL elution volume in Covaris G-tubes was performed by centrifuging at 4200–5000 rpm (Eppendorf 5424 centrifuge) for 90s to achieve fragment sizes of ~20 kb. We prepared DNA libraries employing the Nextera XT library preparation kit and the Nextera XT v2 index kit (Illumina, San Diego, USA). The library was sequenced on a HiSeq4000 (Illumina, San Diego, USA) using the

reagent kit v2 (Oxford Genomics Center, Oxford, UK) to generate 250-bp paired-end reads.

Long-read sequencing. DNA was extracted automatically with the MagnaPure 96 System (Roche, Basilea, Switzerland). We used a minimum concentration of 20 ng/µL for the library preparation with the Rapid Barcoding kit 96 (Oxford Nanopore Technologies, Oxford, UK), following the manufacturer's instructions. The libraries were loaded onto flow cell versions FLO-MIN106 R9.4 MinION (Oxford Nanopore Technologies, Oxford, UK) and sequenced for 72 h. Base calling was performed in real-time with Guppy integrated into MinKNOW (Oxford Nanopore Technologies, Oxford, UK).

3.12 Metagenomics

Metagenomics refers to the study of the totality of the genomic material in a sample to analyze the diversity and functions of a microbial community using sequencing techniques (Pérez-Cobas, Gomez-Valero and Buchrieser, 2020). The study of microbial communities is principally based on marker gene sequencing and whole-genome shotgun metagenomics. In this thesis, we performed 16S rRNA gene sequencing, the most commonly used marker gene to identify bacterial and archaeal communities, and specific targeted metagenomics (ResCap) developed to investigate the ARG profiles in the pooled samples (resistome).

16S rRNA sequencing for microbiome characterization. For each pooling sample (p0, p1), a region of the prokaryotic 16S rRNA was amplified using the forward and reverse primers listed in **Table 2**. The amplified region of a ~550bp corresponded to hypervariable regions V3 and V4 (Klindworth *et al.*, 2013). The sequencing was performed using Mi-Seq 2x300 paired-end (Illumina, San Diego, USA) following the Illumina standard library prep manual for 16S rRNA sequencing (Illumina, 2013).

ResCap targeted metagenomics for ARGs characterization. To study the resistome in pools p0 and p1, we used ResCap (Resistome Capture), a targeted sequence capture platform based on SeqCapEZ (NimbleGene) technology developed in our laboratory by Lanza et al. (Lanza *et al.*, 2018). ResCap improves sensitivity and specificity in detecting ARGs compared to untargeted metagenomic approaches. It consists of a library based on core reference databases comprising well-known and hypothetical genes encoding resistance to antimicrobials (antibiotics, heavy metals, biocides) and production of

specific relaxases (involved in plasmid DNA transfer). In this thesis, we focused on the diversity and presence of ARGs. Probes targeting the antibiotic resistome include 47,806 putative ARGs and 7,963 functionally characterized genes. The workflow consists of i) whole-metagenome shotgun library construction, ii) hybridization and capture, and iii) captured DNA sequencing. This process was achieved in the *Unidad de Genómica Traslacional y Bioinformática* (UCA-GTB) at HURyC with a workflow design supervised by the developers of this method (Lanza *et al.*, 2018).

3.13 Bioinformatic analysis

This section will be divided into analyses referred to genomics and metagenomics.

3.13.1. Genomics

Assembly and annotation. The first step was to assemble and annotate the raw reads obtained from short and long-read sequencing. For Illumina *fastq* files (short read), *de novo* assembly was performed using SPAdes 4.0.0 (Prjibelski *et al.*, 2020), and annotation was done using Bakta 1.7.0 (Schwengers *et al.*, 2021). For Oxford Nanopore *fast5* files (long read), adapter sequences were removed with qcat (Oxford Nanopore), and *fastq* reads were filtered and quality measured with NanoFilt (>10,000 bases) and Filtlong v0.2.039 (500Mbp best reads) before the assembly. Hybrid assemblies were created with Unicycler v0.4.7 (Wick *et al.*, 2017) and checked by visualization with Bandage v0.8.1. Bakta 1.7.0 was also employed to annotate long-read sequences.

Phylogenetic trees. We built a core-based maximum likelihood phylogenetic tree using a pseudo-multisequence alignment generated with FastTreeMP midpoint root (Price, Dehal and Arkin, 2010). Paralogues were removed with Panaroo (Tonkin-Hill *et al.*, 2020), and regions with high-density polymorphisms were excluded with Gubbins (Croucher *et al.*, 2015). The molecular clock and timeframe for the tree were calculated with TempEST (Rambaut *et al.*, 2016) and BactDating (Didelot *et al.*, 2018). The phylogenetic tree was visualized and annotated using the *ggtree* R package version 2.2.4 (Yu, 2020). Metadata was edited and integrated with the tree using iTOL (Letunic and Bork, 2021). Additionally, we built a MASH-based phylogenetic tree with more than 3,000 sequenced genomes from the NCBI using the "similarity_tree" function from *PATO*

R package, also designed and developed in our laboratory (Fernández-de-Bobadilla *et al.*, 2021).

Bacterial taxonomy. We assigned the species taxonomy using three approaches: the function "classifier" of *PATO* R package (Fernández-de-Bobadilla *et al.*, 2021), GTDB-Tk (Chaumeil *et al.*, 2020), a software of the Genome Database Taxonomy (GTDB) (https://gtdb.ecogenomic.org/), and ribosomal MLST (rMLST) (Jolley *et al.*, 2012). We used the reference genomes for each of the methods.

The function "classifier" assigns each query genome to the closest reference genome from the National Center for Biotechnology Information (NCBI) (https://www.ncbi.nlm.nih.gov/taxonomy) by calculating the average nucleotide identity (ANI) of each genome to the reference ones. It assigns a reference species if the ANI is over 95% of the identity. GTDB-Tk assigns each genome to one of the clusters created by GTDB and to the genome they have selected as a reference for the species. rMLST indexes variation of *rps* genes to integrate microbial taxonomy and typing, from which the scheme used for *Serratia* was available at https://pubmlst.org/organisms/serratia-spp.

Bacterial typing. Isolates were classified according to the MLST scheme available at https://pubmlst.org/organisms/serratia-spp. Single nucleotide polymorphisms (SNPs) were obtained using the *PATO* R package function "get_snps". Clade classification was inferred according to the core-based maximum likelihood phylogenetic tree.

Resistome, ResFinder (Bortolaia *et al.*, 2020) was employed to identify intrinsic and acquired ARGs in *Serratia* genomes by comparing input sequences against a comprehensive database of resistance genes. The nucleotide and amino acid sequences of AmpC, AmpR, and AmpD genes were aligned and analyzed using Clustal Omega (https://www.ebi.ac.uk/jdispatcher/msa/clustalo) and Benchling (https://www.benchling.com/).

Plasmidome. For the Illumina data, plasmids were reconstructed from FASTA files and typed using the MOB-recon and MOB-typer modules of the MOB-suite software (Robertson and Nash, 2018). The distance matrix was created using the "accent" function of *PATO* R package, and the plasmid network was built with Cytoscape (https://cytoscape.org/) and managed with the *igraph* R package. For the hybrid plasmid assemblies, annotated FASTA files were visualized and analyzed using Gview (https://server.gview.ca) and Benchling, and clinker (Gilchrist and Chooi, 2021) was used for the gene cluster comparison.

Analysis, visualization of data, and graphical design. The *tidyverse* (Wickham *et al.*, 2019), *ggplot2* (Wickham, 2016) and *lubridate* (Grolemund and Wickham, 2011) R packages were employed for image construction and data analysis. Inkscape 0.92.3 (https://inkscape.org/es/) was used for graphical editing and design.

3.13.2. Metagenomics

Quality control and processing of raw reads. 16S rRNA raw sequencing reads were subjected to quality filtering by trimming sequencing adapters, discarding short and low-quality reads, and removing low-quality extremes using QIIME2 software (https://qiime2.org/). QIIME2 was also used to estimate the Amplicon Single Variants (ASV) using DADA2 algorithm (Callahan *et al.*, 2016) and to perform the taxonomic classification based on the Green Genes database. The analyses were based on the ASV abundance tables collapsed at the species level as a minimum.

ResCap raw reads were mapped against the preformed database following the indications of the published pipeline (Lanza *et al.*, 2018).

Diversity metrics. The diversity and composition of microbial communities are usually estimated using diversity metrics (Kim et al., 2017). The most common way to study diversity is to measure the number of species in a single sample (alpha diversity) and the number of species within various heterogeneous samples (beta diversity).

Alpha diversity is commonly measured by determining the number of species (richness) and species abundance distribution in a single sample (evenness). Chao1 is a common richness estimator, and the Shannon index is the most common diversity index for analyzing species diversity and evenness (Kim et al., 2017). The phylogenetic relatedness of the community members can be measured using Faith's phylogenetic diversity (Faith's PD), estimating the taxonomic distance between taxa present in a sample (Armstrong *et al.*, 2021). These estimators were measured using the *vegan* R package (Oksanen, 2024). Temporal distributions of the alpha diversity metrics were lotted and analyzed using the *splinectomeR* R package (Shields-Cutler *et al.*, 2018).

Beta diversity measures the similarity or dissimilarity between microbiomes in relation to their taxonomic distribution (Su, 2021). It can be based on "non-phylogenetic" distances (Bray-Curtis or Jaccard) or "phylogenetic" distances (unweighted and weighted UniFrac). Bray-Curtis and weighted Unifrac are quantitative, while Jaccard and unweighted Unifrac are qualitative (Pérez-Cobas, Gomez-Valero and Buchrieser, 2020).

Bray-Curtis dissimilarity is the most used index, considering the relative abundance of the taxa. In contrast, the Jaccard index determines the distance considering presence/absence values. Ordination techniques such as principal component analysis (PCA) or non-metric multidimensional scaling (NMDS) help identify data compositional patterns. NMDS analysis for p0 and p1 using the Bray-Curtis dissimilarity matrix was based on the *vegan* R package.

Microbial composition comparison. A barplot showing the average composition of pools p0 and p1 was constructed using *phyloseq* R package (McMurdie and Holmes, 2013). To identify the taxa that explained the differences between each pool (p0, p1), we employed the LEfSe (Linear discriminant analysis Effect Size) test. LEfSe performed non-parametric statistical testing to identify features with significant differential abundance, followed by linear discriminant analysis (LDA) to estimate the effect size of each feature, providing a robust means to discover biomarkers (Segata *et al.*, 2011).

Analysis, visualization of data, and graphical design. The *tidyverse, ggplot2,* and *lubridate* R packages were employed for image construction and data analysis. Inkscape 0.92.3 was used for graphical editing and design.

3.14 Statistical analysis

All statistical analyses were carried out in R version 4.3.0 (https://www.r-project.org/) with additional packages *tydiverse*, *vegan*, *ggplot, ggstatsplot* (Patil, 2021) and *ggpubr* (Kassambara, 2023). For the microbiome 16S rRNA gene, the script implemented in the QIIME2 pipeline was also used.

Parametric (t-test) and nonparametric (Wilcoxon, Kruskal-Wallis, Chi-square, Spearman's r) tests were conducted to assess each case's data. The Shapiro test was used to measure the data's normality. The Adonis test, a nonparametric test equivalent to PERMANOVA, was used to compare the differences in multivariate data among/between groups using the "adonis2 function" in the *vegan* R package.

Normalization for comparing the relative abundance of datasets was achieved using the z-score, also known as the standard score, which describes a value's position relative to the mean.

3.15 Data availability

The genome sequences generated during this study were deposited in the European Bioinformatics Institute database under Bioproject accession number PRJNA1023224 (accessible from January 1st, 2024). Biosample accession numbers for each sequence can be found in **Annex 6**.

The metagenome sequences generated during this study are pending submission along with the submission of the manuscript.

RESULTS.
RESULTADOS.

CHAPTER 1.
THE INFLUENCE OF THE ICU STAY IN THE PATIENT MICROBIOME AND RESISTOME

CAPÍTULO 1.
LA INFLUENCIA DE LA ESTANCIA EN LA UCI EN EL MICROBIOMA Y EN LA RESISTENCIA DEL PACIENTE

4.1.1. Motivation

The risk of selecting, acquiring, and spreading opportunistic antibiotic-resistant pathogens within the hospital occurs mainly in ICUs (Wenzel, 2005). Such risks have been associated with the patient's individual characteristics and basal microbiome, the selective local pressures (consumption of antibiotics and other drugs), the density of colonized patients, and the connectivity among them and health workers (ICU demographic factors). These factors determine the abundance and diversity of ARB reservoirs at the individual level (colonization resistance) and the collective level (colonization pressure) (Bonten, 2012; Le Guern *et al.*, 2021).

Hospital surveillance of AMR is performed as part of the infection control programs to identify microbial species on the WHO Bacterial Priority Pathogens List (WHO Bacterial Priority Pathogens List, 2024). This involves testing “sentinel samples” from patients, such as rectal and/or nasal swabs, and potential environmental reservoirs, primarily surfaces of medical devices or sinks, which are only tested during outbreaks (Grundmann, 2014). This deterministic surveillance approach focuses on a few pathogens and ARGs included in the “watch lists” of the WHO. However, the low sensitivity and specificity of the culturing-based methodology and the generally weak spatiotemporal screening designs may have underestimated patients' contributions to the “ward microbiome” (Coque *et al.*, 2023), encompassing the ensemble of all microbiomes in the ward, including patents, hospital health workers, medical devices, and built environment, thus considering the ward as a unity of surveillance.

We hypothesized that the admission of patients in high-risk hospital areas such as ICUs rapidly changes their gut microbiome, which may shape the ward microbiome and, complementarily, the antibiotic resistome, determining the emergence and spread of HAIs, the leading cause of death. This chapter describes the dynamics of the intestinal microbiome and resistome of the patients admitted at the largest ICU ward throughout a year and the impact of patient intestinal antibiotic-resistome and microbiome. A pooled approach was used to analyze a high number of samples by metagenomics through an extended period and identify periods of risk of infection. With this meta-analysis, we aimed to explain the changes in the microbiome of an established ICU ward and how the microbiome of patients influences these variations.

4.1.2. The ICU microbiome

The ICU ward was analyzed as a **single ecological entity**, or *ecosystem* (Willis, 1997; Coque *et al.*, 2023), with a dynamic microbiome comprising "transient microbes" from patients and clinical staff and "core microbes" inhabiting environmental reservoirs. In this section, we analyzed the contribution of patients ("transient microbes") and how they influenced the ICU microbial dynamics using the pooled approach.

To achieve this objective, we designed a metagenomic analysis of pooled fecal samples (p) from newly admitted patients (p0) and patients who stayed in the ICU for more than five days and collected successively until the patient's discharge (p1) (see section **3.8**). We recovered 728 stool samples from 178 patients during the study. Below, we described the results from the analysis of weekly p0 (n=41) and p1 (n=43) pooled samples. On average, each tube had a final volume of 60 µl (ranging from 20-90 µl) with a concentration of 70 ng/µl (ranging from 20-100 ng/µl). Pooled samples with DNA concentrations below 15 ng/µl and low-quality DNA measurements were excluded from sequencing. Data for the pooled samples are included in **Annex 1**. We successfully sequenced 41 pooled samples for p0 and 43 for p1 for 16S rRNA microbiome studies and 45 pooled samples for p0 and 46 for p1 for resistome analysis. The pooled samples were obtained from 336 patient fecal samples.

4.1.2.1. Alpha and beta diversity from the patient's microbiome

Alpha diversity. **Figure 6A** shows the alpha diversity of the p0 and p1 samples using the Shannon, Chao1, and Faith PD estimators, measuring the abundance, diversity, richness, and phylogenetic relationships, respectively. The significance of the results for Shannon and Chao1 (p-value<0.001) was verified using the Wilcoxon test, which indicates that the microbiome composition of p0 patients had higher species diversity and richness than that of p1 patients. However, the significance for the phylogenetic bacterial diversity within p0 and p1 was not observed (p-value$=0.16$), thus indicating the maintenance of phylogenetically related bacteria within p0 and p1.

We further examined the variation in the diversity of both p0 and p1 samples over time using the Shannon and Chao1 indexes (**Figure 6B**). We observed that the significantly higher overall bacterial diversity for p0 is consistent during the study period, albeit with some variations. Higher values of both Shannon and Chao1 were observed from September to November 2019, in which diversity for p0 decreased.

The variability of the measurements was correlated with the number of patients per pooled sample (**Annex 1**) and the bacterial diversity. A weak positive and significant correlation was found for Shannon (p-value<0.001, r=0.37), Chao1 (p-value<0.001, r=0.5), and Faith PD (p-value<0.05, r=0.2) using Spearman's rank correlation. This indicates that, particularly in terms of richness, the more patients included in the pooled samples, the greater the diversity observed. The temporal tendency of the number of patients per pooled groups p0 and p1 at the time was also inferred (**Annex 2**).

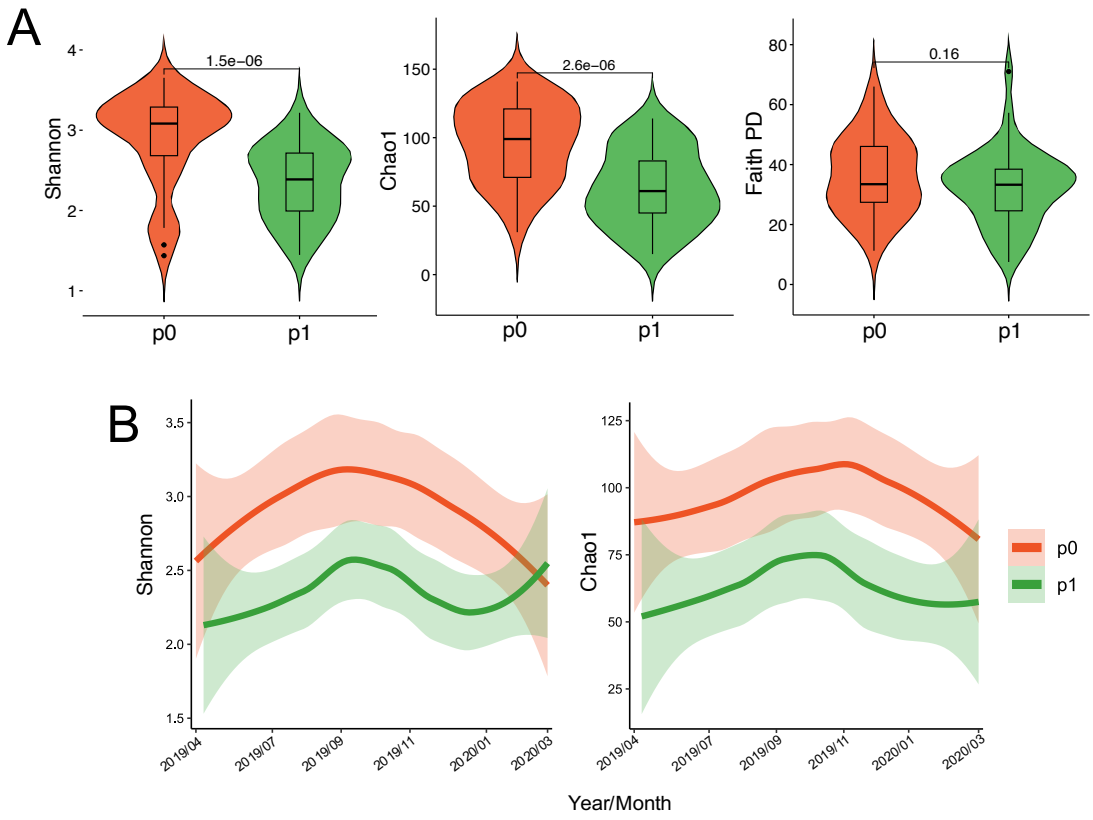

Figure 6 | Alpha diversity of pools p0 and p1.
Panel A) Violin boxplots of the alpha diversity metrics Shannon, Chao1, and Faith PD among the p0 and p1 samples. Significance was calculated using the Wilcoxon test. The boxplots show the median value, and the whiskers extend to the most extreme value.
Panel B) Temporal distribution of Shannon and Chao1 estimators. Graphs were made using the function "geom_smooth" from the *ggplot* R package representing p0 and p1 longitudinal distributions. The X-axis represents the year and month of the pooling and sample obtention, and the Y-axis shows the values for both diversity indexes.

Beta diversity. The difference in taxonomic composition between pooled groups p0 and p1 was explored through Bray-Curtis dissimilarity and Jaccard distance (p-values<0.001) and unweighted and weighted Unifrac (p-values<0.01), being significant for all distances evaluated. As shown in **Figure 7**, based on Bray-Curtis dissimilarity, the taxa associated with p1 pooled samples were more heterogeneously distributed than those of p0 samples.

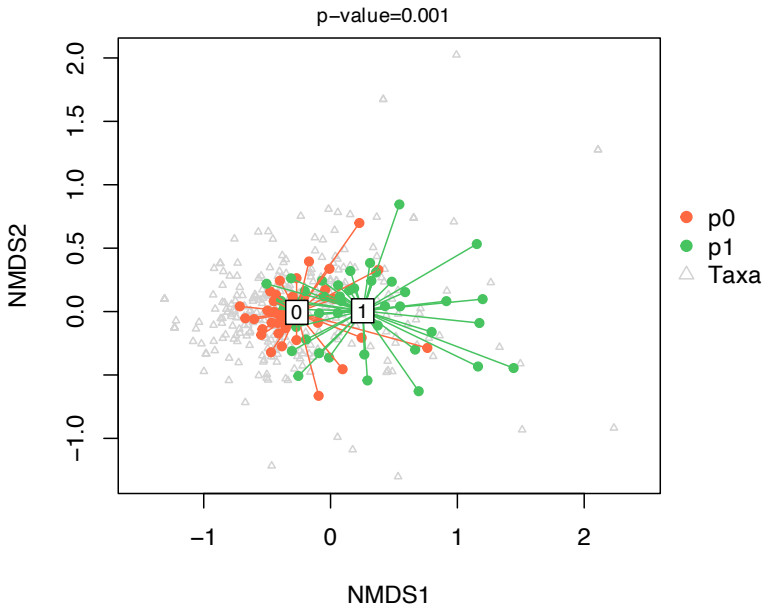

Figure 7 | Taxa distribution of p0 and p1 pooled samples
An NMDS ordination plot based on the Bray-Curtis dissimilarity matrix represents the beta diversity of pooled samples. Colored circles represent each pooled sample, and triangles represent the taxa. Significance was analyzed using the PERMANOVA test.

4.1.2.2. The ICU microbiome composition

As described before, we found significant differences in taxonomic composition between samples of the p0 and p1 pooled groups. Specifically, the relative abundance of taxa associated with a healthy microbiota, such as *Clostridiales, Ruminococcaceae, Methanobacteriaceae* (archaea), *Lactobacillae*, or *Prevotella* (Tap *et al.*, 2009), was significantly higher in p0 than p1 (p-value<0.05) (**Figure 8A**). To specially identify those taxa associated with each group, we used the LEfSe test (see section **3.13.2**) (Segata *et al.*, 2011). This analysis revealed significant enrichment of *Enterococcus, Bacteroides,* and *Staphylococcus saprophyticus* in p1 pooled samples (**Figure 8B)**.

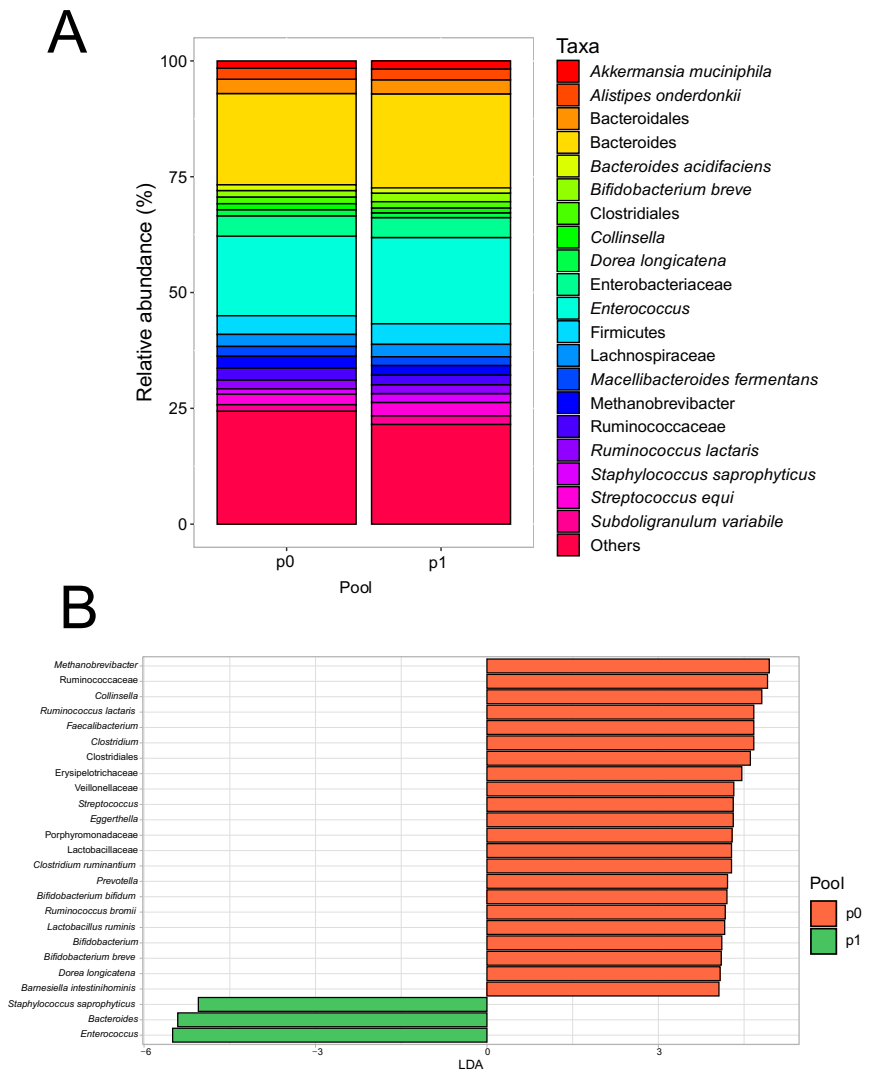

Figure 8 | Gut microbiome comparison between p0 and p1 pooled samples
Panel A) Average relative abundance (%) of the most prevalent taxa (>1%) in p0 and p1 pooled samples
Panel B) LEfSe plot showing taxa with significant and different abundance from p0 and p1 pooled samples. LDA scores (X-axis) > 4 are represented.

4.1.3. The ICU resistome

We analyzed the content of ARGs using a targeted metagenomics approach based on the SeqCapEz technology (see section **3.12**) (Lanza *et al.*, 2018). **Figure 9** shows the diversity of ARGs in p0 and p1 samples using Shannon diversity. The diversity and abundance of ARGs were significantly higher for newly admitted patients (p0) than long-stay patients (p1) (t-test: p-value=0.008).

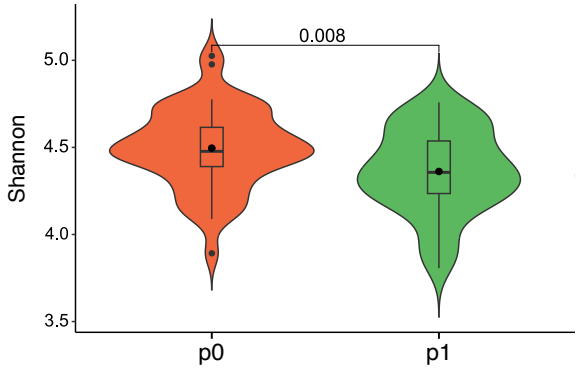

Figure 9 | Violin and box plots showing alpha diversity Shannon index for p0 and p1 pooled samples.
P-values were measured using a t-test.

We identified 7,908 alleles from 540 unique ARGs associated with resistance to macrolides (n=2,042, 25.8%), tetracyclines (n=1,577, 19.9%), aminoglycosides (n=1,506, 19.0%), β-lactams (n=1,188, 15.0%), phenicols (n=493, 6.2%), folate pathway antagonists (n=441, 5.6%), fluoroquinolones (n=217, 2.7%), fosfomycin (n=177, 2.2%), glycopeptides (n=114, n=1.4), and other categories “others” (n=153, 1.9%) (**Figure 10**). In p0, the composition of distinct genes is significantly higher and different than in p1 (ADONIS: p-value<0.01) (**Figure 11**).

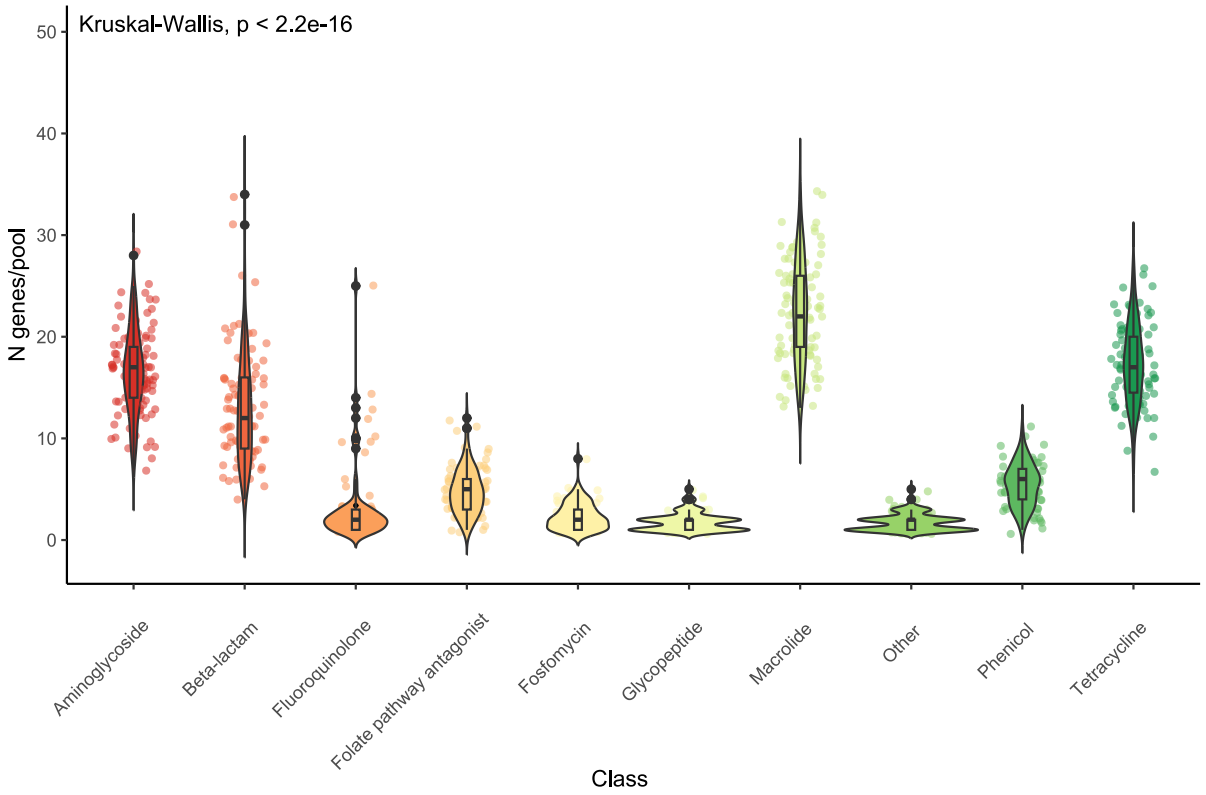

Figure 10 | Violin plots showing the antibiotic families for the ARGs identified
Each dot represents the number of genes in a pooled sample. P-value was measured using the Kruskal-Wallis test.

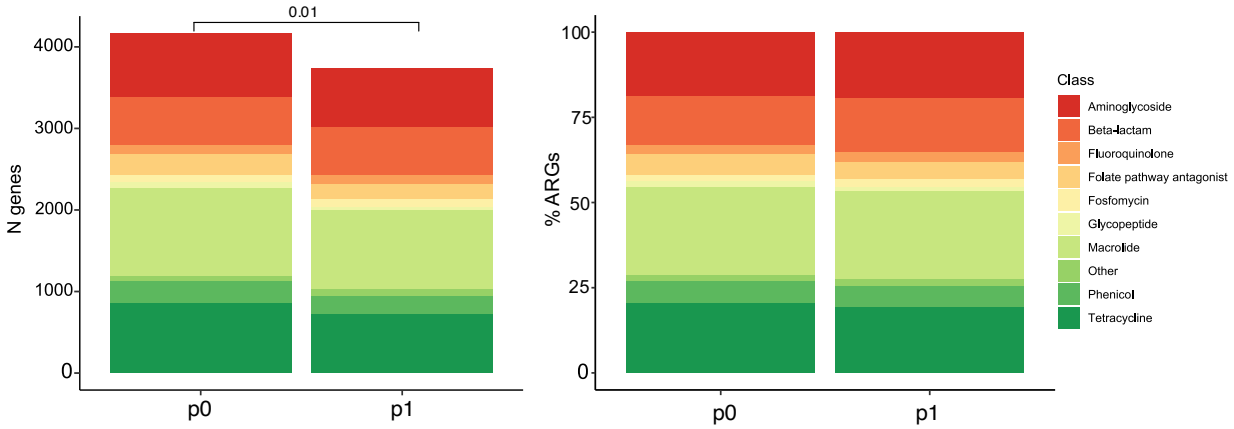

Figure 11 | Composition of ARGs regarding distinct antibiotic families for p0 and p1 pooled samples
The P-value was measured using the ADONIS test (panel on the left). The right panel represented the percentage (%) of those genes.

Figure 12 represents the diversity of alleles, each associated with ARGs of different antibiotic families. β-lactams (n=175), aminoglycosides (n=81), macrolides (n=69), and *tet* (n=63) encompassed the highest number of distinct alleles. Only *tet* alleles (n=63) are found for tetracyclines, even though the number of alleles detected was high.

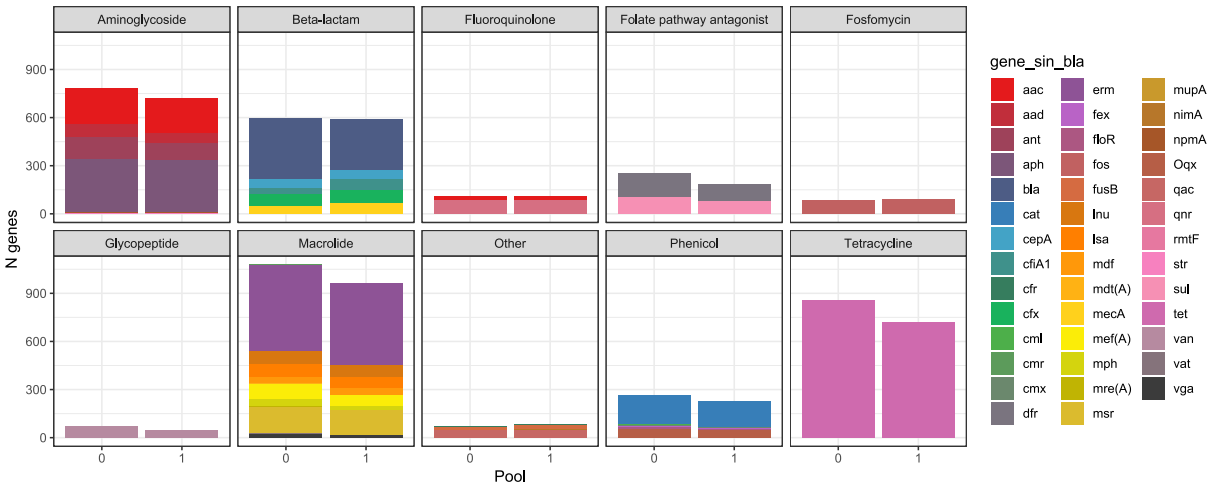

Figure 12 | Diversity of ARGs from different antibiotic families in p0 and p1 samples.

Due to the high recovery of genes of distinct clinical relevance, we focused on analyzing the dynamics of the more frequently associated genes with therapeutic failure.

4.1.3.1. Antibiotic-resistance genes of clinical relevance

ARGs conferring resistance to first-line antibiotics were categorized as "clinically relevant genes" due to their challenging impact on patient treatment and outcome (WHO Bacterial Priority Pathogens List, 2024). Among them, we detected genes conferring resistance to third-generation cephalosporins and carbapenems, identifying ESBLs and carbapenemases in *Enterobacterales* and *Pseudomonas* (*bla*$_{CTX}$, *bla*$_{GES}$, *bla*$_{KPC}$, *bla*$_{OXA}$, *bla*$_{VIM}$), as well as resistance to β-lactams in staphylococci (*mecA*) and glycopeptides in enterococci (*van*). Notably, outbreaks of *K. pneumoniae* KPC-3 and *P. aeruginosa* GES-5, along with polyclonal outbreaks of VIM-1, CTX-M-15, and OXA-48 producers, occurred in the ICU during the last period analyzed and have been reported in several wards of the HURyC for at least the past fifteen years.

The dynamics of these clinically relevant genes over time are shown in **Figure 13A**, illustrating the temporal distribution and prevalence. **Figure 13B** demonstrates the normalized abundance of these genes using the z-score (see section **3.14**). As expected, OXA- and TEM-type enzymes were the most prevalent and abundant β-lactamases, being widely detected in different bacterial species and the environment (Boyd *et al.*, 2022; Ramatla *et al.*, 2023). Some *bla*$_{OXA}$ genes (26 distinct alleles, including the clinically relevant *bla*$_{OXA-48}$) were consistently identified throughout the study. This is the case of *bla*$_{OXA-1}$, usually located on class 1 integrons and often on multiresistant regions of plasmids such as pC15-like IncF carrying *bla*$_{CTX-M-15}$ (Livermore *et al.*, 2019), and *bla*$_{OXA-347}$, associated with the human respiratory tract microbiome (Zhu *et al.*, 2022).

Of particular interest were *bla*$_{OXA-48}$-like genes such as *bla*$_{OXA-48}$ and *bla*$_{OXA-244}$, which have been detected at various points in the study and have been previously reported in hospitals from Spain (Oteo *et al.*, 2013; Boyd *et al.*, 2022). The highest rate of recovery of these *bla*$_{OXA}$-like enzymes was at the end of the mentioned hospital outbreaks (January-March 2020), in which the detection of *bla* genes encoding resistance to first-line antibiotics in the ICU increased, specifically class A β-lactamases *bla*$_{KPC-3}$, *bla*$_{CTX-M-15}$ and *bla*$_{GES}$ alleles. The *mecA* and *van* alleles of *Staphylococcus* spp. and *Enterococcus* spp. respectively, were overrepresented throughout the study.

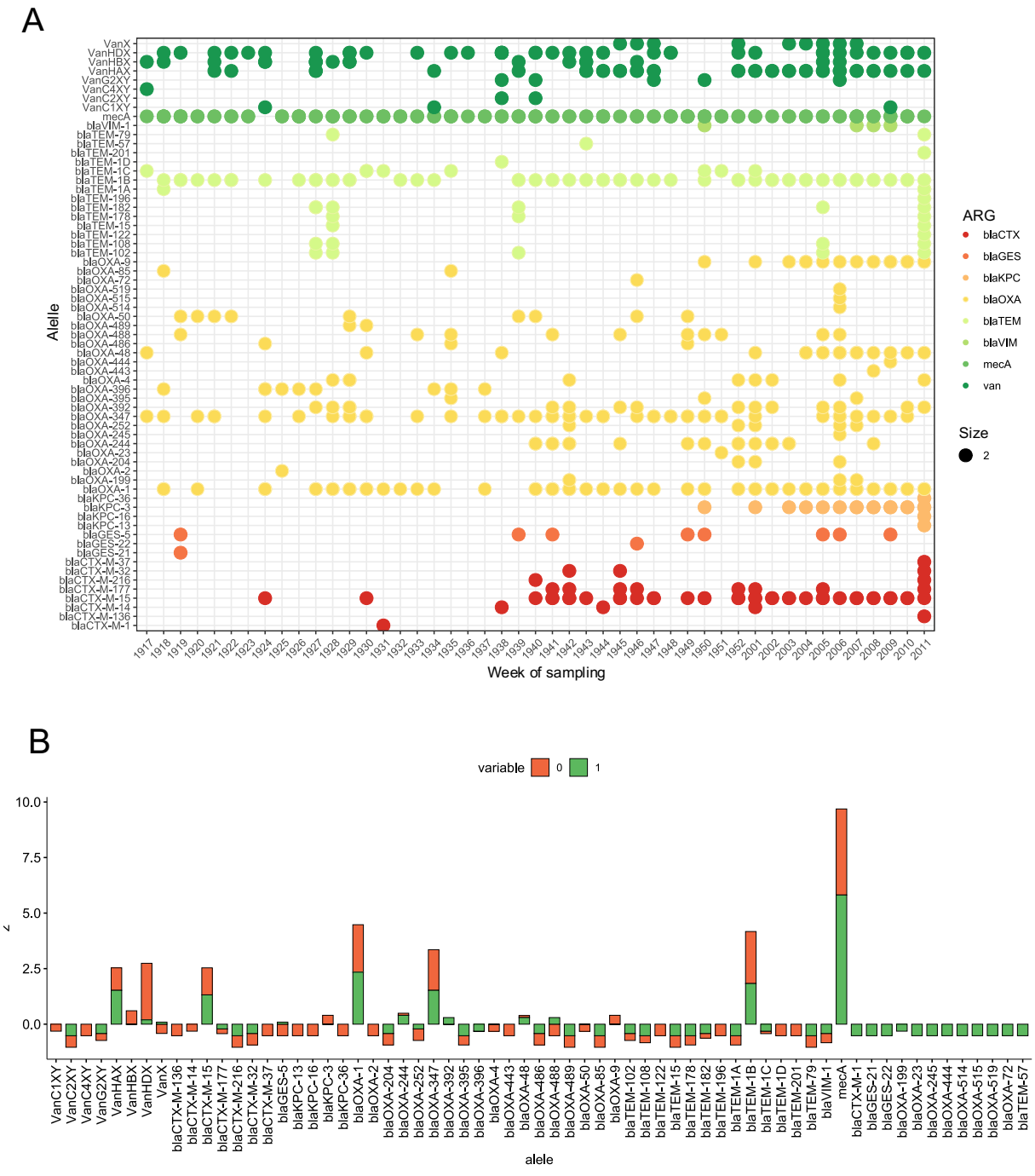

Figure 13 | Clinically relevant gene alleles detected in pooled samples.
Panel A) Temporal distribution of this study's main ARGs.
Panel B) Normalization of ARGs abundance using z-scores. The main clinically relevant alleles are shown with their values for pools p0 and p1 represented in the plot. Positive or negative z-score values indicate abundance above or below the mean, respectively.

4.1.4. Highlights

❖ This chapter emphasizes **the significant impact of extended ICU stays on the gut microbiota of hospitalized patients**, particularly a reduction in bacterial species and gene diversity. The bacterial composition of fecal samples from newly admitted patients', similar to that of a “healthy” microbiota, seems to be impacted by medical interventions prior to the ICU stay. In contrast, the bacterial composition of patients upon entering the ICU becomes more heterogeneous, reflecting **the varied effect of ICU-related interventions on microbiome diversity.** This variation is indicated by the alpha and beta diversity indexes.

❖ This chapter provides a view of the **impact of the ICU length stay to the composition of patients' bacterial gut microbiome and resistome**. While a reduction in microbial diversity is observed in patients with prolonged ICU stays, particular genes and species tend to dominate during and beyond outbreak periods. This suggests that, during these times, the ecological niches within the ICU ward are primarily occupied by either low-risk resistant Gram-positive species (with occasional but infrequent clinical importance) or, eventually, by outbreak-related Gram-negative resistant pathogens, overshadowing the typical commensal bacteria and potentially colonizing environmental reservoirs.

❖ The **use of first-line β-lactam antibiotics**, frequently administered prophylactically in ICU wards, disrupts the microbial community and favors the growth and selection of **Gram-positive bacteria**, particularly *Enterococcus* and *Staphylococcus,* which adapt and thrive in this altered niche. However, the increase of the population size of these species is not always associated with HAIs or outbreaks by these microorganisms.

❖ **ARGs conferring resistance to first-line β-lactam antibiotics** were primarily detected in the p1 pooled samples. Some were intrinsically associated with commensal taxa (e.g., *bla*$_{\text{OXA}}$-like), while others were “transiently” associated with (often hidden) colonization by MDROs (e.g., *bla*$_{\text{GES}}$, *bla*$_{\text{KPC}}$) and/or with hospital outbreaks. This highlights the risk of ARG amplification and dissemination within the patient (colonization/HAI), between patients, or patient-environment, particularly favored by prolonged hospital stays.

CHAPTER 2.
THE INFLUENCE OF THE MICROBIOLOGICAL SURVEILLANCE OF THE ICU WARD ON PATIENT SAFETY (HAIS AND AMR)

CAPÍTULO 2.
LA INFLUENCIA DE LA VIGILANCIA MICROBIOLÓGICA DE LA PLANTA DE UCI EN LA SEGURIDAD DEL PACIENTE (IAAS Y RAM)

4.2.1 Motivation

Advanced omics and high-throughput analyses provide insights into the dynamics of microbial taxa (metagenomes) and ARGs (resistome) (see **Chapter 1**, section **4.1**). However, the epidemiology and drivers of opportunistic pathogens within the hospital must be addressed to prevent healthcare-associated infections (HAIs) and the transmission of antibiotic resistance. In this context, the Division of Healthcare Quality Promotion (DHQP) of the Centers for Disease Control and Prevention (CDC) has highlighted key priority research questions for healthcare, which include: i) understanding the natural history of *colonization* and *infection* by antibiotic-resistant pathogens, ii) identifying the most effective vectors for AMR *transmission*, and iii) ensuring the efficiency of colonization screening methodologies to prevent HAIs and transmission (Centers for Disease Control and Prevention, 2024c).

In the following sections of **Chapter 2**, we explore the predicted relation between colonization estimated in different types of samples and HAI episodes that occurred in the ICU ward of a tertiary hospital over 12 months, taking ICU metrics into account. We further focus on the dynamics of high-risk ARGs, such as those conferring resistance to carbapenems. Finally, we evaluate the efficacy of different methodological strategies for screening patient colonization and, consequently, the "pollution" of high-risk ARGs.

4.2.2 Colonization and Infection Events

We collected data on patients' colonization levels by culturing 487 out of 718 fecal samples into several selective media (see section **3.4**) and gathering information about the data obtained by the Microbiology Service routine weekly surveillance of infections and rectal carrier screening. Information about patients recovered during this study period is in **Annex 3**.

Results for positive samples from fecal culturing are shown in **Figure 14A** and **Figure 14B**, depicting persistence over time and abundance. We mostly detected *Enterococcus* spp. (58.3%), *Staphylococcus* spp. (19.3%), *E. coli* (7.2%), and *Klebsiella* spp. (4.2%). Other bacterial species of clinical interest were recovered less frequently, such as *Pseudomonas* spp. (1.4%), *Enterobacter* spp. (1.2%), *Citrobacter* spp. (0.8%), *Acinetobacter radioresistens* (0.4%), and *S. marcescens* (0.2%). Differences were not significant for samples from newly admitted patients (p0) or long-term patients (p1) (Wilcoxon: p-value>0.05). These results, including the dominance of Gram-positive bacteria, are highly consistent with those presented in the previous chapter (section **4.1**).

The occurrence of patients colonized detected by the Microbiology Laboratory were mainly from rectal swabs (59.4%) (**Figure 15**). Bacterial isolates from this source were mainly reported as ESBL-producing *E. coli* (32.4%) and *Klebsiella* (11.8%), carbapenemase-producing *Klebsiella* (14.7%), *Pseudomonas* (9.8%), and *Serratia* (6.9%); and, also, vancomycin-resistant *Enterococcus* (VRE, 9.8%).

Phenotypic and genotypic antibiotic resistance was only screened for Gram-negative opportunistic pathogens (**Figure 14C**). *Klebsiella* spp. and *Pseudomonas* spp. were the most β-lactam resistant bacteria isolated from feces. They produced ESBLs and carbapenemases, mostly CTX-M with OXA or KPC for *Klebsiella*, and CTX-M or GES for *Pseudomonas*.

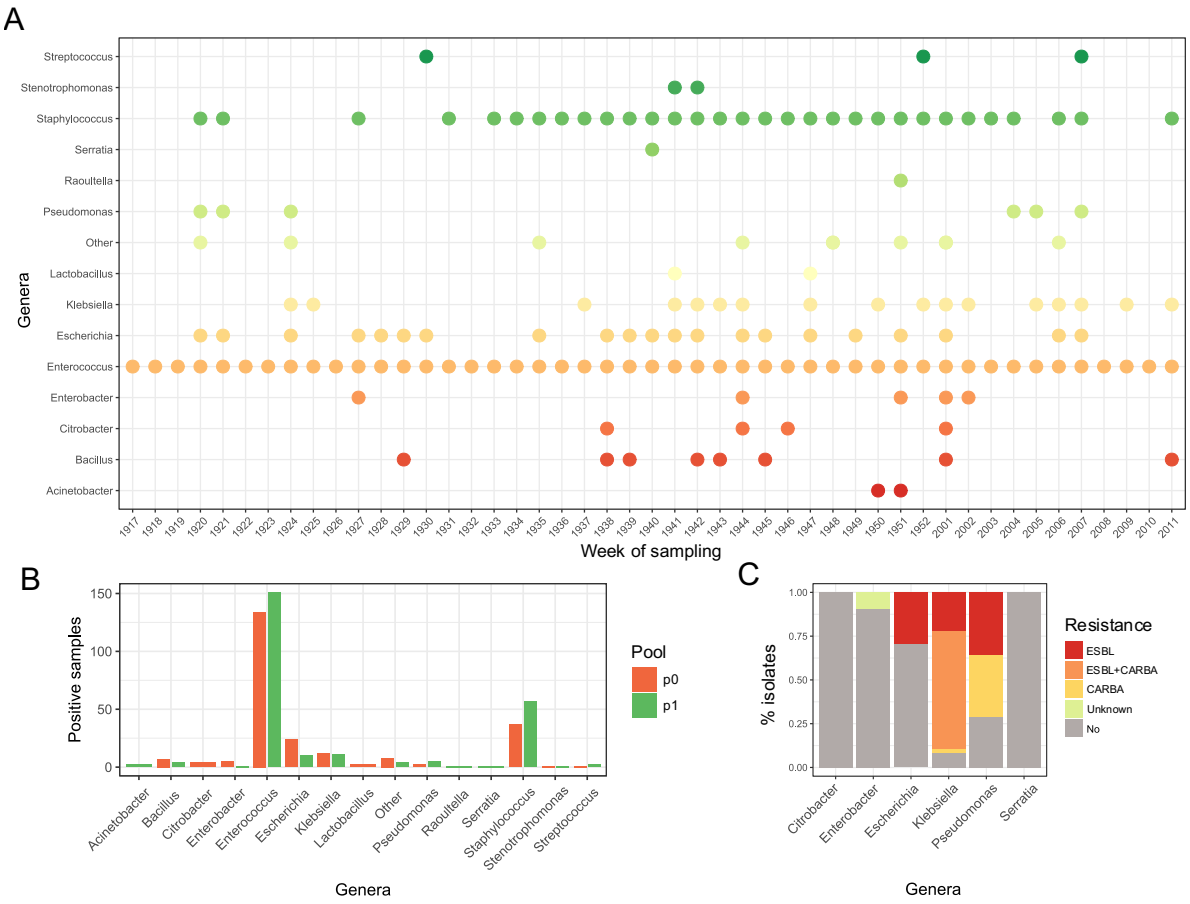

Figure 14 | Culturomics of fecal samples.
Panel A) Temporal distribution of positive samples for the identified genera. The X-axis represents the week of sampling, where the first two digits indicate the year, and the last two represent the week of this year (i.e., 1917, which means the week 17 of the year 2019). The Y-axis displays the bacterial genera identified. The data illustrates the presence and absence of positive samples. Panel B) Isolates obtained from the fecal samples by culturomics. Panel C) Resistant determinants per category for the different Proteobacteria isolates in fecal samples. Abbreviations: CARBA (presence of carbapenemases).

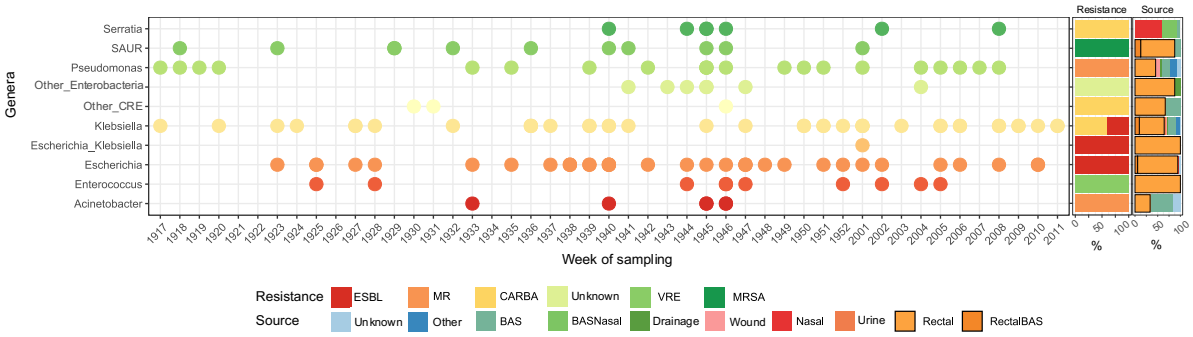

Figure 15 | Colonization events for weekly clinical surveillance events.
The X-axis represents the week of sampling, where the first two digits indicate the year, and the last two represent the week of this year (i.e., 1917, which means the week 17 of the year 2019). The Y-axis displays the bacterial genera analyzed. The panel from the right represents the resistance determinants per category and the source of colonization. Abbreviations: BAS (Bronchoaspirate), SAUR (*S. aureus*), CARBA (presence of carbapenemases).

Concerning the infections, 85 episodes of HAIs were reported, 63 caused by Gram-negative and 22 caused by caused by Gram-positive bacterial species (**Figure 16**). The causal bacterial species were *P. aeruginosa* (19.6%), *K. pneumoniae* (16.3%), *E. coli* (13.0%), and *S. aureus* (12.0%). Only 50.6% of the cases showed antibiotic resistance to the more common antibiotics used in the ICU, mainly driven by carbapenemases and ESBL producers (**Figure 17**). HAIs were mostly catalogued as ventilator-associated pneumonia (NAV, 22.4%), tracheobronchitis (21.2%), urinary tract infection (UTI, 18.8%), and abdominal injuries (14.1%).

In general, ESBL, carbapenemase, and ESBL+carbapenemase producers dominated the colonization and infection events, thriven mainly by *K. pneumoniae* (both), *P. aeruginosa* (both), *E. coli* (ESBL), and *S. marcescens* (carbapenemase). Few events with MRSA or VRE were accounted for.

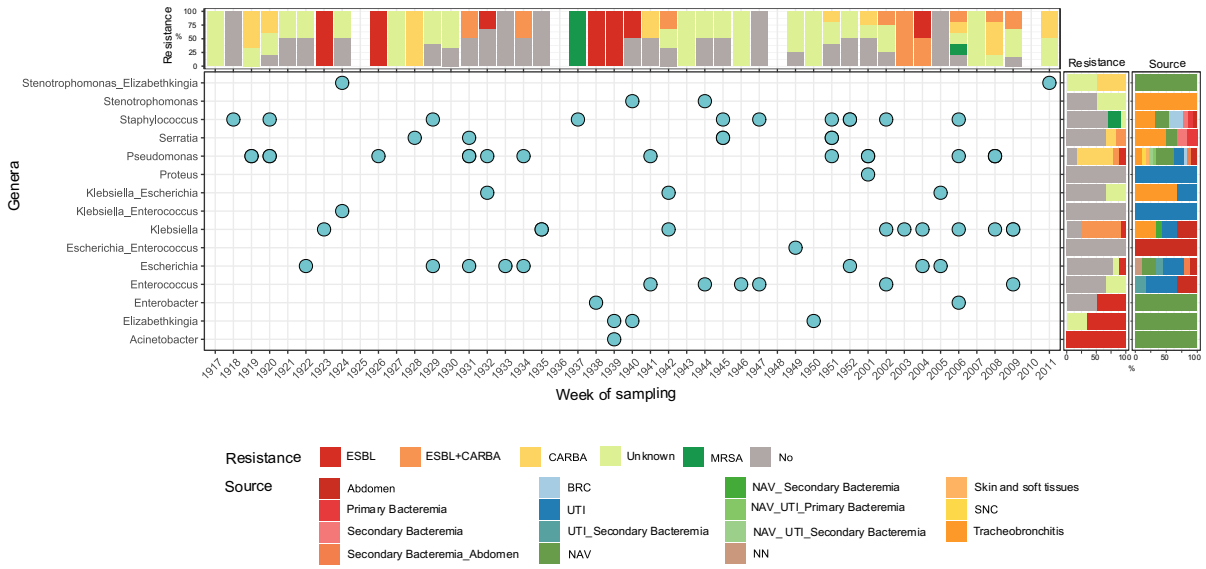

Figure 16 | Nosocomial infection episodes in the ICU
The X-axis represents the week of sampling (the first two numbers represent the year, and the last two represent the week of this year, i.e., 1917, which means the week 17 of the year 2019). The Y-axis represents the bacterial genera analyzed. The resistance determinant per category are represented in the panel from the right and above, and the source of colonization is in the right panel.
Abbreviations: BRC (Central Venous Catheter-related Bloodstream Infections), UTI (Urinary Tract Infection), NAV (Ventilator-associated pneumonia), NN (Nosocomial Pneumonia), SNC (Central Nervous System).

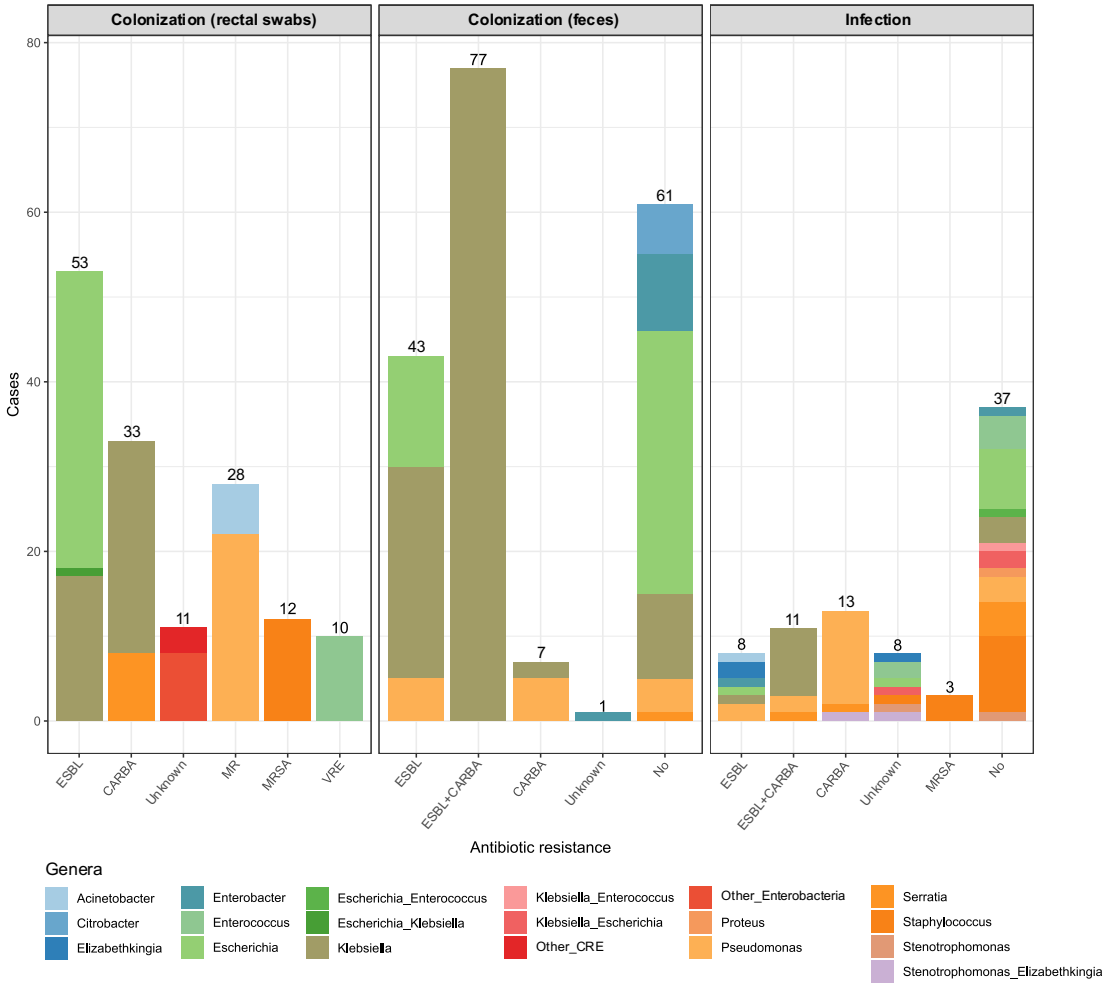

Figure 17 | Resistance determinants per category in the cases of nosocomial infections and comparison of swab and fecal sampling colonization events.
Abbreviations: CARBA (production of carbapenemases and/or resistance to carbapenems), CRE (Carbapenemase-producing *Enterobacteriaceae*), MR (Multidrug-resistant).

Given the clinical relevance of hospital outbreaks associated with carbapenemase production and the detection of nosocomial infections, we focused our analysis on these MDROs and carbapenemase-related events.

4.2.3 Dynamics of carbapenemase-producing *Enterobacterales* in the ICU

In the ICU, carbapenemase-producing bacteria were detected in 34 colonized patients (19 for rectal swabs and 13 for feces) and 17 patients with documented infection. Most cases involved both colonization and infection by *Klebsiella* and *Pseudomonas*and rectal colonization by *S. marcescens* (**Figure 17**).

We selected fecal samples from the collection obtained during the study that tested positive for MDROs producing carbapenemases from colonization or infection events. Total DNA from these individual samples were characterized using the 16S rRNA or shot-gun metagenomics. Selected strains of these events will be subjected to short-read sequencing (Illumina). The objective is to study the dynamics of the abundance and transmission of particular bacterial strains encoding carbapenemases in the context of the ICU microbiome.

First, with the clinicians' collaboration, we elaborated on a preliminary selection of the patients, considering patients who stayed more than two weeks in the ICU (**Annex 4**). To do that, we classified the patients into different groups according to their data about infection or colonization by MDROs. Five groups were obtained from that: 1) patients with HAI-MDRO but not colonized or colonized by a different microorganism; 2) patients colonized with MDRO and non-infected or infected by a different MDRO; 3) patients colonized and infected with the same MDRO; 4) patients infected by non-MDRO or colonized by a different microorganism; 5) control patients neither colonized nor infected by MDROs. This approach aimed to evaluate the causal influence of rectal colonization and infection in developing HAI-MDRO.

4.2.4 Highlights

❖ We detected a high prevalence of *Enterococcus* spp. in fecal samples and well-known hospital pathogens such as *Staphylococcus* spp., *E. coli*, and *Klebsiella* spp. Colonization detected from rectal swabs accounted for ESBL-producers (*E. coli* and *Klebsiella* spp.) and carbapenemase-producers (*Klebsiella* spp.), MDR *Pseudomonas*, MRSA, and VRE.

❖ MDROs cause **half of the HAI cases**. One of the most concerning findings is the widespread resistance to first-line antibiotics used in treating severe Gram-negative bacterial infections, particularly carbapenem-resistant *Klebsiella* and *Pseudomonas*. Carbapenems are often used as a last-resort treatment, so the high prevalence of ESBL- and carbapenemase-producing strains indicates a severe challenge for ICU management, mostly in outbreak circumstances.

❖ The leading sources of ICU infections were ventilator-associated pneumonia and tracheobronchitis, with *P. aeruginosa* and *K. pneumoniae* being the dominant pathogens. This finding underscores the importance of stringent **infection control measures for ventilators and other respiratory equipment** because such conditions appear to facilitate the spread of these bacteria. Ventilators can be contaminated by the patient's secretions, causing bacterial organisms partly from intestinal origin; in a vicious circle, these organisms might multiply in the ventilator and inoculate the respiratory tract.

CHAPTER 3.
THE CONTRIBUTION OF THE ICU ENVIRONMENT TO THE PERSISTENCE OF AMR BACTERIA: THE EXAMPLE OF *Serratia marcescens*

CAPÍTULO 3.
LA CONTRIBUCIÓN DEL ENTORNO DE LA UCI A LA PERSISTENCIA DE LA BACTERIA RAM: EL EJEMPLO DE *Serratia marcescens*

4.3.1 Motivation

The buildings in which modern health care is delivered constitute the "patient care environment." This includes all fixtures and furniture, the water supplied and drained away, or the air circulated down corridors and hallways and into patient and procedure rooms. These environments can become contaminated by pathogens that usually colonize and infect patients or environmental-adapted organisms that can fill the role of opportunistic pathogens. The "patient care environments" are still largely unexplored despite the relevance of understanding pathogen persistence and survival in the physical structure of healthcare institutions and its relationship with transmission risks.

Some opportunistic nosocomial pathogens able to contaminate and persist in abiotic surfaces are AmpC producers, which are arbitrarily grouped under the acronym SPACE (*Serratia, Pseudomonas or Proteus, Acinetobacter, Citrobacter,* and *Enterobacter*) or ESPCM (*Enterobacter, Serratia, Citrobacter, Providencia, Morganella*) group (Tamma *et al.*, 2019; Liu, 2022). The risk of inducing AmpC production varies by β-lactam and by species, complicating treatment decisions. Among them, *Serratia* is often associated with clonal and polyclonal outbreaks of ESBL or carbapenemase producers in our hospital, especially in the ICU and NICU (Tato *et al.*, 2010; Hernández-García *et al.*, 2019; Saralegui *et al.*, 2020; León-Sampedro *et al.*, 2021; Pérez-Viso *et al.*, 2021). *Serratia* has traditionally been considered a nosocomial pathogen that accounts for 1-2% of hospital-acquired infections, which are often associated with unforeseen outbreaks of high morbidity and mortality in pediatric or ICU wards. Contamination from medical devices (e.g., nebulizers, catheters, fomites) and via health-care workers are well-known transmission pathways (Mahlen, 2011). Hospital water sinks are increasingly recognized as abiotic reservoirs of MDR *Serratia* and other *Enterobacterales* during outbreaks (Bourdin et al., 2023; Constantinides et al., 2020; Martineau et al., 2018). Nonetheless, the long-term colonization dynamics of *Serratia* in the hospital environment remain understudied.

Due to its frequent occurrence within our hospital ecosystem and the limited understanding of its ecology, *S. marcescens* was selected as a model organism associated with the "patient care environment". The goals of the work were to evaluate: i) the role of ICU sinks as a reservoir of *Serratia*; ii) the phenotypic and genotypic diversity of *Serratia*; and iii) the dynamics of *Serratia* genomes from sinks and patients in the hospital environment.

4.3.2 *Serratia* in the ICU hospital environment

We analyzed the presence and dynamics of *Serratia* in 2,417 abiotic samples recovered from sinks (n=1,126) and room surfaces (n=1,291) according to what was described in section **3.1**., analyzing more than 13,600 isolates of distinct bacterial species. Bacterial isolates from wet and dry surfaces differ significantly, with sinks being more enriched in Gram-negative bacteria and dry surfaces in Gram-positive bacteria (chi-square: p-value<2.2E-16). For wet surfaces, the most common genera were *Serratia* (43.8%), *Pseudomonas* (37.4%), *Staphylococcus* (35.4%), *Stenotrophomonas* (20.1%), *Achromobacter* (17.2%), *Burkholderia* (16.8%), and *Klebsiella* (16.6%). This high detection of *Enterobacterales* in "wet" (sink) samples (**Figure 18**), especially for *Serratia*, interested us in studying sinks as a reservoir for *Serratia*. The highest recovery rate occurred in period A, overlapping with the ICU outbreak, and drastically decreased during periods B and C. At this time, *Pseudomonas* and *Klebsiella* predominated the ICU sinks.

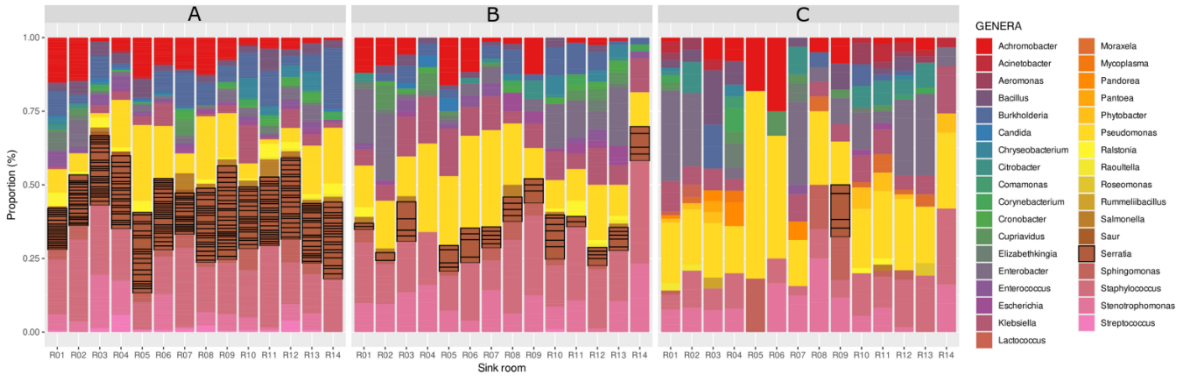

Figure 18 | Bacterial genus proportion in sinks during periods A, B, and C.
Positive samples are observed, *Serratia* marked brownish and bordered in black.

Figure 19 shows the spatiotemporal distribution of the 1,460 isolates of *Serratia*. Most of the colonies tested were preliminarily identified using MALDI-TOF-MS as *S. marcescens* (n=1,270, 88.7%; 428/448, 95.5% samples), *Serratia ureilytica* (n=152, 10.6%; 99/448, 22.1% samples), *Serratia nematodiphila* (n=9, 0.6%; 3/448, 0.7% samples), and *Serratia entomophila* (n=1, 0.1%; 1/448, 0.2% samples). *S. marcescens* and *S. ureilytica* isolates were found in all 14/14 sinks, while *S. entomophila* was detected only once, and *S. nematodiphila* was isolated in a single room during period C. A similar sink colonization pattern by *Serratia* was observed in the sinks of the renewed ICU ward months after opening on a different floor (data not shown).

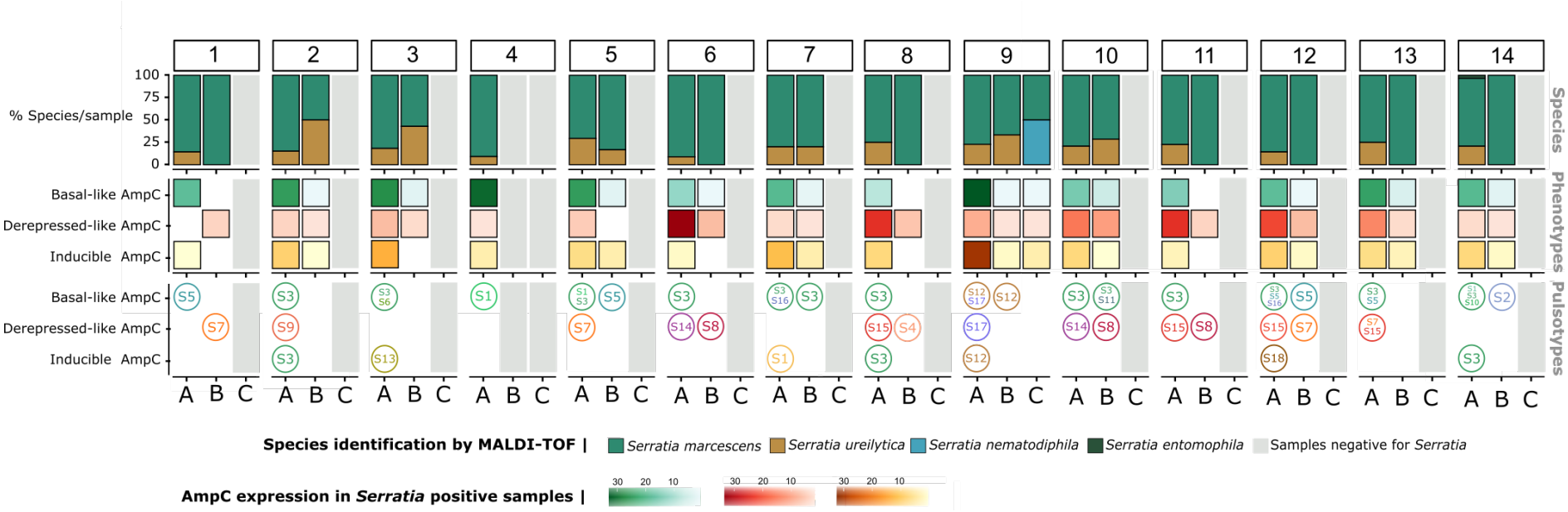

Figure 19 | Spatiotemporal distribution of *Serratia* at ICU.
Columns labeled by numbers embedded in boxes represent the 14 ICU rooms. Capital letters designate the study periods: A (March 2019-February 2020), B (July 2020-February 2021), and C (March 2021-December 2021), according to patient occupancy and use of the ICU hospital space, namely, ICU occupancy before (A) and after SARS-CoV lockdown (B), and patient clearing and conversion of the ward for other purposes unrelated to inpatient care (C). The first line shows the diversity and percentage of each *Serratia* species according to MALDI-TOF MS. The second row reflects the diversity of AmpC phenotypes, each phenotype being represented by a color: i) basal-like expression of the AmpC enzyme (AMC^{S}+FOX^{S}+$3GC^{S}$); ii) derepressed-like AmpC expression (AMC^{R}+FOX^{R}+$3GC^{R}$+$4GC^{R}$±$carbapenems^{R}$), and iii) inducible AmpC β-lactamase expression (AMC^{R}+FOX^{R}+$3GC^{S}$). The third row represents the most common pulsotypes (PT) based on XbaI-digested genomic DNA patterns of isolates with distinct AmpC phenotypes.

4.3.3 Genomic diversity of *Serratia* strains

We selected 94 isolates for detailed clonal and genome typing/clustering analyses. The selection was randomly based on the spatiotemporal distribution of species and phenotypes after eliminating redundancies (same antibiogram, morphology, and sampling site). Preliminary clonal analysis using PFGE typing identified 18 pulsotypes (PTs), with 15 corresponding to *S. marcescens* and three to *S. ureilytica* according to MALDI-TOF (**Figure 19**). Certain PTs, notably PT-S3, were consistently found across most sinks during the study, while others were specific to particular sinks (**Annex 5**). Some PTs expressed different β-lactam phenotypic patterns, while others were associated with a single phenotype. 66 isolates (64 from wet surfaces, two from dry surfaces) representing the spatiotemporal distribution, the diversity of β-lactam-phenotypes, and the PFGE patterns were selected for whole-genome sequencing and genomic analyses.

To further explore the phylogenetic diversity and understand how variation in habitat quality affects *Serratia* populations in the hospital environment, we compared these 66 ICU-environmental isolates with 99 clinical isolates representing the epidemiology (clinical isolates) of *Serratia* in our institution in the last years. The dataset of genomic and epidemiological metadata of the 165 sequenced isolates is summarized in **Annex 6**.

4.3.3.1. Phylogenomic analysis of the core genome of *Serratia*

The chromosome length of the isolates ranged from 4,9 to 5,4 Mbp, with an average G+C content of 59.4% (**Annex 6**). The core genome-based phylogenetic tree in **Figure 20** revealed four major clades with subclades, each corresponding to a designated species (see the following section). Multi-locus Sequence Typing (MLST), yielding new Sequence Types (STs) assigned by the curators of PubMLST (https://pubmlst.org/) (Jolley, Bray and Maiden, 2018), and single nucleotide polymorphisms per megabase (SNPs/Mb) were analyzed in the core genomes of clades and subclades (**Figure 21**). Information about strains grouped in clades is summarized in **Table 3**.

In our hospital, diverse *Serratia* populations coexist. *Serratia* isolated from sinks were primarily grouped in the predominant clades 3 and 4, with some interspersed in clade 2B. Clade 3 showed a difference of 0 to 11,560 SNPs/Mb, median of 9,297 SNPs/Mb, and 27 STs, including highly related isolates from four ICU sinks and patients.

These sink-patient isolates, belonging to ST525, only differed in 0-7 SNPs/Mb and were continuously collected from 2015 to 2020, distinct from the other 36 clinical strains. Some of these clinical isolates corresponded to STs recovered long ago from different wards, each represented by three isolates differing in 5-13 SNPs/Mb. All strains exhibited an AmpC inducible phenotype, except two outbreak isolates with a derepressed-like phenotype that contained an IncL plasmid harboring *bla*$_{\text{OXA-48}}$.

Subclade 4A showed a difference of 0 to 16,498 SNPs/Mb, a median of 4,736 SNPs/Mb, and 5 STs, mainly encompassing highly related genomes from sink isolates with AmpC basal-like expression. ST92 (0-3 SNPs/Mb; isolates from 11 sinks) and ST470 (0-21 SNPs/Mb; isolates from seven sinks) were the most represented STs. ST92 included 21 sink genomes and two clinical isolates collected in 2015 and 2016, one carrying a plasmid harboring *bla*$_{\text{VIM-1}}$, whereas the rest of the 11 sink isolates corresponded to ST470. Three STs correspond to unrelated genomes from clinical isolates (2004-2019).

Subclade 4B showed a difference of 0 to 17,740 SNPs/Mb, a median of 6,376 SNPs/Mb, and 10 STs, comprising both unrelated and clonally related environmental and clinical (outbreak) VIM-1-producing isolates with a depressed-like phenotype (ST424, 0-5 SNPS/Mb, 2017-2020). This epidemic clone was collected from 7/14 ICU sinks for at least 18 months during different outbreaks and persists to date (data not shown).

Table 3 | Metadata about strains from each of the major clades and subclades

Clade/Subclade	N	Species (GTDB)	Origin	Phenotype	MLST	Year
1A	2	*S. nematodiphila*	P(2)	Inducible(2)	ST431(2)	2004(1), 2007(1)
1B	3	*S. marcescens*	P(3)	Inducible(3)	ST459(1), ST503(1), ST511(1)	2003(1), 2009(1), 2016(1)
2A	15	*S. bockelmannii*	P(15)	Inducible(15)	ST31(3), ST197(1), ST407(1), ST416(1), ST420(1), ST432(1), ST445(1), ST446(1), ST448(1), ST500(1), ST502(1), ST507(1), ST510(1)	2004(3), 2005(4), 2006(1), 2007(2), 2011(1), 2012(1), 2013(1), 2015(2)
2B	26	*S. ureilytica*	P(21), S(5)	Inducible(23), Basal-like(3)	ST485(3), ST195(2), ST307(2), ST447(2), ST213(1), ST238(1), ST275(1), ST405(1), ST409(1), ST413(1), ST419(1), ST433(1), ST436(1), ST453(1), ST455(1), ST456(1), ST458(1), ST496(1), ST501(1), ST650(1)	2003(1), 2004(5), 2005(2), 2006(1), 2007(1), 2008(1), 2009(1), 2012(2), 2013(1), 2014(1), 2015(2), 2019(4), 2020(1), NA(1)
3	41	*S. marcescens/nevei*	P(36), S(5)	Inducible(39), Derepressed-like(2)	ST525(5), ST255(3), ST366(3), ST394(3), ST408(3), ST417(2), ST807(2), ST340(1), ST356(1), ST367(1), ST375(1), ST376(1), ST379(1), ST404(1), ST412(1), ST423(1), ST427(1), ST428(1), ST439(1), ST444(1), ST449(1), ST462(1), ST490(1), ST508(1), ST512(1), ST56(1), ST679(1)	2003(2), 2004(3), 2005(2), 2006(1), 2007(3), 2008(2), 2009(3), 2010(1), 2011(4), 2012(2), 2013(1), 2014(2), 2015(2), 2016(3), 2018(2), 2019(5), 2020(1), NA(2)
4A	37	*S. nevei*	S(32), P(5)	Basal-like(29), Inducible(7), Derepressed-like(1)	ST92(23), ST470(11), ST434(1), ST451(1), ST457(1)	2004(1), 2007(1), 2015(1), 2016(2), 2019(25), 2020(7)
4B	41	*S. nevei*	S(22), P(17), D(2)	Derepressed-like(26), Inducible(15)	ST424(25), ST430(5), ST402(3), ST327(1), ST352(1), ST414(1), ST415(1), ST425(1), ST438(1), ST454(1), ST485(1)	2004(2), 2006(4), 2008(1), 2009(1), 2010(1), 2011(1), 2013(1), 2014(1), 2016(2), 2017(2), 2019(17), 2020(7), NA(1)

Abbreviations: D(Dry), N(Nº of genomes), P(Patient), ST(Sequence Type), S(Sink).

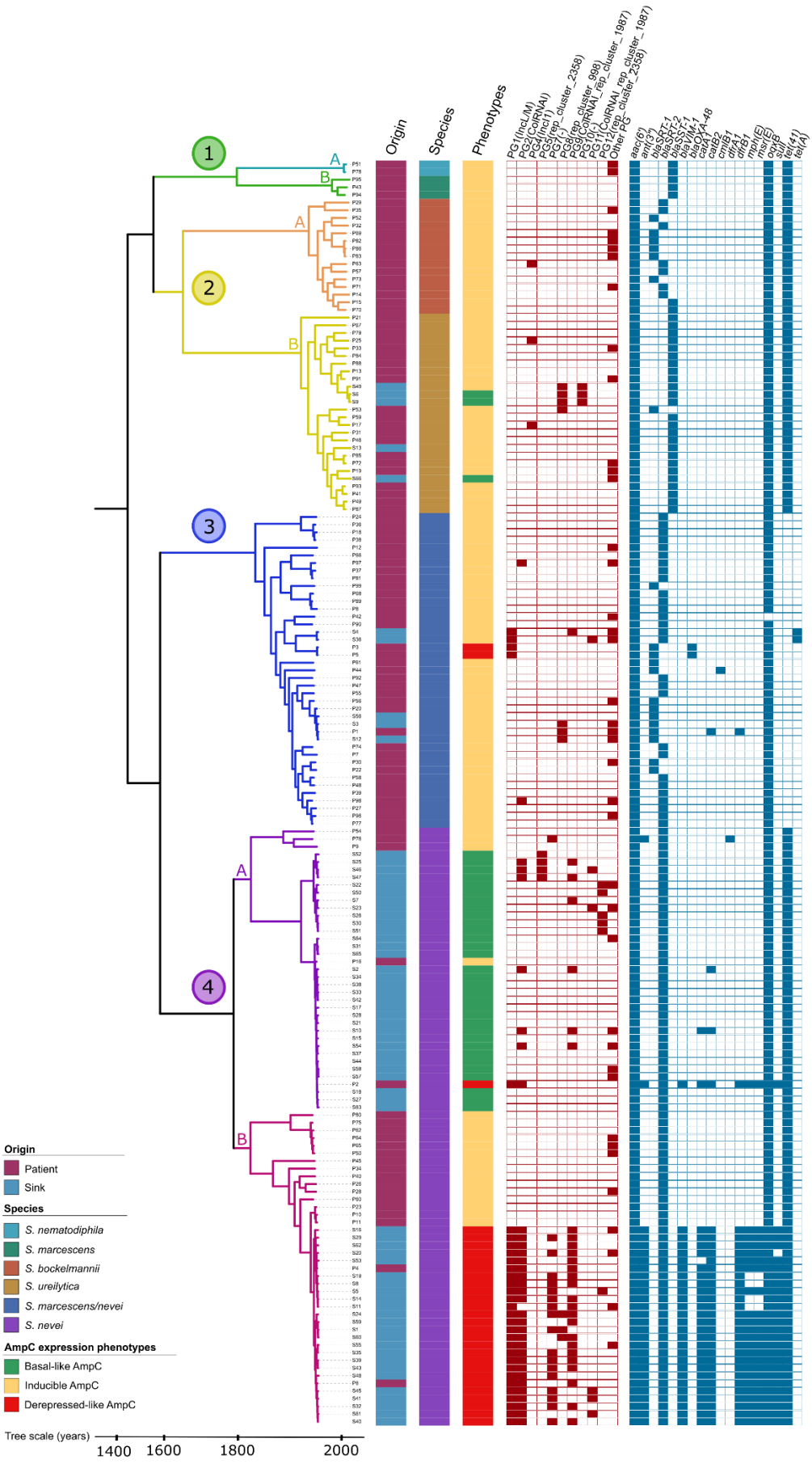
Origin
Species
Phenotypes
PG1(IncL/M)
PG2(ColRNAI)
PG4(IncI1)
PG3(rep_cluster_2358)
PG7(-)
PG8(rep_cluster_998)
PG10(-)
PG11(ColRNAI rep_cluster_1987)
Other PG
aac(6')
aph(3'')
blaSRT-1
blaSRT-2
blaSST-1
blaNMC-1
blaNMA-48
catA2
catB1
dfrA1
dfrB1
mph(E)
msr(E)
sul2
tet(41)
tet(A)
1
2
3
4
A
B
Origin
Patient
Sink
Species
S. nematodiphila
S. marcescens
S. bockelmannii
S. ureilytica
S. marcescens/nevei
S. nevei
AmpC expression phenotypes
Basal-like AmpC
Inducible AmpC
Derepressed-like AmpC
Tree scale (years)
1400
1600
1800
2000

Figure 20 | Phylogenetic structure of 165 isolates from the *S. marcescens* complex at HURyC.
A maximum likelihood tree was built with the 45,720 SNPs taken from the 2,583 core genes. Strains were obtained from sinks and patients (stool, bloodstream, and outbreak-related) from 2003–2020. The main clades and subclades are shaded accordingly (see key). The origin of the sample (patient/sink), the species name according to genome similarity (*S. nematodiphila*, *S. marcescens, S. bockelmannii, S. ureilytica, S. marcescens/nevei, S. nevei*), the AmpC phenotype expression (AmpC basal-like, AmpC inducible, AmpC derepressed-like, no phenotype tested), the plasmid groups (PG, MOB-Typer), and the antibiotic resistance genes (ResFinder) are represented from left to right and labeled accordingly (see keys).

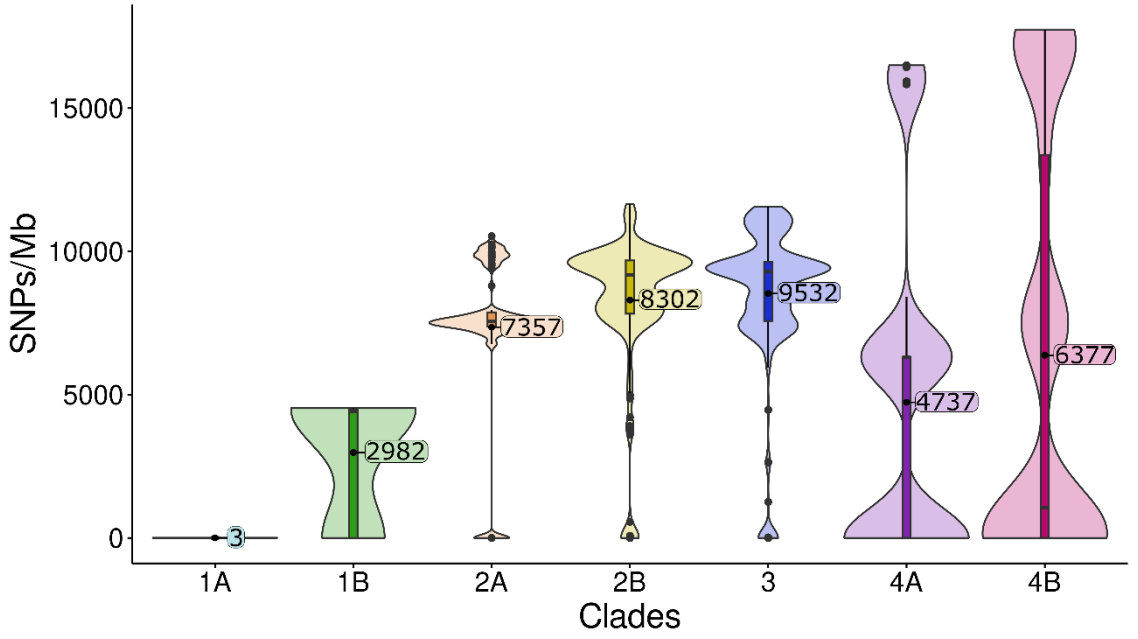

Figure 21 | Violin plot showing the SNPs/Mb distribution among the major clusters of the core *Serratia* genome.
SNPs ranged from 35,533 to 45,719 SNPs/Mb between genomes of clades 1 and 2 (42,009 SNPs/Mb median distance). The significance values (Wilcoxon test + Bonferroni p-adjust) referring to comparisons of distributions of SNPs/Mb across subclades ranged from $p<0.001$ (1A-2A, 1A-2B, 1A-3, 1A-4A, 1A-4B, 2A-2B, 2A-3, 2A-4A, 3-4A, 3-4B, 4A-4B) to $p<0.05$ (1B-2A, 1B-2B, 1B-3, 1B-4B, 2A-4B). Comparisons 1A-1B, 1B-4A, and 2B-3 were not significant ($p>0.05$).

Clades 1 and 2 were less frequent and contained mostly patient strains, with only five environmental isolates from four sinks with inducible and basal-like AmpC phenotype located in subclade 2B (10-11,656 SNPs/MB, median of 9,180, 22 STs). Subclade 2B also included 21 clinical isolates (18 STs). Subclade 2A only accounts for clinical isolates (6,729-10,251 SNPs/Mb, median of 7,565, 13 STs), three of them clonally related (ST31, 0-1 SNP/Mb, 2004). Subclade 1A (ST431, 5 SNPs/Mb, 2004-2007) and

subclade 1B (3 STs) were less represented in our sample, comprising only clinical isolates.

To contextualize our results within the *Serratia* population structure, we conducted a phylogenetic comparison of all available NCBI genomes (**Figure 22**). Our collection reflects a highly similar distribution to the available *Serratia* genomes in databases, confirming that our strains represent human-associated *Serratia*'s known diversity.

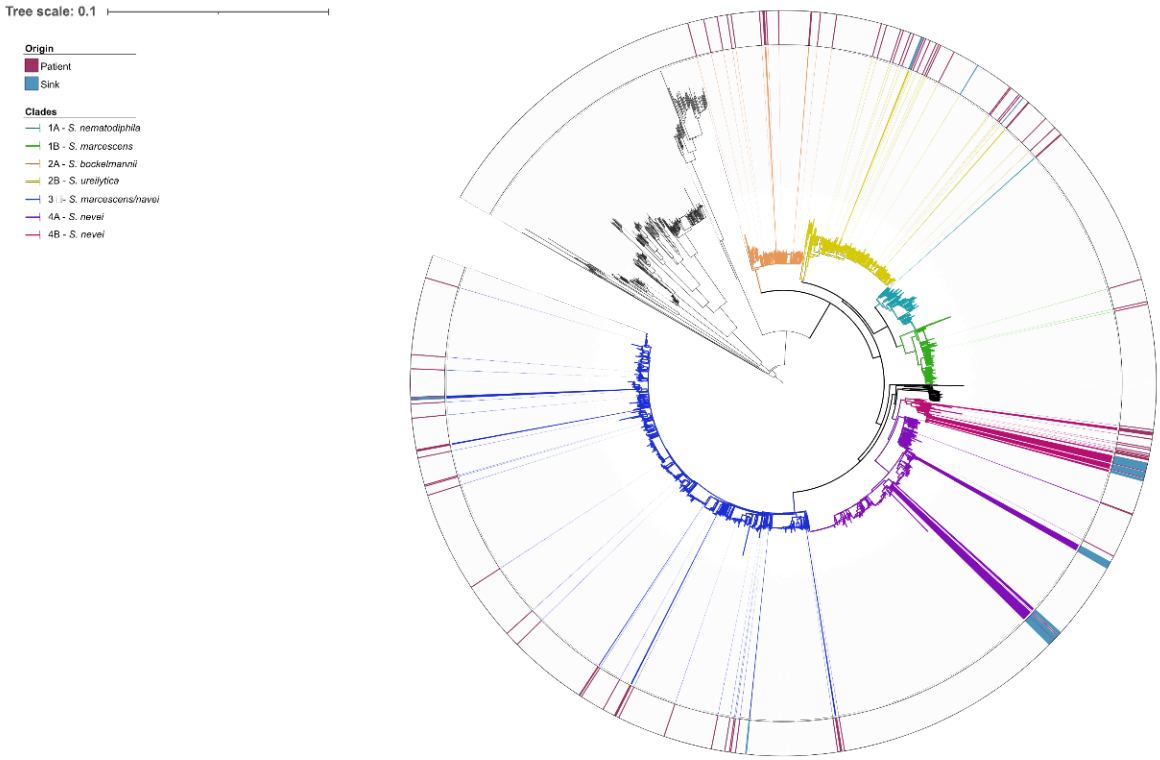

Figure 22 | MASH-based phylogenetic tree of the *Serratia* strains represented in this work compared with other NCBI database sequences (last accessed 12 January 2024).
Clades and subclades from the core-based phylogenetic tree of *Serratia* in this work are represented by branch colors (see key), and the origin (patient/sink) is indicated for the isolates.

4.3.3.2. *Serratia* taxonomy and designation/epidemiological typing

The species taxonomy of *Serratia* has been debated since the description of the genus to date (Ono *et al.*, 2022; Williams *et al.*, 2022). We compared the results for MALDI-TOF-MS for species identification with different genomic tools. The correlation of each clade/subclade with known species was established by comparing these genomes with the GTDB and the NCBI, which are considered the standardized microbial taxonomy

based on genome phylogeny (Parks *et al.*, 2018) (see section **3.13.1** for more details). rMLST, a widely used diversity identifier, was also assessed (Jolley *et al.*, 2012), although it did not consistently reach the species level in most cases. In those taxonomy tools, reference genomes are compared by similarity, obtaining an ANI value. **Table 4** shows each method's results and bacterial classification per clade.

Discrepancies in the species assignment when using GTDB or NCBI genome references were observed for subclade 1A [*S. nematodiphila* vs *S. marcescens*], subclade 2A [*S. bockelmannii* vs *S. ureilityca*], and clade 3 [*S. marcescens* vs. *S. nevei*], although the ANI values for any comparisons were very high.

Table 4 | Taxonomy genomic tools with the ANI value

Clade/Subclade	NCBI (ANI)	GTDB (ANI)	rMLST
1A	*S. marcescens* (98%)	*S. nematodiphila* (98%)	*Serratia* sp.
1B	*S. marcescens* (96%)	*S. marcescens* (99%)	*S. marcescens*
2A	*S. ureilytica* (95%)	*S. bockelmannii* (98%)	*Serratia* sp.
2B	*S. ureilytica* (98%)	*S. ureilityca* (98-99%)	*Serratia* sp.
3	*S. nevei* (95%)	*S. marcescens* (98-99%)	*Serratia* sp.
4A	*S. nevei* (96%)	*S. nevei* (97%)	*Serratia* sp.
4B	*S. nevei* (96-97%)	*S. nevei* (97-98%)	*Serratia* sp.

4.3.4 The resistome of *Serratia*

One of *Serratia*'s main adaptive traits is its capability to express and acquire ARGs, most of which are intrinsically encoded in the chromosome. In this section, we explore *Serratia's* ability to develop intrinsic and acquired resistance to clinically relevant genes while shedding light on its significance in expressing phenotypic traits, enhancing this bacteria's adaptability to select gene pools.

4.3.4.1. Intrinsic resistance

All *Serratia* strains contained chromosomally located genes associated with resistance to various antibiotic families: β-lactams (bla_{AmpC}), aminoglycosides (*aac(6')-Ic*), tetracyclines (*tet*41) (Shaw *et al.*, 1992; Matsumura, Minami and Mitsuhashi, 1998; Thompson *et al.*, 2007), polymyxins (*pmrA*) (Lin *et al.*, 2014) and quinolones (*oqxB*)

(Andres *et al.*, 2013). Efflux pumps of the resistance-nodulation-division (SdeAB, SdeXY, OqxAB), ABC (SmdAB), and small multidrug resistance (SsmE) families associated with resistance to a variety of antibiotics and/or biocides were also detected in all isolates (Sandner-Miranda *et al.*, 2018; Mariscotti and Véscovi, 2021; Shirshikova *et al.*, 2021). *ant(3´´)*-Ia, previously considered part of the intrinsic resistome, was only detected in clade 4 (*S. nevei*). All isolates but those of clade 3 (*S. marcescens/nevei*) contained the allele *tet*41. Of particular interest remain the AmpC β-lactamase due to the intrinsic β-lactam resistance property of *Serratia* and the findings observed along this work for the variety of phenotypes, some described here for the first time, and some others previously reported (Sandner-Miranda *et al.*, 2018).

AmpC β-lactamase expression. Phenotypic and genotypic variability for the housekeeping gene encoding the cephalosporinase AmpC was analyzed in *Serratia*. This enzyme is generically known as "SRT/SST" (a name coined in early papers and coming from *Serratia*-Resistant to β-lactam T-5575-SRT and *Serratia*-Susceptible to β-lactam T-5575-SST, respectively) (Matsumura and Mitsuhashi, 1995; Matsumura, Minami and Mitsuhashi, 1998).

Three phenotypic patterns were identified according to the β-lactam susceptibility profiles, which we designate as basal-like, inducible, and derepressed-like. The basal-like phenotype first described in this work, showed a susceptible pattern for aminopenicillins (AMC^{S}+FOX^{S}+$3GC^{S}$) that is similar to that of *E. coli* but is exceptional for the ESCPM group, and it has not been previously described for *S. marcescens* (Livermore, 1995). The inducible phenotype represents the characteristic *Serratia* phenotype (AMC^{R}+FOX^{R}+$3GC^{S}$), as *Serratia* contains a chromosomal AmpC of inducible character (Tamma *et al.*, 2019). Based on phenotypic studies, the third phenotype was classified as derepressed-like due to its intrinsic nature of AmpC being derepressed (AMC^{R}+FOX^{R}+$3GC^{R}$$\pm$$4GC^{R}$$\pm$$carbapenems^{R}$). However, as described in the following sections, the AmpC derepressed-like phenotype is mimicked in a non-depressed isolate by the presence of the carbapenemase VIM-1 because we did not detect constitutively derepressed-like AmpC patterns in strains lacking bla_{VIM-1}. Resistance to chloramphenicol, gentamicin, and sulfamethoxazole-trimethoprim was observed only among AmpC derepressed-like *Serratia*, whereas susceptibility to ciprofloxacin and tetracycline varied significantly within and between phenotypes. Antibiotic susceptibility is summarized in **Table 5**.

Table 5 | Antibiotic susceptibility patterns based on disk-diffusion (mm of the diameter of the inhibition zone) testing for the three major AmpC phenotypes of *Serratia*

	AMP10	AMC30	FOX30	CTX5	CZD10	FEP30	ATM30	MEM10
Basal-like	S (>14)	S (>19)	I (0-30)	S (>17)	I (0-30)	S (>24)	S (>30)	S (>20)
Inducible	R	R (<19)	R	S (>20)	S (>19)	S (>25)	S (>26)	S (>16)
Derepressed-like	R (0-13)	R (0-18)	R (0-19)	R (0-16)	R (0-18)	I (0-30)	I (0-35)	I (0-30)

	ATM30	CIP5	CHL30	GMN10	TOB10	TET30	SXT25
Basal-like	S (>30)	I (0-30)	S (>22)	S (>17)	S (>16)	I (0-30)	S (>30)
Inducible	S (>26)	I (0-30)	S (>19)	S (>18)	S (>17)	I (0-30)	S (>29)
Derepressed-like	I (0-35)	I (0-30)	R (<17)	I (0-30)	NA	I (0-30)	I (0-30)

All AmpC expression patterns were detected overall the study, although those with the basal-like phenotype (286/448 sink samples, 63.8%) predominated over the "classical" AmpC phenotype either inducible (144/448, 32.1%) or derepressed-like (180/448, 40.2%) (**Figure 19**). *Serratia* isolates exhibiting all three AmpC phenotypes were regularly detected in the same sink sample, although the frequency of each phenotype varied among sinks. During period B, a progressive decrease in the recovery of inducible *Serratia* phenotypes and increased derepressed-like AmpC isolate detection was observed. At the time of writing, all these phenotypes are still being recovered (further studies) from sinks in the former and the new ICU wards.

Clinical isolates were also tested for susceptibility to β-lactams. All 94 blood isolates showed an inducible AmpC phenotype, while the five outbreak isolates exhibited a derepressed-like AmpC phenotype attributed to the VIM-1 production. Isolates with AmpC basal-like expression exhibited MICs to aminopenicillins lower than those producing inducible AmpC (2-8 mg/mL vs. 16/8->64 mg/mL, respectively). **Annex 7** shows the antibiogram images and induction assays representative of each phenotype.

All the genomes encoded the AmpC cephalosporinase and their regulatory proteins AmpR, AmpD, AmpE, and AmpG. However, mutations in AmpC, AmpR, and AmpD were specific to the different clades as observed for other species of *Enterobacterales* (Jacoby, 2009) (**Figure 23**). In addition to the highly conserved AmpC motifs (64SXSK, 150YXN, and 315KTG) and other conserved residues linked to the reference AmpC β-lactamase of *Serratia* SRT/SST in positions N204S, E250D, H355R, and E361D, we observed amino acid variations at positions N86K and R91H located in the middle of an alpha-helix and a bend or turn (Mack *et al.*, 2020; Philippon *et al.*, 2022). Some mutations (GC>AT) in the intergenic region of *ampC*/*ampR* genes were observed (Mahlen *et al.*,

2003). This may increase the number of stop codons and affect the half-life of AmpC, thus decreasing its activity against the antibiotic.

The alignment of AmpR identified a common mutation concerning the reference in position 243, although we detected more differences at the clade level for the alignments of AmpD. The conserved domains previously reported are maintained instead of the one at position 106 of the alignment (Langaee, Dargis and Huletsky, 1998). Two mutations involving clades 3 and 4 are located at positions 122 and 148. To get more knowledge about this topic, please visit the original article (Aracil-Gisbert *et al.*, 2024).

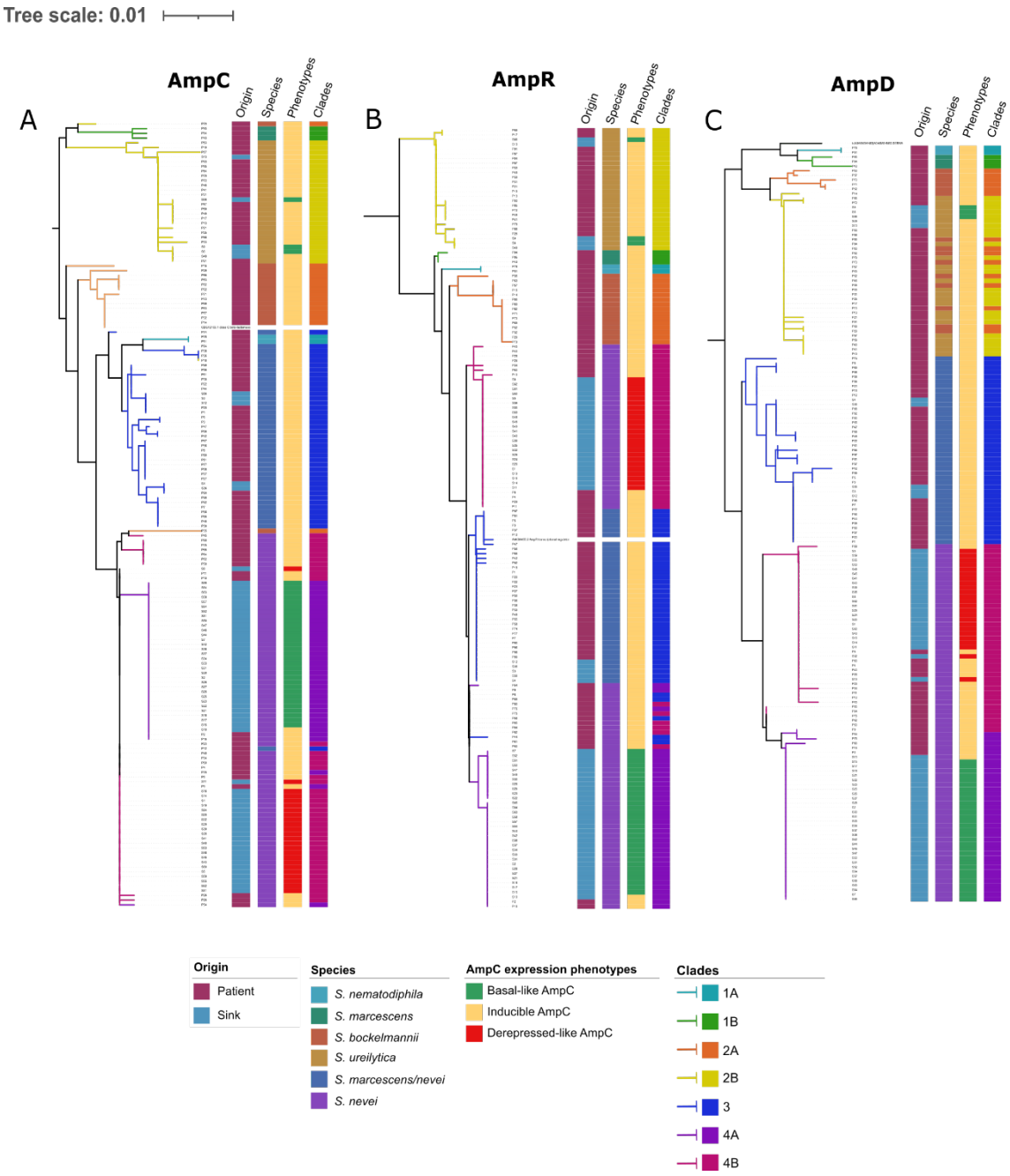

Figure 23 | Phylogenetic analysis of AmpC, AmpR and AmpD enzymes
Phylogenetic tree of a multiple sequence alignment of the AmpC, AmpR, and AmpD protein sequences of *Serratia* spp. (panels A, B, and C, respectively) generated by ClustalW (https://www.ebi.ac.uk/Tools/msa/clustalo/). The epidemiological features of the isolates (β-lactam phenotype, sample origin, *Serratia* species, and clades/subclades) inferred from the core genome phylogenetic tree are represented in bars (see keys).

4.3.4.2. Acquired resistance

The isolates clustered in subclade 4B (ST424) carried a class 1 integron comprising genes that encode resistance to carbapenems (*bla*$_{\text{VIM-1}}$), aminoglycosides (*aac(6')Ib*), chloramphenicol (*catB2*), trimethoprim (*dfrB1*), sulfonamides (*sulI*), and quaternary ammonium salts (*qacEdelta1*) (**Figure 20**). The IS*26*-*msr(E)*-*mph(E)*-IS*26* transposon conferring resistance to macrolides and triamilides but not lincosamides, widely spread in the plasmids of *Enterobacterales* and water systems (Carattoli and Hasman, 2020; Blackwell, Doughty and Moran, 2021), was detected upstream from class 1 integron. *bla*$_{\text{OXA-48}}$ carbapenemase gene was also detected but confined to clinical outbreak isolates.

4.3.5 Highlights

❖ Different populations previously associated with distinct *Serratia* species (*S. marcescens* but also *S. ureilytica* or *S. nevei*) belong to a **single *S. marcescens* species** according to the high value of ANI. This is now designed as the **"*S. marcescens* complex" (SMC).**

❖ The **coexistence of diverse *Serratia* populations of the SMC** within the same ecological niche suggests a high degree of adaptation and diversification to disparate and changing conditions, explaining the survival and persistence of discrete populations in the hospital environment. This **genotypic and phenotypic diversity** complicates the diagnosis and management of infections.

❖ The **variability of AmpC β-lactamase expression** of the SMC populations contrasted with the traditional assertion about the intrinsic resistance to β-lactams of *S. marcescens*. The "basal-like" phenotype was observed for other species of the ESPCM group but not for *S. marcescens*, explaining the efficacy in treating *Serratia* infections with β-lactams in some cases, and reinforcing the need to identify the SMC clusters before implementing therapy.

CHAPTER 4.
THE CONTRIBUTION OF THE ICU WARD TO THE TRANSMISSION OF AMR

CAPÍTULO 4.
LA CONTRIBUCIÓN DE LA UCI A LA TRANSMISIÓN DE LA RAM

4.4.1 Motivation

Broad host-range plasmids, which can replicate stably in diverse bacterial genera (e.g. Gram-negative bacteria such as *Serratia* and *Klebsiella*), play a major role in introducing resistance determinants to opportunistic bacterial species that contribute to nosocomial infections and persistent colonization in humans or hospital environments (Blackwell, Doughty and Moran, 2021). Since the 1970s, plasmids from incompatibility (Inc) groups L and M have been associated with ARGs encoding ESBLs and class A, B, and D carbapenemases (Carattoli *et al.*, 2015; Blackwell, Doughty and Moran, 2021). In particular, a unique epidemic IncL-type plasmid (pOXA-48) is responsible for the worldwide dissemination of *bla*$_{\text{OXA-48}}$, which showed high backbone homology with other IncL/M plasmids (Poirel, Bonnin and Nordmann, 2012; Carattoli *et al.*, 2015).

In our hospital, clonal and polyclonal outbreaks of *Enterobacterales* producing VIM- and OXA-48 carbapenemases that are associated with IncL plasmids have been described since 2005 and 2016, respectively (Tato *et al.*, 2010; León-Sampedro *et al.*, 2021; Pérez-Viso *et al.*, 2021). The variability of plasmid pOXA-48 in our hospital has extensively been studied (Hernández-García et al., 2019; León-Sampedro et al., 2021).

This chapter analyzes the diversity and dynamics of an IncL plasmid encoding *bla*$_{\text{VIM-1}}$ or *bla*$_{\text{OXA-48,}}$ highly similar to the epidemic pOXA-48 circulating in our hospital with emphasis in the role of *Serratia* as a reservoir of broadhost plasmids encoding carbapenemases such as the IncL group.

4.4.2 The plasmidome of *Serratia*

First, we analyzed the plasmidome of the 165 isolates of *Serratia* (see section **4.3**, **Chapter 3**) to identify plasmids encoding carbapenemases (specifically with VIM-1 and OXA-48) and to establish a comprehensive plasmidome landscape of *Serratia,* as it was not well explored until now.

We detected 190 plasmids across the 165 *Serratia* isolates, distributed into ten plasmid groups (PGs) among the different clades (**Table 6**). Plasmids were more common in sink isolates than patient isolates (**Figure 24**). Among those sink strains, L/M plasmids (PG1) predominated. Col and IncF-like (PG7 and PG8) were also common in our collection. Of particular interest are PG1 and PG8, which appear to be transferable between sink *Serratia* populations. From those populations, clades 4A and 4B (*S. nevei*) showed the highest variety of PG associated, followed by clade 3 (*S. marcescens/nevei*).

Table 6 | Plasmid Group dataset

						Origin		**Clades/Subclades**						
PG	**Rep-type**	**N PG**	**Size (kb)**	**Relaxase_Type**	**Mash_ID**	**P**	**S**	**1A**	**1B**	**2A**	**2B**	**3**	**4A**	**4B**
PG1	IncL/M	31	44.0-74.6	MOBP(30), -(1)	CP023251, CP023419, KX230795	5	26	0	0	0	0	4	1	26
PG8	rep_988	10	96.3-107.1	MOBP(10)	CP018916	2	8	0	0	0	4	3	0	3
PG7	-	18	62.2-64.4	-(18)	CP042515	1	17	0	0	0	0	0	1	17
PG10	-	3	37.9	MOBP(3)	CP018921	0	3	0	0	0	3	0	0	0
PG4	IncI1	3	55.2-80.7	MOBF(3)	LT575492	3	0	0	0	1	2	0	0	0
PG5	rep_2358	4	3.6	MOBP(4)	CP034043	0	4	0	0	0	0	0	4	0
PG2	ColRNAI	34	1.5-2.4	-(34)	CP041737	5	29	0	0	0	0	2	7	25
PG9	ColRNAI	27	2.8-5.9	MOBP(27)	CP016867, CP024503, CP024519	2	25	0	0	0	0	1	6	20
PG11	ColRNAI	6	3.3	MOBP,MOBP(6)	CP016867	0	6	0	0	0	0	1	2	3
PG12	ColRNAI	6	3.3-5.8	MOBP(6)	CP016867	0	6	0	0	0	0	0	5	1
Other	multiple	48	1.1-107.1	multiple	multiple	31	17	3	0	9	5	16	7	8

Abbreviations: PG (Plasmid Group), P (Patient), S (Sink).

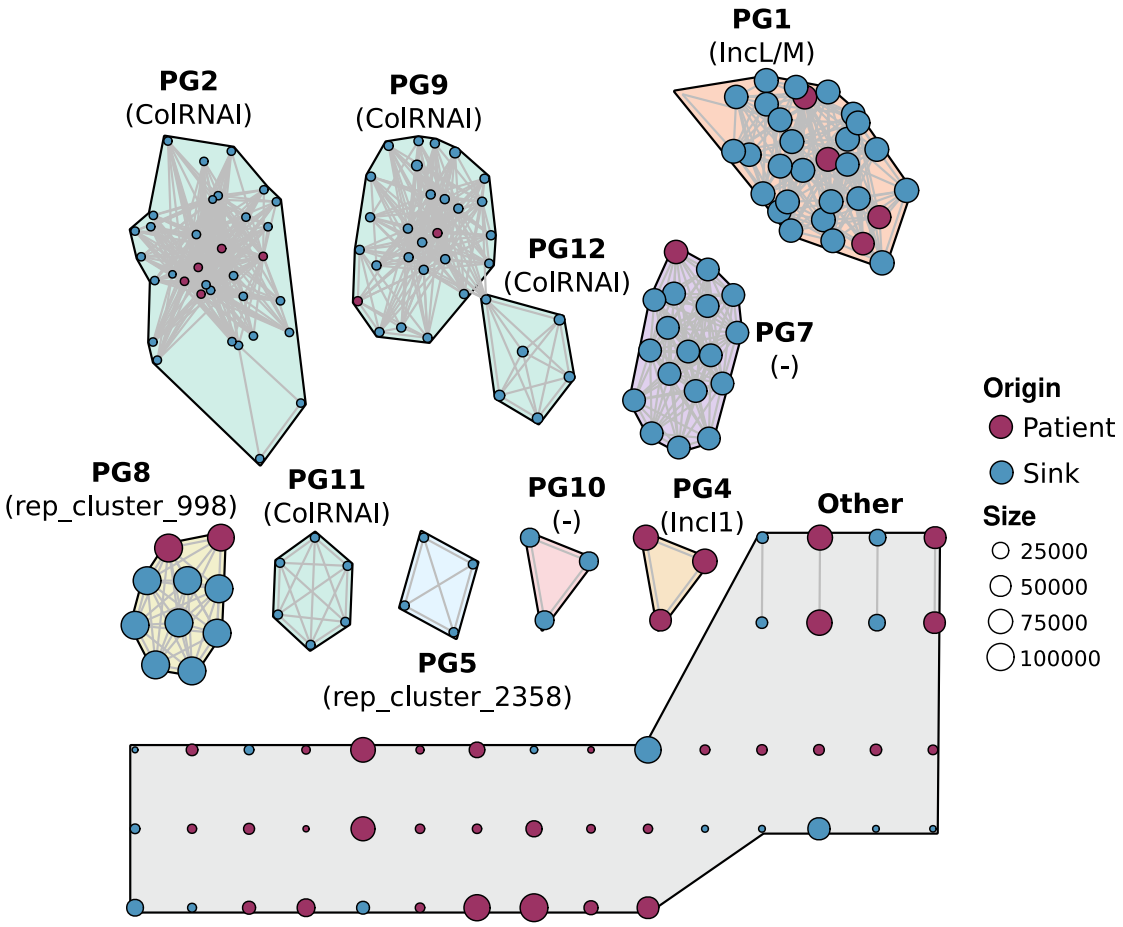

Figure 24 | Plasmidome of the "*S. marcescens* complex".
Plasmid network built with the k-nearest neighbors' algorithm (K-NNN) using the "K-NNN" function of the *PATO* R package. Each node represents one plasmid and is colored according to the origin (patient vs. sink), its molecular weight is proportional to the node size (see keys). A plasmid group (PG) was defined using the Louvain algorithm over the network structure, each plasmid being connected with its best hits (Jaccard similarity >0.5, coverage/size difference <50%). PGs were arbitrarily designated with a number; their replicon content, defined by the MOB-typer tool, is shown below the PG label in brackets.

4.4.3 IncL/M plasmids from the PG1 of *Serratia*

The PG1 comprises plasmids of high epidemiological value belonging to the L and M families (Carattoli *et al.*, 2015; Blackwell, Doughty and Moran, 2021). PG1 is overrepresented by a predominant and highly conserved IncL plasmid (~70kb, 51.4% GC content) carrying a ~6kb class 1 integron harboring *bla*$_{VIM-1}$ (**Figure 25**), which was highly similar to pB77-CPsm (GenBank: MN913381.1; 100% identity, 93% coverage) recovered from *Serratia* outbreak isolates in our hospital since at least 2017 (Pérez-Viso *et al.*, 2021). This plasmid was identified in clinical (n=5) and sink (n=26) isolates of clade 3 (*S. marcescens/nevei*) and clade 4 (*S. nevei*) (**Table 6**). PG1 also grouped a ~81 kb IncM1 plasmid (53.0% GC content) carrying tetracycline resistance genes (*tetA, tetR*) in two sink isolates similar to a plasmid previously described in *E. coli* (Frazão *et al.*, 2019).

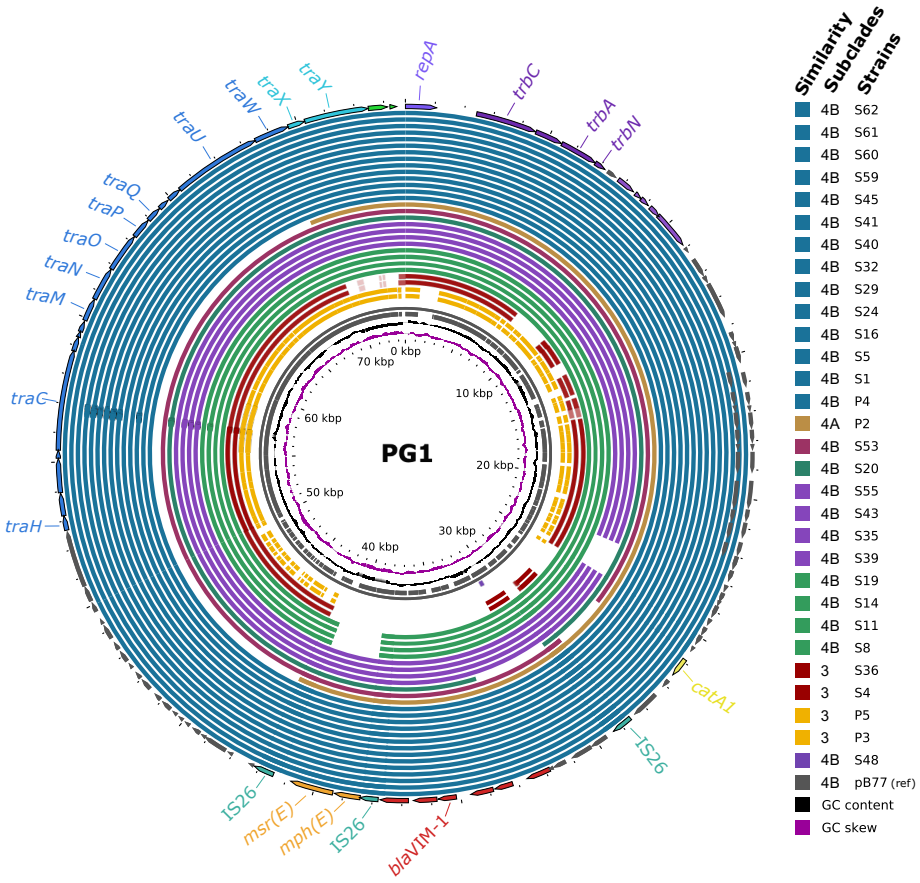

Figure 25 | BLAST Atlas of *S. nevei* IncL plasmids in PG1 compared with IncL epidemic plasmids isolated in our institution.
BLAST was applied to the coding sequences (CDS) within the reference plasmid from this group, obtained through annotation via Bakta of one of the outbreak plasmid strains (pB77, P6 strain) against sequence regions in the query plasmids. The circularized map of the plasmids was

rendered with Gview (https://server.gview.ca/). The inner slots represent the reference's GC skew, GC content, and CDS regions. The colored slots represent plasmid data from PG1 strains, mainly from subclades 3, 4A, and 4B.

4.4.4 IncL plasmids circulating in the hospital

The gene array of the *bla*$_{VIM-1}$ integron (*int*I1-*bla*$_{VIM-1}$-*aac(6')Ib-dfrB1-aadA1-catB2-qacEΔ1/sul1*) was observed in our hospital on a variety of plasmids and species of *Enterobacterales* for years (Tato *et al.*, 2007, 2010; Pérez-Viso *et al.*, 2021) (**Figure 26**). We compared the plasmids isolated and identified in *Serratia* with sequences from other genera found in sinks and patients, particularly those associated with VIM-1 or OXA-48 producers, as it is known that an IncL plasmid harbors these resistance genes.

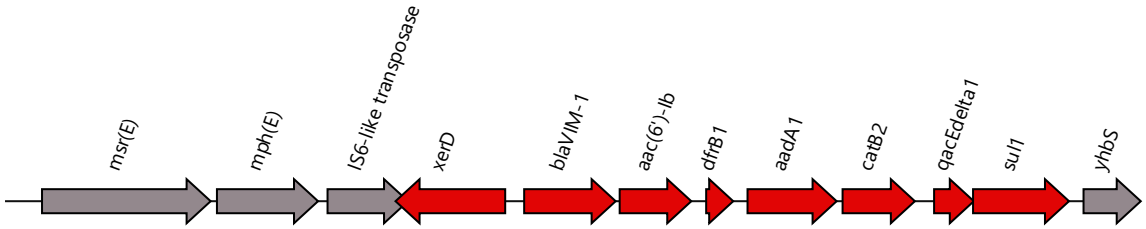

Figure 26 | Class I *bla*$_{VIM-1}$ integron genes (red arrows) and nearby genes (grey arrows)

The comparative analysis revealed 11 variants of the IncL plasmid (**Table 7**). Those plasmid variants differ in few SNPs and/or small indels, rearrangements, or duplications and were detected in isolates of *K. pneumoniae, Klebsiella variicola, Citrobacter cronae,* and *Enterobacter roggenkampii* collected for at least five years (2017-2022) from patients (Tato *et al.*, 2010), and sinks (Guerra-Pinto *et al.*, 2024). It is of note that this plasmid was also isolated in a *K. pneumoniae* encoding *bla*$_{OXA-48}$ instead of the *bla*$_{VIM-1}$ integron, being highly similar to pOXA-48 circulating in our hospital (99.9% identity, 91% coverage) (León-Sampedro *et al.*, 2021). An IncL plasmid variant (IncL11, ~46 kb) from a clinical isolate, lacking a 27,125bp region encoding genes of the conjugation module and categorized as a singleton ("other PGs"), was highly similar to PG1.

Interestingly, we found the *bla*$_{VIM-1}$ integron in the chromosome of certain *P. aeruginosa* isolates from sinks, confirming its promiscuity and ability to be acquired by several heterogeneous bacterial hosts.

Table 7 | Plasmid types harboring *bla*$_{\text{VIM-1}}$ or *bla*$_{\text{OXA-48}}$

Plasmid type	ARG cassette	N	Species	Source	MLST	ICU room	Month/Year
IncL_1+ IncL_1inv	***bla*$_{\text{VIM-1}}$ integron**	12	*S. marcescens*(6), *K. pneumoniae*(3), *K. variicola*(1), *C. cronae*(1), *E. roggenkampii*(1)	Sink(10), Patient(2)	Kv-ST365(1), Kpn-ST985(2), Kpn-ST65(1), Cit-ST102(1)	#1(1), #5(1), #10(5), #11(2), #13(1), #NA(2)	09/2017(1), 01/2018(1), 03/2019(2), 07/2020(2), 08/2020(2), 09/2020(3), 04/2022(1)
IncL_2	***bla*$_{\text{VIM-1}}$ integron**	1	*S. marcescens*(1)	Sink(1)	-	#12(1)	10/2019(1)
IncL_3	***bla*$_{\text{VIM-1}}$ integron**	1	*S. marcescens*(1)	Sink(1)	-	#12(1)	07/2020(1)
IncL_4	***bla*$_{\text{VIM-1}}$ integron**	3	*S. marcescens*(3)	Sink(1)	-	#6(2), #10(1)	03/2019(1), 04/2019(1), 07/2019(1)
IncL_5	*bla*$_{\text{OXA-48}}$	3	*K. pneumoniae*(3)	Sink(1), Patient(2)	Kpn-ST39(3)	#13(1), #14(2)	12/2019(1), 02/2020(2)
IncL_6	***bla*$_{\text{VIM-1}}$ integron**	1	*S. marcescens*(1)	Sink(1)	-	#6(1)	09/2020(1)
IncL_7	***bla*$_{\text{VIM-1}}$ integron**	1	*S. marcescens*(1)	Sink(1)	-	#8(1)	07/2020(1)
IncL_8	***bla*$_{\text{VIM-1}}$ integron**	1	*K. pneumoniae*(1)	Sink(1)	Kpn-ST268(1)	#11(1)	05/2019(1)
IncL_9	***bla*$_{\text{VIM-1}}$ integron**	1	*K. pneumoniae*(1)	Sink(1)	Kpn-ST144(1)	#12(1)	11/2020(1)
IncL_10	***bla*$_{\text{VIM-1}}$ integron**	1	*K. pneumoniae*(1)	Patient(1)	Kpn-ST39(1)	NA(1)	Between 2005-2007
IncL_11	***bla*$_{\text{VIM-1}}$ integron**	1	*S. marcescens*(1)	Patient(1)	-	NA(1)	12/2016(1)

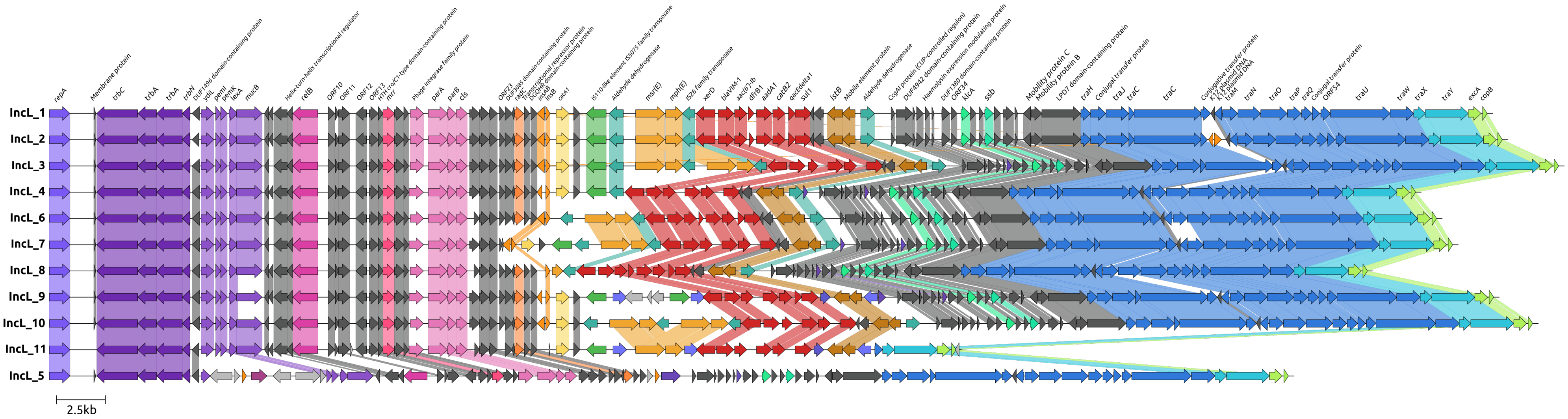

Figure 27 | Pairwise alignment among the IncL plasmid variants.
All genes of the 11 variants of IncL plasmid sequences of *Enterobacterales* obtained through MinION technologies and annotated with Bakta were aligned using clinker with GenBank files (.gbff). A 100% identity is used for cluster similarity.

4.4.5 Highlights

❖ **Sinks act as environmental reservoirs** of bacterial species that harbor and maintain plasmids encoding carbapenemases, thus facilitating their persistence and potentially spread between different species and clonal backgrounds.

❖ **IncL plasmids harboring clinically relevant ARGs** often cause outbreaks in our hospital. The **occurrence of plasmid variants** with small genetic differences (SNPs, indels) and their presence in various species illustrates the evolutionary dynamics of plasmids in hospital environments. These variants can offer insights into plasmid evolution, including host adaptation, diversification, and the directional mechanisms thorugh plasmids acquire and disseminate resistance genes.

DISCUSSION.
DISCUSIÓN.

Hospitals, particularly ICUs, have been suggested as critical hotspots contributing to the acquisition, transmission, and evolution of opportunistic bacterial pathogens and AMR (Centers for Disease Control and Prevention, 2024a). In particular, the environmental opportunistic pathogens, grouped as the SPACE group (*Serratia, Pseudomonas, Acinetobacter, Citrobacter, Enterobacter*), inhabit biotic and abiotic landscapes (Tamma *et al.*, 2019), being responsible for a high number of HAIs (Perkins *et al.*, 2019; Centers for Disease Control and Prevention, 2024b). The risk of infection is influenced by various factors, including patient-specific conditions (e.g., disease severity, underlying disease) and external factors (e.g., antibiotic consumption, colonized abiotic reservoirs). Many studies have approached these issues separately, but the influence of the hospital environment on nosocomial infection and AMR remains understudied. In this thesis, we explored the transient flow and persistence of ARGs and ARB using a novel approach that considered different *units of analysis* (the ICU, the patients) and *indicators* (the microbiome, the genome, the resistome, the plasmid, the gene).

In **Chapter 1**, we demonstrated how the **ICU stay affected the gut microbiota of hospitalized patients** and how such dysbiosis involving the overgrowth of specific opportunistic pathogens contributes to the "microbial pollution" of the ICU. Factors such as antibiotic stewardship, ICU invasive interventions, exposure to a variety of therapeutic drugs, unusual nutritional procedures, and patient characteristics (e.g., age, gender, underlying disease, severity of illness, and prognostic scores) have traditionally been associated with the selection and overgrowth of some *off-targeted* bacterial taxa such as *Lactobacillales*, mostly *Enterococcus* spp. (Ubeda *et al.*, 2010; Arias and Murray, 2012). Gut colonization by enterococci is considered a key risk factor for infection and acquisition of AMR and has been associated with longer ICU stays and treatment costs (Freedberg *et al.*, 2018; Wyres *et al.*, 2021). Most information addressing the impact of the ICU stay in the selection of high-risk clones or genes came from studies focused on cancer or immunocompromised patients (Holland, Fowler and Shelburne, 2014) and performed during endemic and epidemic situations (Gu *et al.*, 2023), always limited on time. The longitudinal study of pooling samples used in this thesis allowed us to explore the resistome and microbiome dynamics and, thus, to gain insights into the factors involved in the emergence and transmission of ARBs and ARGs in high-risk hospital wards. The pooling approach, considering the ICU patient's microbiome as an interactive biological entity, offers an efficient method for screening markers, populations, or alleles in numerous applications (Sham *et al.*, 2002), reducing the project's cost, time, and labor.

Previous studies using pooling' approaches have been focused on screening large populations in environmental settings (Weinberg and Umbach, 1999; Sato *et al.*, 2017; Ushio *et al.*, 2022; Jo, 2023), parasite and disease control in farms and veterinary practices (Nielsen *et al.*, 2021; Goni, Hendrix and Kritchevsky, 2023; Maurizio *et al.*, 2023), contamination and control of food in farms (Dean 2022), or genome-wide association studies for disease prevention (Homer *et al.*, 2008; Craig *et al.*, 2009; Anand *et al.*, 2016), but not for the analysis of AMR dynamics. Our findings confirmed that the microbiota of newly admitted ICU patients, who often have not undergone intensive therapeutic interventions, had gut bacterial communities similar to healthy people. However, as their ICU stay lengthened, gut microbiota dysbiosis is favored by the selective effect of ICU-specific interventions such as antibiotic therapy. Disturbances in their gut microbial communities occur more frequently when patients are in altered physiological states, such as bedridden, mechanically ventilated, or exposed to external factors like widespread antibiotic exposure. Recent studies also highlight the potentially harmful effects of antibiotics on long-term patients (Szychowiak *et al.*, 2022). The positive and negative selection of off-target bacterial taxa (e. g. *Enterococcus* or *Clostridium difficile*) can disrupt the microbiota, affecting the colonization resistance and promoting AMR evolution within the patient's microbiome (Morley, Woods and Read, 2019). This dysbiosis also increases the risk of infection by opportunistic pathogens and MDROs, which account for 20% of all nosocomial infections (Weiner *et al.*, 2016). MDRO infections can reduce the efficacy of antibacterial therapy, increase hospital stay and patient mortality, raise the economic burden, and thus impact the quality of medical care and patient safety (Barrasa-Villar *et al.*, 2017).

Longitudinal studies allowed analyzing the contribution of different factors. Remarkably, we observed an apparent seasonal variability despite the sampling being limited by intrinsic factors of the ICU, such as the availability of clinical staff and the varying conditions of the patients. Seasonal variation in highly occupied ICUs has been suggested previously (Garfield *et al.*, 2001; Galvão *et al.*, 2019). During the winter season (December to March), when the highest patient occupancy in hospital wards occurs (Garfield *et al.*, 2001), we observed an increased detection of ARGs. However, this period is influenced by the coincidence of the onset of the SARS-CoV-2 pandemic and associated quarantine with several bacterial outbreaks. High ward occupancy rates, high antibiotic consumption, and the decay of infection control measures caused by the ICU´s overflow during this period seem to have influenced the sequential and overlapping

outbreaks during this time, as COVID-19 adversely impacted the HAI rates within hospitals (Baker *et al.*, 2022). This is further supported by the absence of outbreaks during the previous months, despite ESBL and carbapenemase genes being detected sporadically without major transmission consequences in the ward.

In **Chapter 2**, we analyzed the dynamics of fecal colonization to understand the factors that trigger *invasion* at the ICU (outbreak emergence) and/or individual (patient infection) levels.

The colonization of bacterial opportunistic pathogens can lead to the development of HAIs, particularly in high-risk hospital wards (Bonten, Willems and Weinstein, 2001). Among the HAIs documented during the longitudinal study performed in this thesis, ventilator-associated pneumonia, and tracheobronchitis were the leading causes of infection, a finding consistent with previous reports (Koenig and Truwit, 2006; Prinz, 2022). The last report of the CDC emphasized the ICUs as the hospital ward with the highest prevalence of HAIs associated with a rate in 2020 of 12.7% of patients with at least one HAI for patients staying more than two days in the ICU, most of which can be preventable (European Centre for Disease Prevention and Control, 2024b). This underscores the importance of stringent infection control measures for ventilators and other respiratory equipment, as such conditions appear to facilitate the spread of these bacteria. Interestingly, while ventilator-associated infections mainly occurred in our ICU, the primary source of colonization was constituted by organisms present in intestinal or fecal samples. Since most infections were pneumonia-related, this suggests an invasion route via the gut-lung axis. Such pathway has been noticed and may be influenced by microbial signals or immune system stimulation (Pérez-Cobas *et al.*, 2021, 2023). Understanding the gut-lung microbial interactions is highly relevant to preventing the development of HAIs or outbreaks in ICUs.

During outbreak periods, there was a marked increase of carbapenem-resistant *Klebsiella* and *Pseudomonas*. The high prevalence of carbapenemase-producing strains constitutes a severe challenge for the ICU management of patients, as carbapenems are often a last-resort treatment (McKenna, 2013). A recent study combining shot-gun metagenomics and genomics of samples from individuals colonized by CRE revealed how colonization is associated with an altered gut ecology and can favor transfer of ARGs even in the absence of overt infection and antibiotic usage (Kang *et al.*, 2022). The ICU-related ecosystem (e.g. persistence of difficult-to-treat microorganisms, vulnerability to infections) (Calvo, Stefani and Migliorisi, 2024) provides the settling scenario for the

rapid proliferation of these outbreak clones that can negatively impact the microbial community of patients and environment, affecting their bacterial biomass and composition and thus facilitating the appearance of outbreaks in ICUs. During non-outbreak periods, however, patients were predominantly colonized by enterococci or staphylococci, consistent with the metagenomics findings in **Chapter 1**. In such cases, colonization can progress to infection and facilitate the spread of MDROs in the ICU. Despite the colonization pressure by these microorganisms, their clinical impact seems to be less marked, as reflected by the absence of records in the clinical microbiology laboratory.

In **Chapter 3**, we further investigated the impact of ICU "microbial pollution" by opportunistic pathogens considered of "critical concern" by the WHO (WHO Bacterial Priority Pathogens List, 2024), using *S. marcescens* as a representative model organism. The results provided unexpected novelties regarding this microbial species' epidemiology, taxonomy, and treatment.

We found a rich diversity of ***S. marcescens*** populations in ICU sinks, **reflecting an advantage over other species to survive and persist in this microenvironment**. This suggests that the known competitive and adaptive capability of *S. marcescens* not only in water, soil, and the rhizosphere (Williams et al., 2022) can be extended across varied built-environment settings. The long persistence of MDR strains, far beyond the end-of-outbreak, highlighted the importance of the water ICU environment as an important reservoir of AMR. Transient antibiotic-resistant opportunistic pathogens that emerged during ICU outbreaks (e.g., carbapenemase or ESBL-producing *Klebsiella* or *Pseudomonas*) can colonize biotic and abiotic reservoirs, displacing the original microbial populations, eventually almost undetectable by culturing. Those MDR populations can limit the growth of original microorganisms in environmental reservoirs so that they are resilient in the environment, even though they have been continually being recovered for subsequent samplings (data not shown). This exemplifies how proliferation can lead to persistence and vice versa. The better the colonizers, the more opportunities to cause infection and contribute to a higher disease burden.

Clarifying the taxonomy of *S. marcescens* helps to understand the genotypic and phenotypic heterogeneity of the species, the adaptation to multiple ecological niches, their phylogenetic relationships, pathogenic potential, and AMR profiles. The taxonomy of the *Serratia* genus has recently been revisited based on comparative phylogenomics, leading to the description of new species/subspecies and the "*S. marcescens* complex" (SMC).

(Ono *et al.*, 2022). Due to the high genomic similarity between the species, our phylogenetic analyses considered distinct populations part of the SMC and confirmed previous studies. Clustering provided a taxonomic tool for classifying organisms into species, noticing that *S. nevei* was the most identified species even though it is rarely present in public databases. The findings showed how species identification might be better explained by considering their phenotypic, genotypic, and ecological (ecotype) characteristics. Species are more than clusters of closely related organisms; the "species structure" can be considered a community strategy to exploit distinct ecological niches in which stable populations can only exist if they are ecologically diverse enough to avoid competition (Cohan, 2001).

The great genotypic and phenotypic diversity among coexisting SMC populations within the same ecological niche, exhibiting distinct and unusual traits such as first-described susceptibility profiles and lack of prodigiosin, confers an interesting topic for future research. This diversity also adds knowledge to the species concept through the wide range of adaptive genetic features of SMC populations (Aracil-Gisbert, Baquero and Coque, 2024). Notably, the basal-like AmpC expression has been observed in SMC for the first time, although it was previously described for other species (Stock *et al.*, 2003; Jacoby, 2009).

In **Chapter 4**, we described the long persistence, dynamics, and evolution of pB77-CpSM, a highly conserved IncL plasmid encoding the VIM-1 carbapenemase found in *S. marcescens* isolates from sinks and patients for years (Pérez-Viso *et al.*, 2021). This plasmid is highly similar to pOXA-48, which has also been collected in our institution for a long time (Hernández-García *et al.*, 2019; León-Sampedro *et al.*, 2021).

The widespread distribution of this IncL plasmid among different species of *Enterobacterales* in sinks agrees with previous studies (David *et al.*, 2020), specifically for a variant that persisted for a long time and sheds light on plasmid transmission and evolution in environmental compartments. The fact that only a few clonal complexes could harbor those plasmids indicates that clonal expansion is suggested as the major cause of plasmid spread, as previously demonstrated mainly for high-risk clones in many different backgrounds (David *et al.*, 2020). In addition to the IncL plasmids, the distribution of different families of plasmids in sink and clinical isolates mirrors the process by which this species easily acquires, maintains, and efficiently facilitates plasmid evolution, probably leading to an ever-increasing host-plasmid synergy. The indirect effect of transmission of ARGs from gut commensals to clinically relevant strains

is getting much attention (Crits-Christoph *et al.*, 2022). Our findings underscored the importance of phylogenetic and ecological similarities between donors and recipients in determining the frequency of ARG transfer in water systems. Stressful environmental conditions further shaped specific traits, assuring the resilience and adaptability of bacterial populations and promoting the evolution and dispersal of MGEs and ARGs in the hospital environment.

The fact that this IncL was maintained in bacterial hosts of different species in the water environment suggests that this microbial community of *Enterobacterales* acts as stable reservoirs of common MGEs. This variation can be extended to the same SMC (Nagano *et al.*, 2023), as long-term plasmid stability can vary even between strains of the same species, as shown for an IncP plasmid (De Gelder *et al.*, 2007). Highly conjugative plasmids may be able to maintain sufficient rates of infectious transmission to persist within microbial communities despite imposing high fitness costs upon their hosts (Bottery, 2022). Some models have suggested the prevalence of host species in the maintenance and evolution of plasmids (Hall *et al.*, 2016). However, those studies have been normally conducted within laboratory conditions. Diverse communities, such as water systems, can contain a high diversity of possible hosts, in which less permissive hosts will introduce a protective effect for the community, as said for the dilution effect in ecology, where diversity assures resilience (Schmidt and Ostfeld, 2001). However, the presence of potential hosts, mainly increasing during outbreaks, and the plasmid transmissibility characteristics will maintain the plasmid in the community, increasing the acquisition probability. Most plasmids detected in SMC populations were not harboring ARGs of clinical relevance. Thus, community composition may, therefore, impact the types of plasmids harbored within them, preferentially selecting plasmids that do not purely rely on infectious transfer but contain other genes that help the survival in those environments. Bacterial resilience in stressed habitats might be influenced by the community acquisition of other genetic elements distinct from ARGs, facilitating the evolution and dispersal of a diverse set of genes and plasmids. The more diverse and abundant a bacterial community, the more likely it can be to exchange gene content. Abundance converts relative minorities into dense populations.

Transmission events of ARGs occur within ecological niches, whether environmental (e.g., surfaces, water systems) or human (e.g., host-associated microbiota) reservoirs, each subjected to varying degrees of selection pressure. In hospital settings, antibiotic exposure is a critical factor driving the selection of ARBs, which can be actively

or passively transmitted. However, in broader ecosystems, survival often depends on the dominance of larger, more abundant microbial populations, able to colonize a broad spectrum of neighbor niches. Adaptive mechanisms, such as horizontal gene transfer and biofilm formation, play a pivotal role in ARG transmission and selection, enabling bacteria to survive various selective pressures. These processes are likely related to the broader dissemination of AMR. Adopting ecological approaches to study AMR is crucial for understanding the dynamics of the resistome and microbiome within hospital ecosystems. This thesis considers the complex interactions between environmental factors, microbial communities, and selective pressures, offering insights into how ARGs persist and spread. By analyzing these dynamics, we can identify critical control points for intervention, focusing on designing strategies to mitigate the risk of AMR dissemination in healthcare and community setting

CONCLUSIONS.
CONCLUSIONES.

The conclusions of this thesis are:

1. The ICU environment, comprising biotic (patients) and abiotic (surfaces, sinks) dimensions and vectors of AMR, is subjected to distinct selective pressures and interventions (use of antibiotics, staff and device rotation, seasonal variations) that influence the dynamics of transmission and selection of ARBs and ARGs. Extended ICU stays consistently impact the gut microbiota of hospitalized patients, reducing bacterial and gene diversity and selecting Gram-positive bacteria, mostly *Enterococcus* spp.

2. A set of ARGs and species of opportunistic pathogens become predominant during outbreaks in the ICU ward, overshadowing the typical commensal bacteria and potentially colonizing environmental reservoirs, thus contributing to the colonization of the "patient care environment" by resistant microbial communities.

3. The interplay between colonization and subsequent infections is evident, particularly during outbreak periods where ARG-harboring strains proliferate. Respiratory equipment, such as ventilators, was identified as a major contributor to HAIs, emphasizing the need for stringent infection control.

4. Hospital water systems, mainly sinks, are reservoirs of a rich microbial and genetic ecosystem. Our ICU, in particular, harbored persistent and coexistent "*S. marcescens* complex" (SMC) populations that adapted to this stressed environment and were able to produce outbreaks. The great phenotypic and genotypic variability observed within the SMC reflected the challenge of characterizing opportunistic pathogens at the subspecies level as well as high-risk clones when treating patients in healthcare settings and the importance of establishing specific infection and control measures.

5. The transmission and exchange of ARGs and plasmids involves the whole ICU patient environment (patients, sink and p-traps). The long persistence of clonal lineages, such as some of the SMC, and the ARGs' intra- and interspecific mobility across microbial populations exemplify how environmental niches can perpetuate AMR.

REFERENCES:
REFERENCIAS

Anand, S. *et al.* (2016) 'Next generation sequencing of pooled samples: Guideline for variants' filtering', *Scientific Reports*, 6(September), pp. 1–9. Available at: https://doi.org/10.1038/srep33735.

Andersson, D.I. and Hughes, D. (2012) 'Evolution of antibiotic resistance at non-lethal drug concentrations', *Drug Resistance Updates*, 15(3), pp. 162–172. Available at: https://doi.org/10.1016/j.drup.2012.03.005.

Andres, P. *et al.* (2013) 'Differential distribution of plasmid-mediated quinolone resistance genes in clinical enterobacteria with unusual phenotypes of quinolone susceptibility from Argentina', *Antimicrob Agents Chemother*, 57(6), pp. 2467–2475. Available at: https://doi.org/10.1128/AAC.01615-12.

Antimicrobial Resistance Collaborators (2022) 'Global Burden of Bacterial Antimicrobial Resistance in 2019: A Systematic Analysis', *Lancet*, 399(10325), pp. 629–655. Available at: https://doi.org/https://doi.org/10.1016/S0140-6736(21)02724-0.

Antimicrobial Resistance Collaborators (2024) 'Global burden of bacterial antimicrobial resistance 1990 – 2021 : a systematic analysis with forecasts to 2050', *The Lancet* [Preprint]. Available at: https://doi.org/10.1016/S0140-6736(24)01867-1.

Aracil-Gisbert, S. *et al.* (2024) 'The ICU environment contributes to the endemicity of the "Serratia marcescens complex" in the hospital setting.', *mBio*, p. e0305423. Available at: https://doi.org/10.1128/mbio.03054-23.

Aracil-Gisbert, S., Baquero, F. and Coque, T.M. (2024) 'Serratia marcescens', *Trends in Microbiology* [Preprint].

Arias, C.A. and Murray, B.E. (2012) 'The rise of the Enterococcus: Beyond vancomycin resistance', *Nature Reviews Microbiology*, 10(4), pp. 266–278. Available at: https://doi.org/10.1038/nrmicro2761.

Armstrong, G. *et al.* (2021) 'Efficient computation of Faith's phylogenetic diversity with applications in characterizing microbiomes', *Genome Research*, 31(11), pp. 2131–2137. Available at: https://doi.org/10.1101/gr.275777.121.

Baker, M.A. *et al.* (2022) 'CDC Prevention Epicenters Program. The Impact of Coronavirus Disease 2019 (COVID-19) on Healthcare-Associated Infections', *Clinical Infectious Diseases*, 74(10), pp. 1748–1754. Available at: https://doi.org/ 10.1093/cid/ciab688.

Baquero, F. *et al.* (2015) 'Public health evolutionary biology of antimicrobial resistance: Priorities for intervention', *Evolutionary Applications*, 8(3), pp. 223–239. Available at: https://doi.org/10.1111/eva.12235.

Baquero, F. *et al.* (2024) 'Selection versus transmission: Quantitative and organismic biology in antibiotic resistance', *Infection, Genetics and Evolution*, 121(February). Available at: https://doi.org/10.1016/j.meegid.2024.105606.

Barrasa-Villar, J.I. *et al.* (2017) 'Impact on Morbidity, Mortality, and Length of Stay of Hospital-Acquired Infections by Resistant Microorganisms', *Clinical Infectious Diseases*, 65(4), pp. 644–652. Available at: https://doi.org/10.1093/cid/cix411.

Berendonk, T.U. *et al.* (2015) 'Tackling antibiotic resistance: The environmental framework', *Nature Reviews Microbiology*, 13(5), pp. 310–317. Available at: https://doi.org/10.1038/nrmicro3439.

Blackwell, G.A., Doughty, E.L. and Moran, R.A. (2021) 'Evolution and dissemination of L and M plasmid lineages carrying antibiotic resistance genes in diverse Gram-negative bacteria', *Plasmid*, 113(April), p. 102528. Available at: https://doi.org/10.1016/j.plasmid.2020.102528.

Bogaerts, P. *et al.* (2013) 'Validation of carbapenemase and extended-spectrum β-lactamase multiplex endpoint PCR assays according to ISO 15189.', *The Journal of antimicrobial chemotherapy*, 68(7), pp. 1576–1582. Available at: https://doi.org/10.1093/jac/dkt065.

Bonten, M., Willems, R. and Weinstein, R. (2001) 'Vancomycin-resistant enterococci: why are they here, and where do they come from?', *The Lancet. Infectious diseases*, 1(5), pp. 314–325. Available at: https://doi.org/10.1016/S1473-3099(01)00145-1.

Bonten, M.J.M. (2012) 'Colonization pressure: A critical parameter in the epidemiology of antibiotic-resistant bacteria', *Critical Care*, 16(4). Available at: https://doi.org/10.1186/cc11417.

Bortolaia, V. *et al.* (2020) 'ResFinder 4.0 for predictions of phenotypes from genotypes.', *The Journal of antimicrobial chemotherapy*, 75(12), pp. 3491–3500. Available at: https://doi.org/10.1093/jac/dkaa345.

Bottery, M.J. (2022) 'Ecological dynamics of plasmid transfer and persistence in microbial communities', *Current Opinion in Microbiology*, 68, p. 102152. Available at: https://doi.org/10.1016/j.mib.2022.102152.

Boyd, S.E. *et al.* (2022) 'OXA-48-Like β-Lactamases: Global Epidemiology, Treatment Options, and Development Pipeline', *Antimicrobial Agents and Chemotherapy*, 66(8). Available at: https://doi.org/10.1128/AAC.00216-22.

Callahan, B.J. *et al.* (2016) 'DADA2: High-resolution sample inference from Illumina amplicon data', *Nature Methods*, 13(7), pp. 581–583. Available at: https://doi.org/10.1038/nmeth.3869.

Calvo, M., Stefani, S. and Migliorisi, G. (2024) 'Bacterial Infections in Intensive Care Units: Epidemiological and Microbiological Aspects', *Antibiotics*, 13(3), pp. 1–15. Available at: https://doi.org/10.3390/antibiotics13030238.

Del Campo, R. *et al.* (2019) 'Biology of hand-to-hand bacterial transmission', *Microbial Transmission*, pp. 203–213. Available at: https://doi.org/10.1128/9781555819743.ch11.

Carattoli, A. *et al.* (2015) 'Differentiation of IncL and IncM Plasmids Associated with the Spread of Clinically Relevant Antimicrobial Resistance', *PLoS One*, 10(5), p. e123063. Available at: https://doi.org/10.1371/journal.pone.0123063.

Carattoli, A. and Hasman, H. (2020) 'PlasmidFinder and In Silico pMLST: Identification and Typing of Plasmid Replicons in Whole-Genome Sequencing (WGS', *Methods Mol Biol*, 2075, pp. 285–294. Available at: https://doi.org/10.1007/978-1-4939-9877-7_20.

Centers for Disease Control and Prevention (2024a) *Considerations for Reducing Risk: Water in Healthcare Facilities*. Available at: https://www.cdc.gov/healthcare-associated-infections/php/toolkit/water-management.html.

Centers for Disease Control and Prevention (2024b) *HAIs: Reports and Data*. Available at: https://www.cdc.gov/healthcare-associated-infections/php/data/index.html.

Centers for Disease Control and Prevention (2024c) *Research Gaps in Patient and Healthcare Personnel Safety.* Atlanta, GA, USA. Available at: https://www.cdc.gov/healthcare-associated-infections/media/pdfs/DHQPs-Research-Questions-508.pdf.

Chaumeil, P.-A. *et al.* (2020) 'GTDB-Tk: a toolkit to classify genomes with the Genome Taxonomy Database', *Bioinformatics*, 36(6), pp. 1925–1927. Available at: https://doi.org/10.1093/bioinformatics/btz848.

CLSI (2023) 'Performance Standards for Antimicrobial Susceptibility Testing', *33rd CLSI supplement M100. Clinical and Laboratory Standards Institute*.

Cohan, F.M. (2001) 'Bacterial Species and Speciation', *Systematic Biology*, 50(4), pp. 513–524. Available at: https://doi.org/10.1080/106351501750435077.

Coque, T.M. *et al.* (2023) 'Antimicrobial Resistance in the Global Health Network: Known Unknowns and Challenges for Efficient Responses in the 21st Century.', *Microorganisms*, 11(4), p. 1050. Available at: https://doi.org/10.3390/microorganisms11041050.

Craig, J.E. *et al.* (2009) 'Rapid inexpensive genome-wide association using pooled whole blood', *Genome Research*, 19(11), pp. 2075–2080. Available at: https://doi.org/10.1101/gr.094680.109.

Crits-Christoph, A. *et al.* (2022) 'Good microbes, bad genes? The dissemination of antimicrobial resistance in the human microbiome', *Gut Microbes*, 14(1). Available at: https://doi.org/10.1080/19490976.2022.2055944.

Croucher, N.J. *et al.* (2015) 'Rapid phylogenetic analysis of large samples of recombinant bacterial whole genome sequences using Gubbins.', *Nucleic acids research*, 43(3), p. e15. Available at: https://doi.org/10.1093/nar/gku1196.

Dalton, K.R. *et al.* (2020) 'One Health in hospitals: How understanding the dynamics of people, animals, and the hospital built-environment can be used to better inform interventions for antimicrobial-resistant gram-positive infections', *Antimicrobial Resistance and Infection Control*, 9(1), pp. 1–17. Available at: https://doi.org/10.1186/s13756-020-00737-2.

David, S. *et al.* (2020) 'Integrated chromosomal and plasmid sequence analyses reveal diverse modes of carbapenemase gene spread among Klebsiella pneumoniae', *Proceedings of the National Academy of Sciences of the United States of America*, 117(40), pp. 25043–25054. Available at: https://doi.org/10.1073/pnas.2003407117.

Didelot, X. *et al.* (2018) 'Bayesian inference of ancestral dates on bacterial phylogenetic trees.', *Nucleic acids research*, 46(22), p. e134. Available at: https://doi.org/10.1093/nar/gky783.

Diorio-Toth, L. *et al.* (2023) 'Intensive care unit sinks are persistently colonized with multidrug resistant bacteria and mobilizable, resistance-conferring plasmids', *mSystems*, 8(4), p. e0020623. Available at: https://doi.org/10.1128/msystems.00206-23.

Dunne, W.M. and Hardin, D.J. (2005) 'Use of several inducer and substrate antibiotic combinations in a disk approximation assay format to screen for AmpC induction in patient isolates of Pseudomonas aeruginosa, Enterobacter spp., Citrobacter spp., and Serratia spp.', *Journal of Clinical Microbiology*, 43(12), pp. 5945–5949. Available at: https://doi.org/10.1128/JCM.43.12.5945-5949.2005.

EClinicalMedicine (2021) 'Antimicrobial resistance: a top ten global public health threat.', *EClinicalMedicine*. England, p. 101221. Available at: https://doi.org/10.1016/j.eclinm.2021.101221.

European Centre for Disease Prevention and Control (2021) *ECDC strategic framework for the integration of molecular and genomic typing into European surveillance and multi-country outbreak investigations - 2019-2021. Stockholm: ECDC; 2019*. Available at: https://www.ecdc.europa.eu/en/publications-data/ecdc-strategic-framework-integration-molecular-and-genomic-typing-european.

European Centre for Disease Prevention and Control (2024a) *Considerations for Reducing Risk: Water in Healthcare Facilities*, *Centers for Disease Control and Prevention*. Available at: https://www.cdc.gov/healthcare-associated-infections/php/toolkit/water-management.html?CDC_AAref_Val=https://www.cdc.gov/hai/prevent/environment/water.html (Accessed: 27 September 2024).

European Centre for Disease Prevention and Control (2024b) *Healthcare-associated infections in intensive care units*, *ECDC. Annual Epidemiological Report for 2020. Stockholm: ECDC*. Available at: https://doi.org/10.54044/rami.2022.01.07.

Fernández-de-Bobadilla, M.D. *et al.* (2021) 'PATO: Pangenome Analysis Toolkit', *Bioinformatics*, 37(23), pp. 4564–4566. Available at: https://doi.org/10.1093/bioinformatics/btab697.

Frazão, N. *et al.* (2019) 'Horizontal gene transfer overrides mutation in Escherichia coli colonizing the mammalian gut', *Proceedings of the National Academy of Sciences*, 116(36), pp. 17906–17915. Available at: https://doi.org/10.1073/pnas.1906958116.

Freedberg, D.E. *et al.* (2018) 'Pathogen colonization of the gastrointestinal microbiome at intensive care unit admission and risk for subsequent death or infection', *Intensive Care Medicine*, 44(8), pp. 1203–1211. Available at: https://doi.org/10.1007/s00134-018-5268-8.

Freedberg, D.E. *et al.* (2022) ' Are There Bad ICU Rooms? Temporal Relationship between Patient and ICU Room Microbiome, and Influence on Vancomycin-Resistant Enterococcus Colonization ', *mSphere*, 7(1), pp. 1–9. Available at: https://doi.org/10.1128/msphere.01007-21.

Galvão, G. *et al.* (2019) 'Seasonal variation of clinical characteristics and prognostic of adult patients admitted to an intensive care unit', *Revista da Associacao Medica Brasileira (1992)*, 65(11), pp. 1374–1383. Available at: https://doi.org/10.1590/1806-9282.65.11.1374.

Garfield, M. *et al.* (2001) 'Seasonal variation in admission rates to intensive care units', *Anaesthesia*, 56(12), pp. 1136–1140. Available at: https://doi.org/10.1046/j.1365-2044.2001.01984.x.

De Gelder, L. *et al.* (2007) 'Stability of a promiscuous plasmid in different hosts: No guarantee for a long-term relationship', *Microbiology*, 153(2), pp. 452–463. Available at: https://doi.org/10.1099/mic.0.2006/001784-0.

Gilchrist, C.L.M. and Chooi, Y.-H. (2021) 'clinker & clustermap.js: Automatic generation of gene cluster comparison figures', *Bioinformatics*, 37(16), pp. 2473–2475. Available at: https://doi.org/10.1093/bioinformatics/btab007.

Goni, J.I., Hendrix, K. and Kritchevsky, J. (2023) 'Recovery of Salmonella bacterial isolates from pooled fecal samples from horses.', *Journal of veterinary internal medicine*, 37(1), pp. 323–327. Available at: https://doi.org/10.1111/jvim.16586.

Grolemund, G. and Wickham, H. (2011) 'Dates and Times Made Easy with lubridate', *Journal of Statistical Software*, 40(3), pp. 1–25. Available at: https://www.jstatsoft.org/v40/i03/.

Grundmann, H. (2014) 'Towards a global antibiotic resistance surveillance system: A primer for a roadmap', *Upsala Journal of Medical Sciences*, 119(2), pp. 87–95. Available at: https://doi.org/10.3109/03009734.2014.904458.

Gu, G.Y. *et al.* (2023) 'Risk of multi-drug-resistant organism acquisition from prior bed occupants in the intensive care unit: a meta-analysis', *Journal of Hospital Infection*, 139, pp. 44–55. Available at: https://doi.org/10.1016/j.jhin.2023.06.020.

Le Guern, R. *et al.* (2021) 'Colonization resistance against multi-drug-resistant bacteria: a narrative review', *Journal of Hospital Infection*, 118, pp. 48–58. Available at: https://doi.org/10.1016/j.jhin.2021.09.001.

Gilbert, J.A. and Stephens, B. (2018) 'Microbiology of the built environment', *Nature Reviews Microbiology*, 16(11), pp. 661-670. Available at: https://doi.org/10.1038/s41579-018-0065-5.

Guerra-Pinto, N. *et al.* (2024) 'The environmental microbiome of hospital patient and non-patient areas reveals the influence of human activity in the dynamics of antimicrobial resistance', in *34th European Congress of Clinical Microbiology and Infectious Diseases (ECCMID)*.

Gupta, G., Tak, V. and Mathur, P. (2014) 'Detection of AmpC β Lactamases in Gram-negative Bacteria', *Journal of laboratory physicians*, 6(1), pp. 1–6. Available at: https://doi.org/10.4103/0974-2727.129082.

Hall, J.P.J. *et al.* (2016) 'Source-sink plasmid transfer dynamics maintain gene mobility in soil bacterial communities.', *Proceedings of the National Academy of Sciences of the United States of America*, 113(29), pp. 8260–8265. Available at: https://doi.org/10.1073/pnas.1600974113.

Harris, P.A. *et al.* (2009) 'Research electronic data capture (REDCap)--a metadata-driven methodology and workflow process for providing translational research informatics support.', *Journal of biomedical informatics*, 42(2), pp. 377–381. Available at: https://doi.org/10.1016/j.jbi.2008.08.010.

Harris, P.A. *et al.* (2019) 'The REDCap consortium: Building an international community of software platform partners.', *Journal of biomedical informatics*, 95, p. 103208. Available at: https://doi.org/10.1016/j.jbi.2019.103208.

Hernández-García, M. *et al.* (2019) 'Intestinal co-colonization with different carbapenemase-producing Enterobacterales isolates is not a rare event in an OXA-48 endemic area', *eClinicalMedicin*, 17(15), pp. 72–79. Available at: https://doi.org/10.1016/j.eclinm.2019.09.005.

Hernando-Amado, S. *et al.* (2019) 'Defining and combating antibiotic resistance from One Health and Global Health perspectives.', *Nature microbiology*, 4(9), pp. 1432–1442. Available at: https://doi.org/10.1038/s41564-019-0503-9.

Holland, T., Fowler, V.G. and Shelburne, S.A. (2014) 'Invasive gram-positive bacterial infection in cancer patients', *Clinical Infectious Diseases*, 59(Suppl 5), pp. S331–S334. Available at: https://doi.org/10.1093/cid/ciu598.

Homer, N. *et al.* (2008) 'Multimarker analysis and imputation of multiple platform pooling-based genome-wide association studies', *Bioinformatics*, 24(17), pp. 1896–1902. Available at: https://doi.org/10.1093/bioinformatics/btn333.

Huijbers, P.M.C., Flach, C.F. and Larsson, D.G.J. (2019) 'A conceptual framework for the environmental surveillance of antibiotics and antibiotic resistance', *Environment International*, 130(May), p. 104880. Available at: https://doi.org/10.1016/j.envint.2019.05.074.

Illumina (2013) '16S Metagenomic Sequencing Library', *Illumina.com*, (B), pp. 1–28. Available at: http://support.illumina.com/content/dam/illumina-support/documents/documentation/chemistry_documentation/16s/16s-metagenomic-library-prep-guide-15044223-b.pdf.

Jacoby, G.A. (2009) 'AmpC β-Lactamases', *Clinical Microbiology Reviews*, 22(1), p. 161. Available at: https://doi.org/10.1128/CMR.00036-08.

Jo, T.S. (2023) 'Pooling of intra-site measurements inflates variability of the correlation between environmental DNA concentration and organism abundance', *Environmental Monitoring and Assessment*, 195(8). Available at: https://doi.org/10.1007/s10661-023-11539-5.

Jolley, K.A. *et al.* (2012) 'Ribosomal multilocus sequence typing: universal characterization of bacteria from domain to strain.', *Microbiology (Reading, England)*, 158(Pt 4), pp. 1005–1015. Available at: https://doi.org/10.1099/mic.0.055459-0.

Jolley, K.A., Bray, J.E. and Maiden, M.C.J. (2018) 'Open-access bacterial population genomics: BIGSdb software, the PubMLST.org website and their applications.', *Wellcome open research*, 3, p. 124. Available at: https://doi.org/10.12688/wellcomeopenres.14826.1.

Kang, J.T.L. *et al.* (2022) 'Long-term ecological and evolutionary dynamics in the gut microbiomes of carbapenemase-producing Enterobacteriaceae colonized subjects.', *Nature microbiology*, 7(10), pp. 1516–1524. Available at: https://doi.org/10.1038/s41564-022-01221-w.

Kassambara, A. (2023) *ggpubr: 'ggplot2' Based Publication Ready Plots*, *R package version 0.6.0*. Available at: https://rpkgs.datanovia.com/ggpubr/.

Kaur, J. *et al.* (2013) 'Modified Double Disc Synergy Test to Detect ESBL Production in Urinary Isolates of Escherichia coli and Klebsiella pneumoniae', *Journal of clinical and diagnostic research : JCDR*, 7(2), pp. 229–233. Available at: https://doi.org/https://doi.org/10.7860/JCDR/2013/4619.2734.

Kim, B.-R. *et al.* (2017) 'Deciphering Diversity Indices for a Better Understanding of Microbial Communities.', *Journal of microbiology and biotechnology*, 27(12), pp. 2089–2093. Available at: https://doi.org/10.4014/jmb.1709.09027.

Kim, U. *et al.* (2024) 'Hospital water environment and antibiotic use: key factors in a nosocomial outbreak of carbapenemase-producing Serratia marcescens', *Journal of Hospital Infection*, 151, pp. 69–78. Available at: https://doi.org/10.1016/j.jhin.2024.04.021.

Kizny Gordon, A. *et al.* (2017) 'The Hospital Water Environment as a Reservoir for Carbapenem-Resistant Organisms Causing Hospital-Acquired Infections-A Systematic Review of the Literature', *Clinical Infectious Diseases*, 64(10), pp. 1435–1444. Available at: https://doi.org/10.1093/cid/cix132.

Klindworth, A. *et al.* (2013) 'Evaluation of general 16S ribosomal RNA gene PCR primers for classical and next-generation sequencing-based diversity studies', *Nucleic acids research*, 41(1). Available at: https://doi.org/10.1093/NAR/GKS808.

Knelson, L.P. *et al.* (2014) ' A Comparison of Environmental Contamination by Patients Infected or Colonized with Methicillin-Resistant Staphylococcus aureus or Vancomycin-Resistant Enterococci: A Multicenter Study ', *Infection Control & Hospital Epidemiology*, 35(7), pp. 872–875. Available at: https://doi.org/10.1086/676861.

Koenig, S.M. and Truwit, J.D. (2006) 'Ventilator-associated pneumonia: Diagnosis, treatment, and prevention', *Clinical Microbiology Reviews*, 19(4), pp. 637–657. Available at: https://doi.org/10.1128/CMR.00051-05.

Langaee, T.Y., Dargis, M. and Huletsky, A. (1998) 'An ampD Gene in Pseudomonas aeruginosa Encodes a Negative Regulator of AmpC β-Lactamase Expression', *Antimicrobial Agents and Chemotherapy*, 42(12), p. 3296. Available at: https://doi.org/10.1128/aac.42.12.3296.

Lanza, V.F. *et al.* (2018) 'In-depth resistome analysis by targeted metagenomics', *Microbiome*, 6(1), pp. 1–14. Available at: https://doi.org/10.1186/s40168-017-0387-y.

León-Sampedro, R. *et al.* (2021) 'Pervasive transmission of a carbapenem resistance plasmid in the gut microbiota of hospitalized patients', *Nature Microbiology*, 6, pp. 606–616. Available at: https://doi.org/10.1038/s41564-021-00879-y.

Letunic, I. and Bork, P. (2021) 'Interactive Tree Of Life (iTOL) v5: an online tool for phylogenetic tree display and annotation', *Nucleic Acids Research*, 49(W1), pp. W293–W296. Available at: https://doi.org/10.1093/nar/gkab301.

Li, H. *et al.* (2024) 'EDTA enables to alleviate impacts of metal ions on conjugative transfer of antibiotic resistance genes', 257(April). Available at: https://doi.org/10.1016/j.watres.2024.121659.

Lin, Q.Y. *et al.* (2014) 'Serratia marcescens arn, a PhoP-regulated locus necessary for polymyxin B resistance.', *Antimicrobial agents and chemotherapy*, 58(9), pp. 5181–5190. Available at: https://doi.org/10.1128/AAC.00013-14.

Liu, L. (2022) 'Amped-up Enterobacterales Debate', *Contagion*, 7(5).

Liu, X. *et al.* (2022) 'Research Progress on Bacterial Membrane Vesicles and Antibiotic Resistance', *International Journal of Molecular Sciences*, 23(19). Available at: https://doi.org/10.3390/ijms231911553.

Livermore, D.M. (1995) 'beta-Lactamases in laboratory and clinical resistance', *Clinical Microbiology Reviews*, 8(4), pp. 557–584. Available at: https://doi.org/10.1128/CMR.8.4.557.

Livermore, D.M. *et al.* (2019) 'OXA-1 β-lactamase and non-susceptibility to penicillin/β-lactamase inhibitor combinations among ESBL-producing Escherichia coli', *Journal of Antimicrobial Chemotherapy*, 74(2), pp. 326–333. Available at: https://doi.org/10.1093/jac/dky453.

Mack, A.R. *et al.* (2020) 'A Standard Numbering Scheme for Class C β-Lactamases', *Antimicrobial Agents and Chemotherapy*, 64(3), pp. e01841-19. Available at: https://doi.org/10.1128/AAC.01841-19.

Mahlen, S.D. *et al.* (2003) 'Analyses of ampC gene expression in Serratia marcescens reveal new regulatory properties', *Journal of Antimicrobial Chemotherapy*, 54(4), pp. 791–802. Available at: https://doi.org/10.1093/jac/dkg133.

Mahnert, A. *et al.* (2019) 'Man-made microbial resistances in built environments', *Nature Communications*, 10(1), pp. 1–12. Available at: https://doi.org/10.1038/s41467-019-08864-0.

Mariscotti, J.F. and Véscovi, E.G. (2021) 'Serratia marcescens RamA expression is under PhoP-dependent control and modulates lipid a-related gene transcription and antibiotic resistance phenotypes', *Journal of Bacteriology*, 203(13). Available at: https://doi.org/10.1128/JB.00523-20/ASSET/3AFB7733-2476-4C2E-9313-60DECDAC8EF9/ASSETS/IMAGES/LARGE/JB.00523-20-F0008.JPG.

Matsumura, N., Minami, S. and Mitsuhashi, S. (1998) 'Sequences of homologous beta-lactamases from clinical isolates of Serratia marcescens with different substrate specificities', *Antimicrobial Agents and Chemotherapy*, 42(1), pp. 176–179. Available at: https://doi.org/10.1128/AAC.42.1.176.

Matsumura, N. and Mitsuhashi, S. (1995) 'A beta-lactamase from Serratia marcescens hydrolyzing the 2-carboxypenam T-5575', *Antimicrobial Agents and Chemotherapy*, 39(9), pp. 2132–2134. Available at: https://doi.org/10.1128/AAC.39.9.2132.

Maurizio, A. *et al.* (2023) 'Comparing pooled and individual samples for estimation of gastrointestinal strongyles burden and treatment efficacy in small ruminants', *Veterinary Parasitology*, 318(April), p. 109935. Available at: https://doi.org/10.1016/j.vetpar.2023.109935.

McKenna, M. (2013) 'Antibiotic resistance: The last resort', *Nature*, 499, pp. 394–396. Available at: https://doi.org/10.1038/499394a.

McMurdie, P.J. and Holmes, S. (2013) 'Phyloseq: An R Package for Reproducible Interactive Analysis and Graphics of Microbiome Census Data', *PLoS ONE*, 8(4). Available at: https://doi.org/10.1371/journal.pone.0061217.

Mitchell, B.G. *et al.* (2015) 'Risk of organism acquisition from prior room occupants: A systematic review and meta-analysis', *Journal of Hospital Infection*, 91(3), pp. 211–217. Available at: https://doi.org/10.1016/j.jhin.2015.08.005.

Monstein, H.J. *et al.* (2007) 'Multiplex PCR amplification assay for the detection of blaSHV, blaTEM and blaCTX-M genes in Enterobacteriaceae', *APMIS*, 115(12), pp. 1400–1408. Available at: https://doi.org/10.1111/j.1600-0463.2007.00722.x.

Morley, V.J., Woods, R.J. and Read, A.F. (2019) 'Bystander Selection for Antimicrobial Resistance: Implications for Patient Health', *Trends in Microbiology*, 27(10), pp. 864–877. Available at: https://doi.org/10.1016/j.tim.2019.06.004.

Nagano, D.S. *et al.* (2023) 'Systematic analysis of plasmids of the Serratia marcescens complex using 142 closed genomes', *Microbial Genomics*, 9(11), pp. 1–15. Available at: https://doi.org/10.1099/mgen.0.001135.

Nielsen, M.K. *et al.* (2021) 'Diagnosing Strongylus vulgaris in pooled fecal samples', *Veterinary Parasitology*, 296, p. 109494. Available at: https://doi.org/https://doi.org/10.1016/j.vetpar.2021.109494.

Oksanen, J. (2024) 'Vegan: ecological diversity', *The Comprehensive R Archive Network*, 0, p. 11. Available at: https://cran.r-project.org/package=vegan.

Ono, T. *et al.* (2022) 'Global population structure of the Serratia marcescens complex and identification of hospital-adapted lineages in the complex', *Microbial Genomics*, 8(3), p. 000793. Available at: https://doi.org/10.1099/mgen.0.000793.

Oteo, J. *et al.* (2013) 'Emergence of OXA-48-producing Klebsiella pneumoniae and the novel carbapenemases OXA-244 and OXA-245 in Spain.', *The Journal of antimicrobial chemotherapy*, 68(2), pp. 317–321. Available at: https://doi.org/10.1093/jac/dks383.

PAHO (2024) *Health in All Policies*, *Panamerican Public Health Association*. Available at: https://www.paho.org/en/topics/health-all-policies#:~:text=Health in All Policies (HiAP,population health and health equity. (Accessed: 4 December 2024).

Parks, D.H. *et al.* (2018) 'A standardized bacterial taxonomy based on genome phylogeny substantially revises the tree of life.', *Nature biotechnology*, 36(10), pp. 996–1004. Available at: https://doi.org/10.1038/nbt.4229.

Patil, I. (2021) 'Visualizations with statistical details: The "ggstatsplot" approach', *Journal of Open Source Software*, 6(61), p. 3167. Available at: https://doi.org/10.21105/joss.03167.

Pérez-Cobas, A.E. *et al.* (2021) 'Altered Ecology of the Respiratory Tract Microbiome and Nosocomial Pneumonia.', *Frontiers in microbiology*, 12, p. 709421. Available at: https://doi.org/10.3389/fmicb.2021.709421.

Pérez-Cobas, A.E. *et al.* (2023) 'Ecology of the respiratory tract microbiome', *Trends in Microbiology*, 31(9), pp. 972–984. Available at: https://doi.org/10.1016/j.tim.2023.04.006.

Pérez-Cobas, A.E., Gomez-Valero, L. and Buchrieser, C. (2020) 'Metagenomic approaches in microbial ecology: An update on whole-genome and marker gene sequencing analyses', *Microbial Genomics*, 6(8), pp. 1–22. Available at: https://doi.org/10.1099/mgen.0.000409.

Pérez-Viso, B. *et al.* (2021) 'Characterization of carbapenemase-producing Serratia marcescens and whole-genome sequencing for plasmid typing in a hospital in Madrid, Spain (2016-18', *Journal of Antimicrobial Chemotherapy*, 76(1), pp. 110–116. Available at: https://doi.org/10.1093/jac/dkaa398.

Pérez-Viso, B. *et al.* (2024) 'A long-term survey of Serratia spp. bloodstream infections revealed an increase of antimicrobial resistance involving adult population.', *Microbiology spectrum*, 12(2), p. e0276223. Available at: https://doi.org/10.1128/spectrum.02762-23.

Perkins, K.M. *et al.* (2019) 'Investigation of healthcare infection risks from water-related organisms: Summary of CDC consultations, 2014-2017.', *Infection control and hospital epidemiology*, 40(6), pp. 621–626. Available at: https://doi.org/10.1017/ice.2019.60.

Philippon, A. *et al.* (2022) 'Class C β-Lactamases: Molecular Characteristics', *Clinical Microbiology Reviews*, 35(3), p. e0015021. Available at: https://doi.org/10.1128/cmr.00150-21.

Plipat, N. *et al.* (2013) 'The dynamics of methicillin-resistant Staphylococcus aureus exposure in a hospital model and the potential for environmental intervention.', *BMC infectious diseases*, 13, p. 595. Available at: https://doi.org/10.1186/1471-2334-13-595.

Poirel, L. *et al.* (2011) 'Multiplex PCR for detection of acquired carbapenemase genes', *Diagn Microbiol Infect Dis*, 70(1), pp. 119–123. Available at: https://doi.org/10.1016/j.diagmicrobio.2010.12.002.

Poirel, L., Bonnin, R.A. and Nordmann, P. (2012) 'Genetic features of the widespread plasmid coding for the carbapenemase OXA-48', *Antimicrobial Agents and Chemotherapy*, 56(1), pp. 559–562. Available at: https://doi.org/10.1128/AAC.05289-11.

Price, L.B. *et al.* (2017) 'Colonizing opportunistic pathogens (COPs): The beasts in all of us', *PLoS Pathogens*, 13(8), pp. 1–8. Available at: https://doi.org/10.1371/journal.ppat.1006369.

Price, M.N., Dehal, P.S. and Arkin, A.P. (2010) 'FastTree 2 – Approximately Maximum-Likelihood Trees for Large Alignments', *PLOS ONE*, 5(3), pp. 1–10. Available at: https://doi.org/10.1371/journal.pone.0009490.

Prinz, R. (2022) 'Environmental Measures Disrupt Transmission of HAIs', *Infection Control Today*, 26(4). Available at: https://www.infectioncontroltoday.com/view/environmental-measures-disrupt-transmission-of-hais.

Prjibelski, A. *et al.* (2020) 'Using SPAdes De Novo Assembler', *Current Protocols in Bioinformatics*, 70(1), p. e102. Available at: https://doi.org/https://doi.org/10.1002/cpbi.102.

Ramatla, T. *et al.* (2023) '"One Health" perspective on prevalence of co-existing extended-spectrum β-lactamase (ESBL)-producing Escherichia coli and Klebsiella pneumoniae: a comprehensive systematic review and meta-analysis', *Annals of Clinical Microbiology and Antimicrobials*, 22(1), pp. 1–17. Available at: https://doi.org/10.1186/s12941-023-00638-3.

Rambaut, A. *et al.* (2016) 'Exploring the temporal structure of heterochronous sequences using TempEst (formerly Path-O-Gen).', *Virus evolution*, 2(1), p. vew007. Available at: https://doi.org/10.1093/ve/vew007.

Ramos, T. *et al.* (2015) 'Spatial and temporal variations in indoor environmental conditions, human occupancy, and operational characteristics in a new hospital building.', *PloS one*, 10(3), p. e0118207. Available at: https://doi.org/10.1371/journal.pone.0118207.

Riley, L.W. (2014) 'Pandemic lineages of extraintestinal pathogenic Escherichia coli', *Clinical Microbiology and Infection*, 20(5), pp. 380–390. Available at: https://doi.org/10.1111/1469-0691.12646.

Robertson, J. and Nash, J.H.E. (2018) 'MOB-suite: software tools for clustering, reconstruction and typing of plasmids from draft assemblies', *Microb Genom*, 4(8), p. e000206. Available at: https://doi.org/10.1099/mgen.0.000206.

Rodríguez, I. *et al.* (2021) 'A 21-Year Survey of Escherichia coli from Bloodstream Infections (BSI) in a Tertiary Hospital Reveals How Community-Hospital', *mSphere*, 6(6), p. e0086821.

Sambrook, J., Fritsch, E. and Maniatis, T. (1989) 'Molecular Cloning, A Laboratory Manual (Second Edition)', *Cold Spring Harbor* [Preprint]. Available at: https://doi.org/https://doi.org/10.1002/jobm.3620300824.

Sandner-Miranda, L. *et al.* (2018) 'The Genomic Basis of Intrinsic and Acquired Antibiotic Resistance in the Genus Serratia', *Frontiers in microbiology*, 9, p. 828. Available at: https://doi.org/10.3389/fmicb.2018.00828.

Saralegui, C. *et al.* (2020) 'Genomics of Serratia marcescens Isolates Causing Outbreaks in the Same Pediatric Unit 47 Years Apart: Position in an Updated Phylogeny of the Species',

Frontiers in microbiology, 11, p. 451. Available at: https://doi.org/10.3389/fmicb.2020.00451.

Sato, H. *et al.* (2017) 'Usefulness and limitations of sample pooling for environmental DNA metabarcoding of freshwater fish communities', *Scientific Reports*, 7(1), pp. 1–12. Available at: https://doi.org/10.1038/s41598-017-14978-6.

Schmidt, K.A. and Ostfeld, R.S. (2001) 'Biodiversity and the dilution effect in disease ecology', *Ecology*, 82(3), pp. 609–619.

Schwengers, O. *et al.* (2021) 'Bakta: rapid and standardized annotation of bacterial genomes via alignment-free sequence identification', *Microbial Genomics*, 7(11), p. 000685. Available at: https://doi.org/10.1099/mgen.0.000685.

Segata, N. *et al.* (2011) 'Metagenomic biomarker discovery and explanation.', *Genome biology*, 12(6), p. R60. Available at: https://doi.org/10.1186/gb-2011-12-6-r60.

Sham, P. *et al.* (2002) 'DNA pooling: A tool for large-scale association studies', *Nature Reviews Genetics*, 3(11), pp. 862–871. Available at: https://doi.org/10.1038/NRG930.

Shaw, K.J. *et al.* (1992) 'Characterization of the chromosomal aac(6')-Ic gene from Serratia marcescens', *Antimicrobial Agents and Chemotherapy*, 36(7), pp. 1447–55. Available at: https://doi.org/doi:

Shields-Cutler, R.R. *et al.* (2018) 'SplinectomeR enables group comparisons in longitudinal microbiome studies', *Frontiers in Microbiology*, 9(APR), pp. 1–7. Available at: https://doi.org/10.3389/fmicb.2018.00785.

Shirshikova, T. V. *et al.* (2021) 'The ABC-Type Efflux Pump MacAB Is Involved in Protection of Serratia marcescens against Aminoglycoside Antibiotics, Polymyxins, and Oxidative Stress', *mSphere*, 6(2). Available at: https://doi.org/10.1128/MSPHERE.00033-21/ASSET/DF515A0D-A5E9-484F-886D-1E26B9098636/ASSETS/IMAGES/MEDIUM/MSPHERE.00033-21-F0006.GIF.

Stock, I. *et al.* (2003) 'Natural antibiotic susceptibility of strains of Serratia marcescens and the S. liquefaciens complex: S', *International Journal of Antimicrobial Agents*, 22(1), pp. 35–47.

Struelens, M.J. and Ludden, C. (2024) 'Real-time genomic surveillance for enhanced control of infectious diseases and antimicrobial resistance', (April), pp. 1–23. Available at: https://doi.org/10.3389/fsci.2024.1298248.

Su, X. (2021) 'Elucidating the Beta-Diversity of the Microbiome: from Global Alignment to Local Alignment', *mSystems*, 6(4). Available at: https://doi.org/10.1128/msystems.00363-21.

Szychowiak, P. *et al.* (2022) 'The role of the microbiota in the management of intensive care patients', *Annals of Intensive Care*, 12(1). Available at: https://doi.org/10.1186/s13613-021-00976-5.

Tamma, P.D. *et al.* (2019) 'A Primer on AmpC β-Lactamases: Necessary Knowledge for an Increasingly Multidrug-resistant World', *Clinical infectious diseases : an official publication of the Infectious Diseases Society of America*, 69(8), pp. 1446–1455. Available at: https://doi.org/10.1093/cid/ciz173.

Tap, J. *et al.* (2009) 'Towards the human intestinal microbiota phylogenetic core', *Environmental Microbiology*, 11(10), pp. 2574–2584. Available at: https://doi.org/10.1111/j.1462-2920.2009.01982.x.

Tato, M. *et al.* (2007) 'Complex clonal and plasmid epidemiology in the first outbreak of enterobacteriaceae infection involving VIM-1 metallo-β-lactamase in Spain: Toward endemicity?', *Clinical Infectious Diseases*, 45(9), pp. 1171–1178. Available at: https://doi.org/10.1086/522288.

Tato, M. *et al.* (2010) 'Dispersal of carbapenemase blaVIM-1 gene associated with different Tn402 variants, mercury transposons, and conjugative plasmids in Enterobacteriaceae and Pseudomonas aeruginosa', *Antimicrobial Agents and Chemotherapy*, 54(1), pp. 320–327. Available at: https://doi.org/10.1128/AAC.00783-09.

Thompson, S.A. *et al.* (2007) 'Novel tetracycline resistance determinant isolated from an environmental strain of Serratia marcescens', *Applied and environmental microbiology*, 73(7), pp. 2199–2206. Available at: https://doi.org/10.1128/AEM.02511-06.

Tonkin-Hill, G. *et al.* (2020) 'Producing polished prokaryotic pangenomes with the Panaroo pipeline.', *Genome biology*, 21(1), p. 180. Available at: https://doi.org/10.1186/s13059-020-02090-4.

Ubeda, C. *et al.* (2010) 'Vancomycin-resistant Enterococcus domination of intestinal microbiota is enabled by antibiotic treatment in mice and precedes bloodstream invasion in humans', *The Journal of Clinical Investigation*, 120(12), pp. 4332–4341. Available at: https://doi.org/10.1172/JCI43918DS1.

United Nations Environment Programme (2023) *Bracing for Superbugs: Strengthening environmental action in the One Health response to antimicrobial resistance*, *Geneva*. Available at: https://doi.org/10.18356/9789210025799.

Ushio, M. *et al.* (2022) 'An efficient early-pooling protocol for environmental DNA metabarcoding', *Environmental DNA*, 4(6), pp. 1212–1228. Available at: https://doi.org/10.1002/edn3.337.

Verhougstraete, M. *et al.* (2024) 'Impact of terminal cleaning in rooms previously occupied by patients with healthcare-associated infections', *PloS one*, 19(7), p. e0305083. Available at: https://doi.org/10.1371/journal.pone.0305083.

van der Waaij, D., Berghuis-de Vries, J.M. and Lekkerkerk-v, L. (1971) 'Colonization resistance of the digestive tract in conventional and antibiotic-treated mice.', *The Journal of hygiene*, 69(3), pp. 405–411. Available at: https://doi.org/10.1017/s0022172400021653.

Weinberg, C.R. and Umbach, D.M. (1999) 'Using Pooled Exposure Assessment to Improve Efficiency in Case-Control Studies', (September), pp. 718–726.

Weiner, L.M. *et al.* (2016) 'Antimicrobial-Resistant Pathogens Associated with Healthcare-Associated Infections: Summary of Data Reported to the National Healthcare Safety Network at the Centers for Disease Control and Prevention, 2011-2014', *Infection Control and Hospital Epidemiology*, 37(11), pp. 1288–1301. Available at: https://doi.org/10.1017/ice.2016.174.

Wellington, E.M.H. *et al.* (2013) 'The role of the natural environment in the emergence of antibiotic resistance in Gram-negative bacteria', *The Lancet Infectious Diseases*, 13(2), pp. 155–165. Available at: https://doi.org/10.1016/S1473-3099(12)70317-1.

Wenzel, R.P. (2005) *Stalking microbes: a relentless pursuit of infection control*, *AuthorHouse Ltd.: Bloomington, IN, USA*. Available at: https://doi.org/10.1179/cim.2006.7.3.179.

WHO Bacterial Priority Pathogens List (2024) *WHO Bacterial Priority Pathogens List, 2024: bacterial pathogens of public health importance to guide research, development and strategies to prevent and control antimicrobial resistance*. Geneva: World Health Organization.

Wick, R.R. *et al.* (2017) 'Unicycler: resolving bacterial genome assemblies from short and long sequencing reads', *PLoS Comput Biol*, 13(6), p. e1005595.

Wickham, H. (2016) *ggplot2: Elegant Graphics for Data Analysis*, *Springer-Verlag New York*. Available at: https://doi.org/https://doi.org/10.1007/978-3-319-24277-4.

Wickham, H. *et al.* (2019) 'Welcome to the Tidyverse', *Journal of Open Source Software*, 4(43), p. 1686. Available at: https://doi.org/10.21105/joss.01686.

Williams, D.J. *et al.* (2022) 'The genus Serratia revisited by genomics', *Nature Communications*, 13, p. 5195. Available at: https://doi.org/10.1038/s41467-022-32929-2.

Willis, A.J. (1997) 'The ecosystem: An evolving concept viewed historically', *Functional Ecology*, 11(2), pp. 268–271. Available at: https://doi.org/10.1111/j.1365-2435.1997.00081.x.

Wyres, K.L. *et al.* (2021) 'Genomic surveillance of antimicrobial resistant bacterial colonisation and infection in intensive care patients.', *BMC infectious diseases*, 21(1), p. 683. Available at: https://doi.org/10.1186/s12879-021-06386-z.

Yu, G. (2020) 'Using ggtree to Visualize Data on Tree-Like Structures', *Current Protocols in Bioinformatics*, 69(1), p. e96. Available at: https://doi.org/https://doi.org/10.1002/cpbi.96.

Zhu, D. *et al.* (2022) 'Emergence of plasmid-mediated tigecycline, β-lactam and florfenicol resistance genes tet(X), blaOXA-347 and floR in Riemerella anatipestifer isolated in China', *Poultry Science*, 101(10), p. 102057. Available at: https://doi.org/10.1016/j.psj.2022.102057.

ANNEXES.
ANEXOS.

Annex 1 | Pooling design data.
In the Pool and Week columns, the first two numbers refer to the year and are followed by numbers denoting the week (i.e: 1917 = year 2019, week 17; 0 means pools at the time of admission; 1, after five days of admission in the ICU).

Pool	Week	Variable	N patients	Initial date	End date	Total volume (µl)	Final Conc (ng/µl)
1917_0	1917	p0	3	2019-04-22	2019-04-28	60	30
1918_0	1918	p0	3	2019-04-29	2019-05-05	60	50
1918_1	1918	p1	1	2019-04-29	2019-05-05	60	100
1919_0	1919	p0	3	2019-05-06	2019-05-12	60	50
1919_1	1919	p1	3	2019-05-06	2019-05-12	45	20
1920_0	1920	p0	2	2019-05-13	2019-05-19	40	40
1920_1	1920	p1	4	2019-05-13	2019-05-19	60	30
1921_0	1921	p0	7	2019-05-20	2019-05-26	70	20
1921_1	1921	p1	2	2019-05-20	2019-05-26	50	20
1922_0	1922	p0	3	2019-05-27	2019-06-02	60	70
1922_1	1922	p1	2	2019-05-27	2019-06-02	60	20
1923_0	1923	p0	3	2019-06-03	2019-06-09	60	40
1923_1	1923	p1	3	2019-06-03	2019-06-09	45	30
1924_0	1924	p0	4	2019-06-10	2019-06-16	60	30
1924_1	1924	p1	2	2019-06-10	2019-06-16	40	30
1925_0	1925	p0	1	2019-06-17	2019-06-23	60	70
1925_1	1925	p1	4	2019-06-17	2019-06-23	60	30
1926_0	1926	p0	2	2019-06-24	2019-06-30	40	45
1926_1	1926	p1	3	2019-06-24	2019-06-30	60	50
1927_0	1927	p0	4	2019-07-01	2019-07-07	60	30
1927_1	1927	p1	2	2019-07-01	2019-07-07	60	70
1928_0	1928	p0	1	2019-07-08	2019-07-14	60	70
1928_1	1928	p1	4	2019-07-08	2019-07-14	60	45
1929_0	1929	p0	8	2019-07-15	2019-07-21	80	35
1929_1	1929	p1	4	2019-07-15	2019-07-21	60	50
1930_0	1930	p0	4	2019-07-22	2019-07-28	60	70
1930_1	1930	p1	6	2019-07-22	2019-07-28	60	35
1931_1	1931	p1	7	2019-07-29	2019-08-04	70	45
1932_0	1932	p0	2	2019-08-05	2019-08-11	60	70
1932_1	1932	p1	2	2019-08-05	2019-08-11	50	50
1933_0	1933	p0	4	2019-08-12	2019-05-18	60	30
1933_1	1933	p1	1	2019-08-12	2019-05-18	60	70
1934_0	1934	p0	2	2019-08-19	2019-08-25	60	70
1934_1	1934	p1	4	2019-08-19	2019-08-25	60	25
1935_0	1935	p0	6	2019-08-26	2019-09-01	60	40
1935_1	1935	p1	2	2019-08-26	2019-09-01	50	40
1936_1	1936	p1	4	2019-09-02	2019-09-08	48	30
1937_0	1937	p0	2	2019-09-09	2019-09-15	50	50
1937_1	1937	p1	3	2019-09-09	2019-09-15	90	100
1938_0	1938	p0	5	2019-09-16	2019-09-22	60	30
1938_1	1938	p1	4	2019-09-16	2019-09-22	60	50

1939_0	1939	p0	7	2019-09-23	2019-09-29	70	40
1939_1	1939	p1	4	2019-09-23	2019-09-29	60	50
1940_0	1940	p0	2	2019-09-30	2019-10-06	60	70
1940_1	1940	p1	6	2019-09-30	2019-10-06	60	40
1941_0	1941	p0	7	2019-10-07	2019-10-13	70	25
1941_1	1941	p1	3	2019-10-07	2019-10-13	60	50
1942_0	1942	p0	2	2019-10-14	2019-10-20	60	70
1942_1	1942	p1	6	2019-10-14	2019-10-20	60	40
1943_0	1943	p0	5	2019-10-21	2019-10-27	60	19
1943_1	1943	p1	3	2019-10-21	2019-10-27	90	70
1944_0	1944	p0	3	2019-10-28	2019-11-03	60	40
1944_1	1944	p1	4	2019-10-28	2019-11-03	40	50
1945_0	1945	p0	6	2019-11-04	2019-11-10	60	40
1945_1	1945	p1	5	2019-11-04	2019-11-10	60	30
1946_0	1946	p0	2	2019-11-11	2019-11-17	60	70
1946_1	1946	p1	4	2019-11-11	2019-11-17	60	40
1947_0	1947	p0	2	2019-11-18	2019-11-24	40	30
1947_1	1947	p1	3	2019-11-18	2019-11-24	60	70
1948_0	1948	p0	5	2019-11-25	2019-12-01	60	70
1948_1	1948	p1	3	2019-11-25	2019-12-01	60	50
1949_0	1949	p0	3	2019-12-02	2019-12-08	36	24
1949_1	1949	p1	5	2019-12-02	2019-12-08	60	30
1950_0	1950	p0	5	2019-12-09	2019-12-15	60	60
1950_1	1950	p1	2	2019-12-09	2019-12-15	40	50
1951_0	1951	p0	1	2019-12-16	2019-12-22	30	51
1951_1	1951	p1	5	2019-12-16	2019-12-22	60	25
1952_0	1952	p0	4	2019-12-23	2019-12-29	60	50
1952_1	1952	p1	4	2019-12-23	2019-12-29	40	50
2001_0	2001	p0	6	2019-12-30	2020-01-05	60	60
2001_1	2001	p1	3	2019-12-30	2020-01-05	60	70
2002_0	2002	p0	3	2020-01-06	2020-01-12	60	70
2002_1	2002	p1	1	2020-01-06	2020-01-12	40	70
2003_0	2003	p0	4	2020-01-13	2020-01-19	40	60
2003_1	2003	p1	8	2020-01-13	2020-01-19	60	70
2004_0	2004	p0	2	2020-01-20	2020-01-26	60	70
2004_1	2004	p1	5	2020-01-20	2020-01-26	60	70
2005_0	2005	p0	2	2020-01-27	2019-02-02	60	70
2005_1	2005	p1	7	2020-01-27	2019-02-02	70	70
2006_0	2006	p0	7	2020-02-03	2020-02-09	57	60
2006_1	2006	p1	4	2020-02-03	2020-02-09	60	70
2007_0	2007	p0	1	2020-02-10	2020-02-16	60	70
2007_1	2007	p1	8	2020-02-10	2020-02-16	60	70
2008_0	2008	p0	3	2020-02-17	2020-02-23	45	50
2008_1	2008	p1	5	2020-02-17	2020-02-23	60	70
2009_0	2009	p0	3	2020-02-24	2020-03-01	60	70
2009_1	2009	p1	6	2020-02-24	2020-03-01	60	70

2010_0	2010	p0	2	2020-03-02	2020-03-08	40	60
2010_1	2010	p1	5	2020-03-02	2020-03-08	60	70
2011_0	2011	p0	2	2020-03-09	2020-03-15	60	70
2011_1	2011	p1	2	2020-03-09	2020-03-15	20	60

Annex 2 | Temporal tendency of the number of patients per pool and pooled group

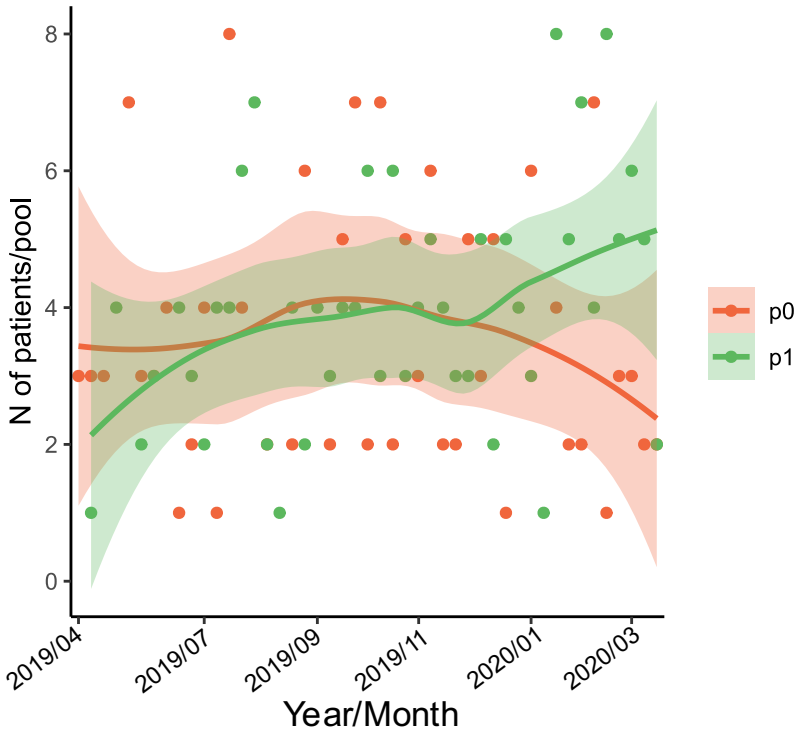

Annex 3 | Clinical information about the patients in the study

Variable		All participants (n=349)	Participants with sampled stool (n=178)
		N=349	**N=178 (51.0%)**
Patients re-admitted		15 (n=364)	13 (n=188)
Age, median(range)	years	60 (16-88)	60 (23-86)
Age, mean(range)	years	59 (16-88)	61 (23-86)
Sex	1.Male	220 (63.0%)	108 (61.7%)
	2.Female	126 (36.1%)	67 (38.3%)
	3.NA	3 (0,9%)	0 (0.0%)
Hospitalization days Hospitalized in ICU, median (range)		6 (1-92)	12 (1-76)
Hospitalized in ICU, mean (range)		11 (1-92)	17 (1-76)
Citizenship	1.African	5 (1,4%)	1 (0.6%)
	2.Asian	2 (0,6%)	1 (0.6%)
	3.European	12 (3,4%)	8 (4.6%)
	4.Latinoamerican	18 (5.2%)	4 (2.3%)
	5.Northamerican	1 (0.3%)	0 (0.0%)
	6.Spanish/European	306 (87.7%)	159 (90.9%)
	7.NA	5 (1.4%)	2 (1.1%)
		N=364	**N= 188**
Type of admission at ICU	1.Medical	321 (88.2%)	171 (91.0%)
	2.Surgical	34 (9,3%)	14 (7.5%)
	3.Trauma	7 (1.9%)	2 (1.1%)
	4.NA	2 (0.6%)	1 (0.5%)
SOFA score, median (range)		8 (0-24)	9 (0-24)
SOFA score, mean (range)		8 (0-24)	9 (0-24)
Mortality	1.Yes	48 (13,2%)	27 (14.4%)
	2.No	280 (76.9%)	139 (74.0%)
	3.NA	36 (9.9%)	22 (11.7%)
		N=349	**N=175**
Inmunocompromised	1.Yes	72 (20,6%)	46 (26.3%)
	2.No	272 (77.9%)	128 (73.1%)
	3.NA	5 (1.4%)	1 (0.6%)
		N=364	**N=188**
Sepsis at admission	1.Yes	165 (45.3%)	109 (58.0%)
	2.No	194 (53.3%)	76 (40.4%)
	3.NA	5 (1.4%)	3 (1.6%)

Annex 4 | Work tables for groups of patients with cases of colonization and infection with ESBL and carbapenemase-producing microorganisms. Legend: light blue (group 1), purple (group 2), orange (group 3), dark blue (group 4). See section **4.2.3** for descriptions. Green bars indicate the length of stay for the patients.

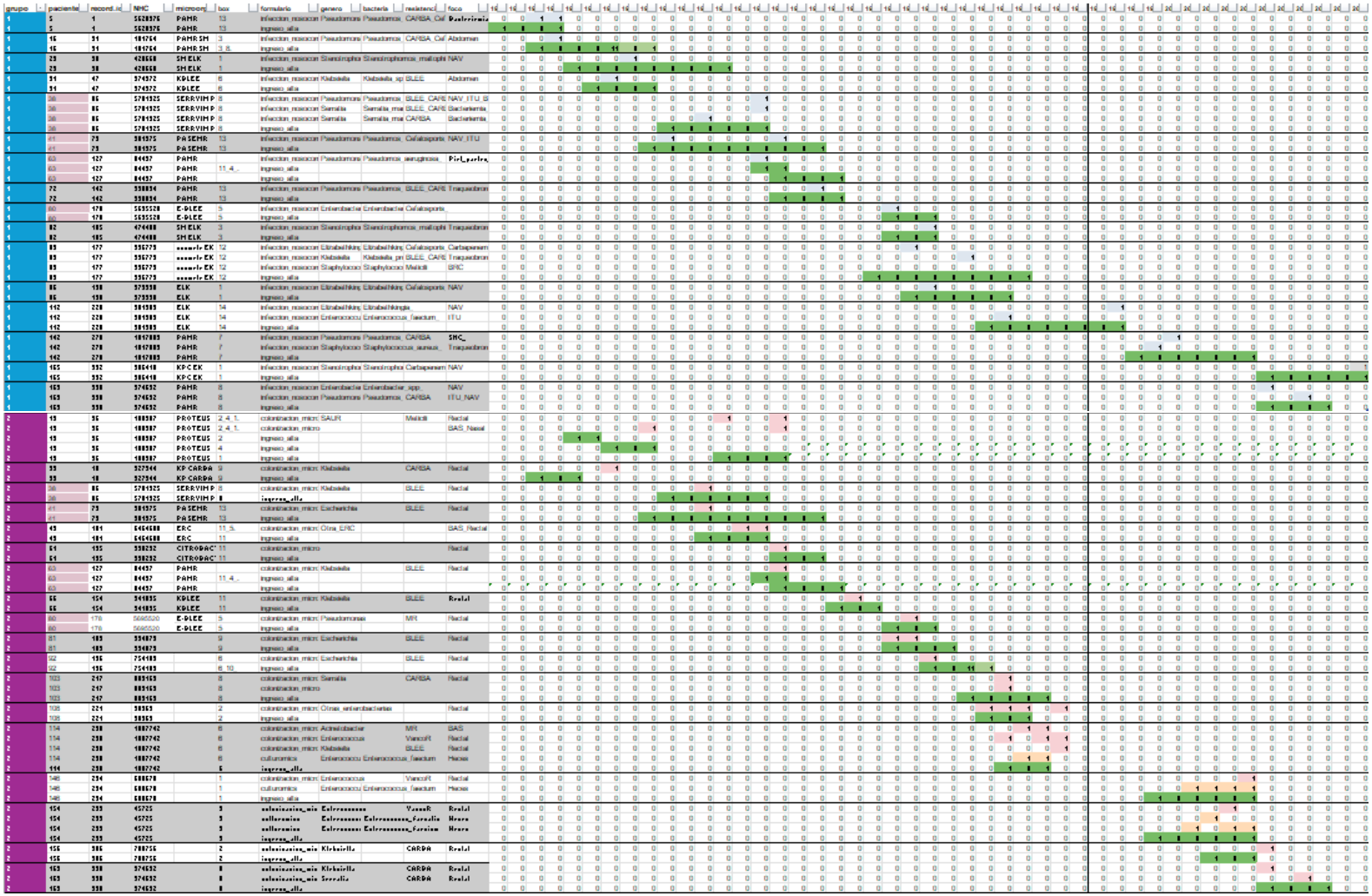

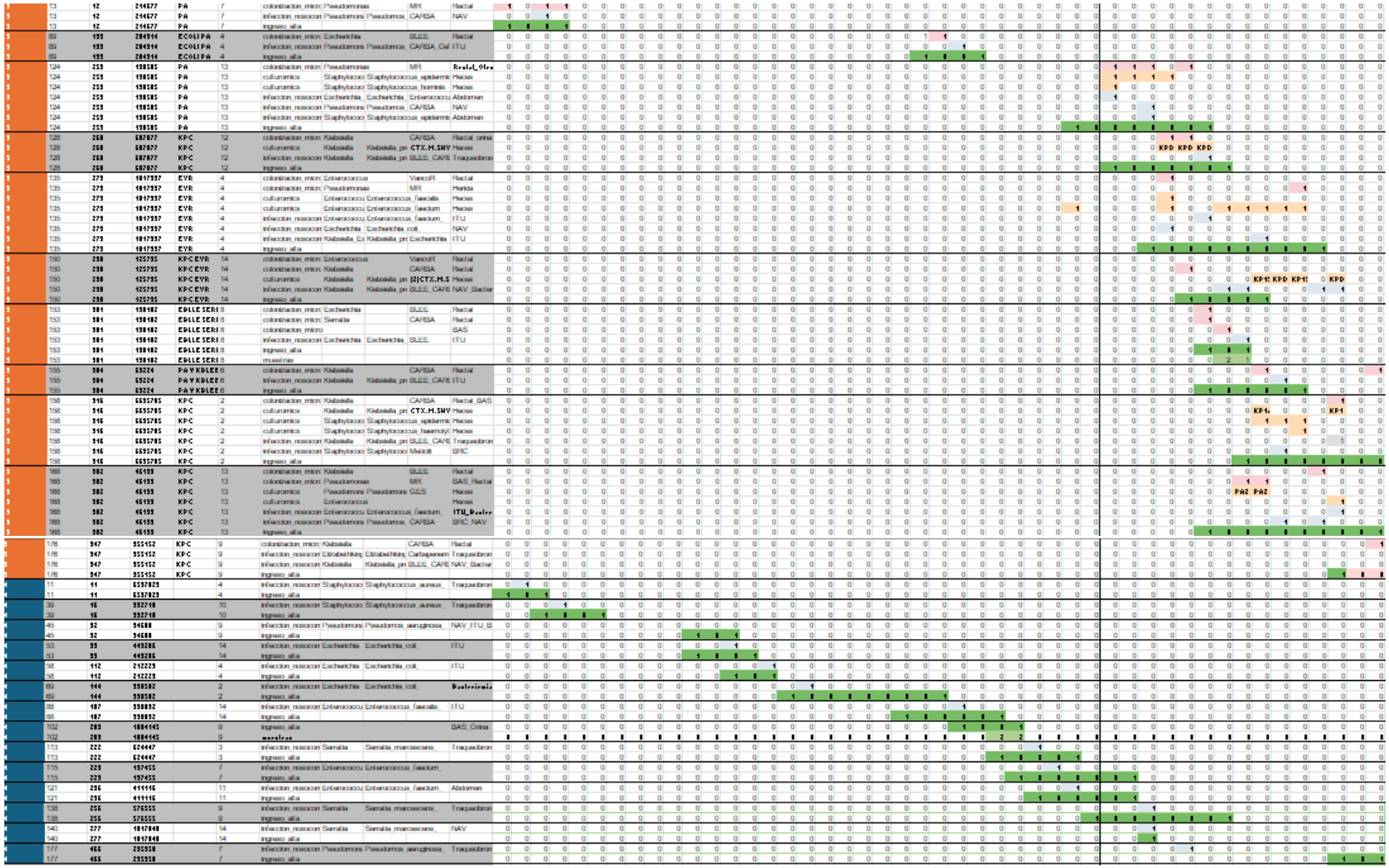

Annex 5 | Pulsotype list

Pulsotype	n	n room	Room number	Week of sampling	Period of isolation	AmpC phenotype	Specie
PT-S1	10	4/14	#4, #5, #7, #14	4(3), 11(1), 16(1) 18(1), 20(1), 27(1), 29(1), 32(1)	Mar 2019 - Feb 2020	Basal-like(9), Inducible(1)	*S. nevei*
PT-S10	1	1/14	#14	31(1)	Feb 2020	Basal-like(1)	*S. nevei*
PT-S11	2	2/14	#10, #13	38(1), 39(1)	Sep - Nov 2020	Basal-like(2)	*S. nevei*
PT-S12	5	1/14	#9	5(2), 7(1), 21(1), 37(1)	Mar 2019 - Sep 2020	Basal-like(2), Inducible(3)	*S. nevei*
PT-S13	1	1/14	#3	16(1)	Jun 2019	Inducible(1)	*S. nevei*
PT-S14	6	3/14	#6, #7, #10	5(2), 8(1), 10(1), 19(1), 23(1)	Mar - Oct 2019	Derepressed-like(6)	*S. nevei*
PT-S15	9	4/14	#8, #11, #12, #13	4(1), 6(1), 7(1), 9(1), 11(1),19(2), 20(1), 22(1)	Mar - Oct 2019	Derepressed-like(9)	*S. nevei*
PT-S16	2	2/14	#7, #12	15(1), 28(1)	Jun - Nov2019	Basal-like(2)	*S. nevei*
PT-S17	8	1/14	#9	4(1), 5(1), 6(1), 7(1), 9(1), 10(2), 19(1)	Mar - Jul 2019	Basal-like(7), Derepressed-like(1)	*S. ureilytica*
PT-S18	2	1/14	#12	4(1), 8(1)	Mar - Apr 2019	Inducible(2)	*S. nevei*
PT-S2	1	1/14	#14	38(1)	Sep 2020	Basal-like(1)	*S. ureilytica*
PT-S3	25	11/14	#2, #3, #5, #6, #7, #8, #10, #11, #12, #13, #14	4(5), 5(1), 6(1), 8(3), 9(1), 10(2), 12(1), 13(2), 16(2), 17(1), 23(1), 24(1), 32(1), 34(1), 38(1)	Mar 2019 - Sep 2020	Basal-like(21), Inducible(3), Derepressed-like(1)	*S. nevei*
PT-S4	2	1/14	#8	34(1), 37(1)	Jul - Sep 2019	Derepressed-like(2)	*S. nevei*
PT-S5	10	4/14	#1, #5, #12, #13	9(2), 11(1), 14(1), 18(1), 20(1), 29(2), 37(1), 38(1)	Apr 2019 - Sep 2020	Basal-like(10)	*S. nevei*
PT-S6	2	1/14	#3	4(1), 17(1)	Mar - Jun 2019	Basal-like(2)	*S. nevei*
PT-S7	4	4/14	#8, #12, #13	9(1), 22(1), 34(1), 37(1)	Apr 2019 - Sep 2020	Derepressed-like(4)	*S. nevei*
PT-S8	3	3/14	#6, #10, #11	6(1), 10(1), 11(1)	Sep 2019	Derepressed-like(3)	*S. nevei*
PT-S9	1	1/14	#2	9(1)	Apr 2019	Derepressed-like(1)	*S. ureilytica*

Annex 6 | Epidemiological and genomic characteristics of the 165 *Serratia* strains

Strain	BioSample	Origin	Source	Date	Hospital ward	GC	MLST	GTDB	Clade	ID	Phenotype
P1	SAMN37645927	P	Stool	2019-09-17	ICU Medical	59.6	ST525	Sm/Sn	3	F495	Inducible
P10	SAMN37645928	P	BSI	2016-08-05	Gastroenterology	59.5	ST402	Sn	4B	16083201	Inducible
P11	SAMN37645929	P	BSI	2016-05-24	Gastroenterology	59.6	ST402	Sn	4B	16093693	Inducible
P12	SAMN37645930	P	BSI	2016-12-06	ICU Medical	59.6	ST404	Sm/Sn	3	16105146	Inducible
P13	SAMN37645931	P	BSI	2015-02-16	Urology	59.7	ST405	Su	2B	15028310	Inducible
P14	SAMN37645932	P	BSI	2015-11-06	Emergencies	59.4	ST500	Sb	2A	15100018	Inducible
P15	SAMN37645933	P	BSI	2015-06-14	Anesthesia/REA	59.3	ST407	Sb	2A	15100893	Inducible
P16	SAMN37645934	P	BSI	2015-06-23	Anesthesia/REA	59.3	ST92	Sn	4A	15107433	Inducible
P17	SAMN37645935	P	BSI	2015-05-08	Emergencies	59.6	ST650	Su	2B	15132730	Inducible
P18	SAMN37645936	P	BSI	2015-03-09	Emergencies	59.9	ST408	Sm/Sn	3	15147908	Inducible
P19	SAMN37645937	P	BSI	2015-05-10	Plastic surgery	59.5	ST409	Su	2B	15168441	Inducible
P2	SAMN37645938	P	BAS	2016-12-13	ICU Medical	59.3	ST92	Sn	4A	P60	Derepressed-like
P20	SAMN37645939	P	BSI	2015-11-19	Nephrology	59.8	ST525	Sm/Sn	3	15197978	Inducible
P21	SAMN37645940	P	BSI	2014-01-13	Oncology	59.4	ST501	Su	2B	14006167	Inducible
P22	SAMN37645941	P	BSI	2014-03-26	Gastroenterology	60.0	ST379	Sm/Sn	3	14051405	Inducible
P23	SAMN37645942	P	BSI	2014-02-06	Emergencies	59.5	ST402	Sn	4B	14090492	Inducible
P24	SAMN37645943	P	BSI	2014-06-22	Emergencies	60.1	ST412	Sm/Sn	3	14102016	Inducible
P25	SAMN37645944	P	BSI	2013-06-13	Cardiac surgery	59.6	ST413	Su	2B	13092327	Inducible
P26	SAMN37645945	P	BSI	2013-09-29	Internal medicine	59.6	ST414	Sn	4B	13147047	Inducible
P27	SAMN37645946	P	BSI	2013-10-29	Emergencies	60.1	ST394	Sm/Sn	3	13164892	Inducible
P28	SAMN37645947	P	BSI		Cardiology	59.4	ST415	Sn	4B	13179079	Inducible
P29	SAMN37645948	P	BSI	2013-12-16	Traumatology	59.4	ST416	Sb	2A	13191200	Inducible
P3	SAMN37645949	P	Bone	2018-11-27	ICU Medical	59.9	ST417	Sm/Sn	3	H28	Derepressed-like
P30	SAMN37645950	P	BSI	2012-01-30	Emergencies	59.9	ST679	Sm/Sn	3	12023282	Inducible
P31	SAMN37645951	P	BSI	2012-02-13	Emergencies	59.7	ST213	Su	2B	12031246	Inducible
P32	SAMN37645952	P	BSI	2012-05-24	Emergencies	59.2	ST502	Sb	2A	12090842	Inducible
P33	SAMN37645953	P	BSI	2012-09-07	Pneumology	59.6	ST419	Su	2B	12118255	Inducible
P34	SAMN37645954	P	BSI	2011-07-01	Emergencies	59.9	ST352	Sn	4B	11003224	Inducible
P35	SAMN37645955	P	BSI	2011-08-22	Gastroenterology	58.7	ST420	Sb	2A	11132886	Inducible
P36	SAMN37645956	P	BSI	2011-11-09	General surgery	60.0	ST408	Sm/Sn	3	11142169	Inducible
P37	SAMN37645957	P	BSI	2011-04-10	ICU pediatric	60.0	ST366	Sm/Sn	3	11156328	Inducible
P38	SAMN37645958	P	BSI	2011-04-10	ICU pediatric	60.0	ST408	Sm/Sn	3	11156328	Inducible
P39	SAMN37645959	P	BSI	2010-09-28	Traumatology	59.8	ST423	Sm/Sn	3	10148459	Inducible
P4	SAMN37645960	P	WE	2017-10-01	ICU Medical	59.6	ST424	Sn	4B	M52	Derepressed-like
P40	SAMN37645961	P	BSI	2010-12-28	Cardiac surgery	59.5	ST425	Sn	4B	10198397	Inducible
P41	SAMN37645962	P	BSI	2009-04-01	General surgery	59.6	ST307	Su	2B	9000612	Inducible
P42	SAMN37645963	P	BSI	2009-02-26	ICU pediatric	59.6	ST356	Sm/Sn	3	9028827	Inducible
P43	SAMN37645964	P	BSI	2009-07-13	Hematology	59.3	ST503	Sm	1B	9106440	Inducible
P44	SAMN37645965	P	BSI	2009-11-10	Nephrology	59.8	ST427	Sm/Sn	3	9152171	Inducible
P45	SAMN37645966	P	BSI	2009-01-11	Nephrology	59.4	ST327	Sn	4B	9164384	Inducible
P46	SAMN37645967	P	BSI	2009-08-11	Emergencies	59.4	ST238	Su	2B	9164384	Inducible
P47	SAMN37645968	P	BSI	2008-03-17	ICU Medical	60.1	ST56	Sm/Sn	3	8039167	Inducible
P48	SAMN37645969	P	BSI	2008-06-29	Cardiology	60.0	ST428	Sm/Sn	3	8095646	Inducible
P49	SAMN37645970	P	BSI	2008-09-30	General surgery	59.6	ST195	Su	2B	8139425	Inducible

P5	SAMN37645971	P	WE	2018-01-22	ICU Medical	59.9	ST417	Sm/Sn	3	I54	Derepressed-like
P50	SAMN37645972	P	BSI	2008-11-20	Cardiac surgery	59.4	ST430	Sn	4B	8170607	Inducible
P51	SAMN37645973	P	BSI	2007-02-02	Oncology	59.6	ST431	Snm	1A	7014608	Inducible
P52	SAMN37645974	P	BSI	2007-11-05	Neurosurgery	59.3	ST432	Sb	2A	7062281	Inducible
P53	SAMN37645975	P	BSI	2007-05-23	ICU Medical	59.0	ST433	Su	2B	7066586	Inducible
P54	SAMN37645976	P	BSI	2007-06-22	ICU Medical	59.9	ST434	Sn	4A	7082986	Inducible
P55	SAMN37645977	P	BSI	2007-07-13	ICU Medical	59.8	ST367	Sm/Sn	3	7096967	Inducible
P56	SAMN37645978	P	BSI	2007-06-08	ICU Medical	60.0	ST376	Sm/Sn	3	7104931	Inducible
P57	SAMN37645979	P	BSI	2007-05-11	ICU Medical	59.3	ST507	Sb	2A	7149110	Inducible
P58	SAMN37645980	P	BSI	2007-06-11	Oncology	59.9	ST490	Sm/Sn	3	7140819	Inducible
P59	SAMN37645981	P	BSI	2006-06-02	ICU Medical	59.4	ST436	Su	2B	6014736	Inducible
P6	SAMN37645982	P	BAS	2017-03-09	ICU Medical	59.2	ST424	Sn	4B	B77	Derepressed-like
P60	SAMN37645983	P	BSI	2006-03-29	ICU Medical	59.3	ST438	Sn	4B	6039197	Inducible
P61	SAMN37645984	P	BSI	2006-04-20	Emergencies	60.0	ST508	Sm/Sn	3	6049262	Inducible
P62	SAMN37645985	P	BSI	2006-07-14	Nephrology	59.4	ST430	Sn	4B	6089946	Inducible
P63	SAMN37645986	P	BSI	2006-08-21	ICU Medical	59.1	ST510	Sb	2A	6106176	Inducible
P64	SAMN37645987	P	BSI	2006-11-29	Emergencies	59.4	ST430	Sn	4B	6153760	Inducible
P65	SAMN37645988	P	BSI	2006-12-21	Cardiology	59.4	ST430	Sn	4B	6163834	Inducible
P66	SAMN37645989	P	BSI	2005-01-28	ICU Medical	60.0	ST444	Sm/Sn	3	5012095	Inducible
P67	SAMN37645990	P	BSI	2005-02-02	Internal medicine	59.7	ST275	Su	2B	5014409	Inducible
P68	SAMN37645991	P	BSI	2005-05-16	Cardiology	60.0	ST255	Sm/Sn	3	5062348	Inducible
P69	SAMN37645992	P	BSI	2005-11-08	ICU pediatric	58.9	ST197	Sb	2A	5100738	Inducible
P7	SAMN37645993	P	BSI	2016-01-26	General surgery	60.1	ST375	Sm/Sn	3	16014874	Inducible
P70	SAMN37645994	P	BSI	2005-08-29	ICU Medical	58.9	ST445	Sb	2A	5106719	Inducible
P71	SAMN37645995	P	BSI	2005-04-11	ICU Medical	59.4	ST446	Sb	2A	5135676	Inducible
P72	SAMN37645996	P	BSI	2005-11-17	ICU Medical	59.5	ST447	Su	2B	5141155	Inducible
P73	SAMN37645997	P	BSI	2005-12-29	Emergencies	59.2	ST448	Sb	2A	5160926	Inducible
P74	SAMN37645998	P	BSI	2004-01-16	ICU Medical	60.0	ST449	Sm/Sn	3	4005946	Inducible
P75	SAMN37645999	P	BSI	2004-01-30	Emergencies	59.4	ST430	Sn	4B	4012794	Inducible
P76	SAMN37646000	P	BSI	2004-11-03	Oncology	59.6	ST451	Sn	4A	4031621	Inducible
P77	SAMN37646001	P	BSI	2004-02-04	Nephrology	60.1	ST394	Sm/Sn	3	4041502	Inducible
P78	SAMN37646002	P	BSI	2004-05-24	ICU Medical	59.6	ST431	Snm	1A	4063668	Inducible
P79	SAMN37646003	P	BSI	2004-06-25	ICU Medical	59.7	ST453	Su	2B	4078963	Inducible
P8	SAMN37646004	P	BSI	2016-06-03	General surgery	60.0	ST255	Sm/Sn	3	16042908	Inducible
P80	SAMN37646005	P	BSI	2004-07-07	ICU pediatric	59.6	ST454	Sn	4B	04083707	Inducible
P81	SAMN37646006	P	BSI	2004-10-08	Internal medicine	60.0	ST366	Sm/Sn	3	04096178	Inducible
P82	SAMN37646007	P	BSI	2004-01-10	ICU Medical	59.2	ST31	Sb	2A	0415461	Inducible
P83	SAMN37646008	P	BSI	2004-10-29	Internal medicine	59.3	ST31	Sb	2A	04130050	Inducible
P84	SAMN37646009	P	BSI	2004-05-11	General surgery	59.5	ST455	Su	2B	04132499	Inducible
P85	SAMN37646010	P	BSI	2004-05-11	ICU Medical	59.2	ST447	Su	2B	04132857	Inducible
P86	SAMN37646011	P	BSI	2004-11-11	Internal medicine	58.8	ST31	Sb	2A	04134935	Inducible
P87	SAMN37646012	P	BSI	2004-10-12	General surgery	59.6	ST195	Su	2B	04148281	Inducible
P88	SAMN37646013	P	BSI	2004-12-23	Emergencies	59.5	ST456	Su	2B	04154569	Inducible
P89	SAMN37646014	P	BSI	NA	NA	59.9	ST255	Sm/Sn	3	03001623	Inducible
P9	SAMN37646015	P	BSI	2016-06-03	General surgery	59.4	ST457	Sn	4A	16042908	Inducible
P90	SAMN37646016	P	BSI	2003-10-02	Otolaryngology	60.0	ST439	Sm/Sn	3	03002128	Inducible

P91	SAMN37646017	P	BSI	NA	NA	59.6	ST458	Su	2B	03002607	Inducible
P92	SAMN37646018	P	BSI	2003-09-13	ICU Medical	59.9	ST340	Sm/Sn	3	03013328	Inducible
P93	SAMN37646019	P	BSI	2003-10-31	ICU Medical	59.4	ST307	Su	2B	03125580	Inducible
P94	SAMN37646020	P	BSI	2003-11-17	Traumatology	59.4	ST459	Sm	1B	03132289	Inducible
P95	SAMN37646021	P	BSI	2016-04-24	Emergencies	59.5	ST511	Sm	1B	16074964	Inducible
P96	SAMN37646022	P	BSI	2012-03-27	ICU Medical	60.1	ST394	Sm/Sn	3	12058178	Inducible
P97	SAMN37646023	P	BSI	2011-07-19	ICU Medical	59.9	ST366	Sm/Sn	3	11117169	Inducible
P98	SAMN37646024	P	BSI	NA	NA	59.7	ST512	Sm/Sn	3	10134885	Inducible
P99	SAMN37646025	P	BSI	2009-01-30	ICU Medical	60.0	ST462	Sm/Sn	3	9013298	Inducible
S1	SAMN37645926	S	Drain	2020-07-15	ICU Medical	59.5	ST424	Sn	4B	11227	Derepressed-like
S10	SAMN37645861	S	Drain	2019-10-04	ICU Medical	58.9	ST92	Sn	4A	1267	Inducible
S11	SAMN37645862	S	Surface	2019-10-07	ICU Medical	59.5	ST424	Sn	4B	5452	Derepressed-like
S12	SAMN37645863	S	Surface	2019-09-10	ICU Medical	59.5	ST525	Sm/Sn	3	6499	Inducible
S13	SAMN37645864	S	Surface	2019-06-19	ICU Medical	59.3	ST465	Su	2B	4078	Inducible
S14	SAMN37645865	S	Surface	2019-10-23	ICU Medical	59.6	ST424	Sn	4B	7132	Derepressed-like
S15	SAMN37645866	S	Drain	2019-04-04	ICU Medical	59.3	ST92	Sn	4A	1113	Basal-like
S16	SAMN37645867	S	Drain	2019-03-27	ICU Medical	58.6	ST424	Sn	4B	862	Derepressed-like
S17	SAMN37645868	S	Surface	2019-10-30	ICU Medical	59.3	ST92	Sn	4A	7373	Basal-like
S18	SAMN37645869	S	Drain	2019-06-19	ICU Medical	59.3	ST92	Sn	4A	4086	Basal-like
S19	SAMN37645870	D	VT	2019-04-24	ICU Medical	59.6	ST424	Sn	4B	1773	Derepressed-like
S2	SAMN37645871	S	Drain	2019-06-26	ICU Medical	59.1	ST92	Sn	4A	4462	Inducible
S20	SAMN37645872	S	Drain	2019-04-04	ICU Medical	59.5	ST424	Sn	4B	1116	Derepressed-like
S21	SAMN37645873	S	Drain	2019-06-19	ICU Medical	59.3	ST92	Sn	4A	4297	Basal-like
S22	SAMN37645874	S	Drain	2019-06-26	ICU Medical	53.1	ST470	Sn	4A	4405	Basal-like
S23	SAMN37645875	S	Drain	2019-11-27	ICU Medical	59.1	ST470	Sn	4A	9176	Basal-like
S24	SAMN37645876	S	Drain	2019-06-03	ICU Medical	58.8	ST424	Sn	4B	5712	Derepressed-like
S25	SAMN37645877	S	Drain	2019-04-10	ICU Medical	59.2	ST470	Sn	4A	6262	Basal-like
S26	SAMN37645878	S	Drain	2019-03-07	ICU Medical	59.1	ST470	Sn	4A	4893	Basal-like
S27	SAMN37645879	S	Drain	2019-06-03	ICU Medical	59.3	ST92	Sn	4A	5925	Inducible
S28	SAMN37645880	S	Surface	2019-05-29	ICU Medical	59.3	ST92	Sn	4A	2977	Basal-like
S29	SAMN37645881	S	Drain	2019-04-10	ICU Medical	59.5	ST424	Sn	4B	6266	Derepressed-like
S3	SAMN37645882	S	Drain	2019-03-13	ICU Medical	59.4	ST525	Sm/Sn	3	168	Inducible
S30	SAMN37645883	S	Drain	2019-04-10	ICU Medical	59.1	ST470	Sn	4A	6066	Basal-like
S31	SAMN37645884	S	Drain	2019-04-04	ICU Medical	59.3	ST92	Sn	4A	5677	Basal-like
S32	SAMN37645885	S	Drain	2019-10-07	ICU Medical	59.6	ST424	Sn	4B	5586	Derepressed-like
S33	SAMN37645886	S	Surface	2019-10-23	ICU Medical	59.3	ST92	Sn	4A	7131	Basal-like
S34	SAMN37645887	S	Surface	2019-06-03	ICU Medical	59.4	ST92	Sn	4A	5842	Basal-like
S35	SAMN37645888	D	Pot	2019-10-04	ICU Medical	59.6	ST424	Sn	4B	1375	Derepressed-like
S36	SAMN37645889	S	Drain	2019-06-03	ICU Medical	60.0	ST807	Sm/Sn	3	5725	Inducible
S37	SAMN37645890	S	Drain	2019-10-04	ICU Medical	59.3	ST92	Sn	4A	1349	Basal-like
S38	SAMN37645891	S	Surface	2019-06-03	ICU Medical	59.3	ST92	Sn	4A	5844	Basal-like
S39	SAMN37645892	S	Drain	2019-10-04	ICU Medical	59.5	ST424	Sn	4B	1378	Derepressed-like
S4	SAMN37645893	S	Drain	2019-04-04	ICU Medical	60.0	ST807	Sm/Sn	3	1154	Inducible
S40	SAMN37645894	S	Surface	2019-03-20	ICU Medical	59.6	ST424	Sn	4B	496	Derepressed-like
S41	SAMN37645895	S	Drain	2019-10-16	ICU Medical	59.3	ST424	Sn	4B	6899	Derepressed-like
S42	SAMN37645896	S	Surface	2019-04-24	ICU Medical	59.3	ST92	Sn	4A	1751	Basal-like

S43	SAMN37645897	S	Surface	2019-10-07	ICU Medical	59.6	ST424	Sn	4B	5514	Derepressed-like
S44	SAMN37645898	S	Drain	2019-04-04	ICU Medical	59.3	ST92	Sn	4A	1150	Basal-like
S45	SAMN37645899	S	Surface	2019-05-16	ICU Medical	59.6	ST424	Sn	4B	2231	Derepressed-like
S46	SAMN37645900	S	Drain	2019-05-06	ICU Medical	59.2	ST470	Sn	4A	3146	Basal-like
S47	SAMN37645901	S	Drain	2019-12-12	ICU Medical	59.2	ST470	Sn	4A	9453	Basal-like
S48	SAMN37645902	S	P-trap	2020-09-16	ICU Medical	59.4	ST424	Sn	4B	12139	Derepressed-like
S49	SAMN37645903	S	Drain	2019-10-04	ICU Medical	59.4	ST485	Su	2B	1269	Inducible
S5	SAMN37645904	S	Drain	2019-03-13	ICU Medical	59.0	ST424	Sn	4B	85	Derepressed-like
S50	SAMN37645905	S	Drain	2019-06-03	ICU Medical	59.1	ST470	Sn	4A	5805	Basal-like
S51	SAMN37645906	S	Drain	2019-06-19	ICU Medical	59.1	ST470	Sn	4A	4125	Basal-like
S52	SAMN37645907	S	P-trap	2020-09-28	ICU Medical	59.0	ST470	Sn	4A	12432	Basal-like
S53	SAMN37645908	S	Surface	2020-09-16	ICU Medical	59.6	ST424	Sn	4B	12239	Derepressed-like
S54	SAMN37645909	S	Drain	2020-07-15	ICU Medical	59.0	ST92	Sn	4A	11108	Basal-like
S55	SAMN37645910	S	Surface	2020-07-15	ICU Medical	59.2	ST424	Sn	4B	11132	Derepressed-like
S56	SAMN37645911	S	P-trap	2020-09-16	ICU Medical	59.8	ST525	Sm/Sn	3	12887	Inducible
S57	SAMN37645912	S	Drain	2020-09-28	ICU Medical	59.0	ST92	Sn	4A	12929	Basal-like
S58	SAMN37645913	S	P-trap	2020-09-28	ICU Medical	59.3	ST92	Sn	4A	12935	Basal-like
S59	SAMN37645914	S	Drain	2020-09-28	ICU Medical	59.5	ST485	Sn	4B	12928	Derepressed-like
S6	SAMN37645915	S	Surface	2019-10-04	ICU Medical	59.3	ST485	Su	2B	1395	Basal-like
S60	SAMN37645916	S	P-trap	2020-09-28	ICU Medical	59.4	ST424	Sn	4B	13049	Derepressed-like
S61	SAMN37645917	S	Drain	2020-07-15	ICU Medical	59.5	ST424	Sn	4B	11237	Derepressed-like
S62	SAMN37645918	S	Drain	2019-10-16	ICU Medical	59.6	ST424	Sn	4B	6923	Derepressed-like
S63	SAMN37645919	S	Drain	2020-05-11	ICU Medical	59.2	ST92	Sn	4A	13611	Basal-like
S64	SAMN37645920	S	Drain	2020-02-13	ICU Medical	59.2	ST92	Sn	4A	10319	Basal-like
S65	SAMN37645921	S	Drain	2020-02-27	ICU Medical	59.3	ST92	Sn	4A	10514	Basal-like
S66	SAMN37645922	S	P-trap	2020-09-28	ICU Medical	59.3	ST496	Su	2B	13134	Basal-like
S7	SAMN37645923	S	Drain	2019-12-06	ICU Medical	59.4	ST470	Sn	4A	3914a	Basal-like
S8	SAMN37645924	S	Surface	2019-03-13	ICU Medical	58.9	ST424	Sn	4B	92	Derepressed-like
S9	SAMN37645925	S	Drain	2019-10-07	ICU Medical	59.3	ST485	Su	2B	5551	Basal-like

Abbreviations: BAS (bronchoaspirate), BSI (Bloodstream Infection), D (Dry surface), P (Patient), S (Sink), S (*S. bockelmannii*), Sm (*S. marcescens*), Sn (*S. nevei*), Snm (*S. nematodiphila*), Su (*S. ureilytica*), VT (Ventilator's touchscreen), WE (Wound exudate).

Annex 7 | Induction assays

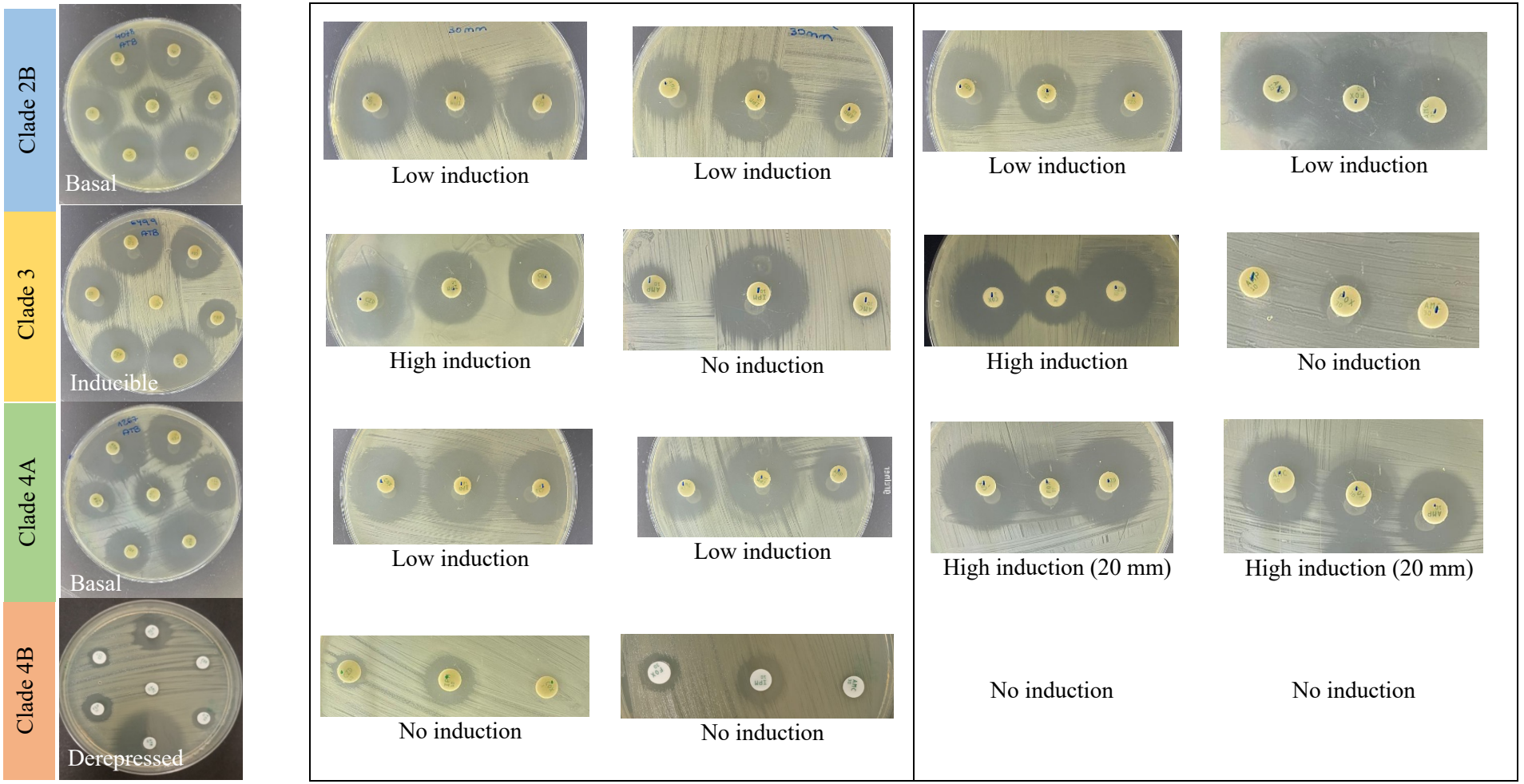

M i s c h i e f

m a n a g e d .

Cover and Design by: ANA MURCIA JOVER
@anitamursia